A study on the antagonistic targeting of thymic stromal lymphopoietin (TSLP) as a potential therapeutic strategy for *Asthma bronchiale*

Dissertation

In order to obtain the academic degree

Doctor rerum naturalium (Dr. rer nat.)

Submitted to the Council of the Medical Faculty,

Friedrich Schiller University, Jena

by Nilabh Ranjan, M.Sc. (Biotechnology)

Born on April 08, 1982 in Sitapur, India

Reviewer/Expert:

1. **Prof. Dr. Karl-Heinz Friedrich (Supervisor/Reviewer 1)**

   Group Leader Signal Transduction
   Institute für Biochemie-II
   Friedrich Schiller University, Jena

2. **Prof. Dr. Dr. rer. nat. Aria Baniahmad (Co-Supervisor/Reviewer 2)**

   Group Leader (Molekular genetics)
   Institute für Humangenetics
   Friedrich Schiller University, Jena

3. **Prof. Dr. rer. nat. Gerhard Müller-Newen (Reviewer 3)**

   Institute of Biochemistry and Molecular Biology
   University Hospital Aachen, RWTH Aachen

Date of the public defense: **1.12.2015**

‘‘The most beautiful thing we can experience is the mysterious.

It is the source of all true art and science.”

— Albert Einstein

Table of Contents

Abbreviations

AD	Atopic dermatitis
AHR	Airway hyperresponsiveness
(B)-ALL	Acute lymphoblastic leukemia of B cells
APC	Antigen presenting cells/Allphycocyanin
APS	Ammoniumperoxidisulphate
AR	Allergic rhinitis
Bp	Base pair
BAL	Bronchoalveolar lavage
BGH	Bovine growth hormone
BMDC	Bone marrow derived dendritic cells
BSA	Bovine serum albumin
CD	Crohn's disease
CD (number)	Cluster of differentiation
CDR3	Complementarity determining region 3
COPD	Chronic obstructive pulmonary disease
cDNA	Complementary DNA
CRLF2/TSLPR	Cytokine receptor like factor/TSLP receptor
CLP	Cecal ligation and puncture
CXCL	Chemokine ligand
CO_2	Carbon dioxide
DCs	Dendritic cells
DMEM	Dulbecco´s modified eagle medium
DMSO	Dimethylsulfoxide
DNA	Deoxyribonucleic acid
dNTP	Deoxyribonucleoside triphosphate
ELISA	Enzyme linked immunosorbent assay
EoE	Eosinophilic esophagitis
Exo/Int	Extracellular/intracellular
EDTA	Ethylenediamintetraacetic acid
FITC	Fluoresceinisothiocyanate
$FOXP3^+$	Forkhead box P3

FCS	Fetal calf serum
FEV1	Forced expiratory volume in one s
GM-CSF	Granulocyte-macrophage colony stimulation factor
Hyb	Hybrid
h/m	Human/mice
HPLC	High pressure liquid chromatography
HRP	Horse radish peroxidase
Ig	Immunoglobulin
IRF1	Interferon regulatory factor1
IL	Interleukin
IFN	Interferon
IL-7Rα	Interleukin-7 receptor α
IBD	Inflammatory bowel disease
JAK	Janus kinase
LC	Langerhans cells
NF-κB	Nuclear factor-kappa B
PBS	Phoshate buffered saline
PCR	Polymerase chain reaction
PFA	Paraformaldehyde
RNA	Ribonucleic acid
RT	Room temperature
mAb	Monoclonal antibody
MBP	Maltose binding protein
Muc2	Mucin gene
mTSLP	Murine thymic stromal lymphopoetin
MVF	measles virus fusion protein
NS	Netherton syndrome
Nod	nucleotide-binding oligomerization domain containing protein
NK	Natural killer cells
NS	Netherton's syndrome
OX40L	OX40 ligand (CD134)
PE	Phycoerythrin

PAR-2	Protease-activated receptor 2
PSMA	Prostate-specific membrane antigen
ROS	Reactive oxygen species
RXR	Retinoid X receptor
UC	Ulcerative colitis
SNP	Single nucleotide polymorphism
SPINK5	Serine peptidase inhibitor Kazal-type 5
SPC	Surfactant protein C
STAT	Signal transducers and activators of transcription
SV40	Simian virus 40
Th2	T helper 2 cells
TGF	Transforming growth factor
TARC	Thymus and activation-regulated chemokine
TLR	Toll-like receptor
TMB	Tetramethylbenzidine
TNF-α	Tumor necrosis factor alpha
Treg	Regulatory T cells
UC	Ulcerative colitis
γ_c	Common γ receptor chain

Units

s	Second
min	Minute
h	Hour(s)
pg	Picogram
µg	Microgram
mg	Milligram
g	Gram
µl	Microlitre
ml	Millilitre
mM	Millimol per Litre
M	Mol per Litre
°C	degree Celsius
%	Percent
|x|g	Centrifugal force unit
Bp	Base pair
U	Unit (µmol/min)
Da	Dalton
A	Ampere
V	Volt

Summary

In recent years, **T**hymic **s**tromal **l**ympho**p**oietin (TSLP) has emerged as a master switch for actuating cellular inflammation and local remodeling in asthmatic airways. Originally discovered as a growth and proliferation factor of the B cells, thymic stromal lymphopoietin (TSLP) is now implicated in immune system related effects on several cells including B cells, basophils, $CD4^+$, $CD8^+$ and natural killer T cells, dendritic cells, eosinophils, epithelial cells and mast cells. The structural and immune cells express TSLP at the site of allergen entry in the airways. TSLP regulates the T helper 2 (Th2) cells humoral immunity by upregulation of a ligand, OX40L, on the surface of the dendritic cells (DCs), which activates the naive Th0 cells to active Th2 lymphocytes. The role of TSLP in the promotion of Th2 responses has been panoptically studied in the context of several allergic disorders. The experimental work in this thesis is focused on the creation of tools to study/manipulate the signaling of murine TSLP/TSLPR system and thus help us in a better understanding of targeting the TSLP induced signal transduction during allergic inflammation. The studies involved development of a TSLPR expressing luciferase gene based murine cellular model, as well as an inducible TSLP secreting epithelial-dendritic cell based model as readouts. The process involved production, purification and characterization of murine TSLP (mTSLP) as a fusion protein with maltose binding protein (MBP) i.e. mTSLP-MBP and mutant I37E mTSLP-MBP. Exo-mTSLPR domain soluble protein was also produced as a competitive inhibitor and it was then used to generate an anti murine TSLPR antibody for the detection of mTSLPR receptors on the cells. These tools have been successfully tested on the readout systems as mentioned above. The I37E mTSLP-MBP mutant showed partially competitive effects in the cellular readouts. The mTSLPR showed an effective blocking of mTSLP induced signaling. The anti mouse TSLPR antibody could bind to the TSLPR receptors on the cells but it was found to be non inhibitory in nature.

By generating the above mentioned inhibitory proteins, novel strategies have been developed to analyze and specifically inhibit TSLP induced immunological activation. The results from these cellular model based studies are in agreement with those obtained from studies involving similar molecules designed for studying human TSLP-TSLPR system in our group in the past. These results cumulatively prove that a successful blockade of the human/murine TSLP-TSLPR system is possible. These results offer an insight into multifaceted roles of TSLP and could potentially pave the way for therapeutic manipulations of allergic disorders.

Zusammenfassung

In den letzten Jahren trat TSLP (Thymic Stromal Lymphopoietin) als ein Hauptakteur in der Auslösung von zellulären Entzündungsreaktionen sowie in asthmatisch bedingten Umbauprozessen in den Atemwegen hervor. TSLP wurde ursprünglich als Wachstums- und Proliferationsfaktor von B-Zellen identifiziert. Heute weiß man, dass TSLP in Effekte des Immunsystems auf verschiedene Zellen wie B-Zellen, Basophile, $CD4^+$-, $CD8^+$- und Natürliche Killer-T-Zellen, Dendritische Zellen, Eosinophile, Epithelzellen sowie Mastzellen involviert ist. In den Atemwegen wird TSLP in Struktur- und Immunzellen am Ort des Allergeneintritts exprimiert. Dabei reguliert TSLP die humorale Immunantwort von Typ2-Helfer-Zellen (Th2-Zellen) über die Aktivierung des OX40-Liganden auf der Oberfläche von Dendritischen Zellen, wodurch wiederum naive T-Helferzellen zu aktiven Th2-Lymphozyten aktiviert werden. Im Kontext verschiedener allergischer Erkrankungen wurde die Rolle von TSLP in der Promotion der Th2-Antwort umfassend studiert. Der experimentelle Teil der vorliegenden Arbeit war fokussiert auf die Entwicklung von Werkzeugen, um die Signalprozesse des murinen TSLP/TSLP-Rezeptor-Systems zu studieren bzw. manipulieren, mit dem Ziel, die TSLP-induzierten Signal-Transduktionsprozesse während der allergischen Reaktion besser zu verstehen und zu beeinflussen. Die Studien beinhalteten die Entwicklung von „Readout"-Systemen, einerseits eines Luziferase-Reportergen-Assays gekoppelt an die TSLPR-Expression in einem murinen Zellmodell sowie andererseits ein induzierbares dendritisches Epithelzellmodellsystem zur Sekretion von TSLP. Die Arbeit beinhaltete die Produktion, Aufreinigung und Charakterisierung von murinem TSLP als Fusionsprotein mit Maltose-bindendem Protein (MBP), dem mTSLP-MBP und der Mutante I37E mTSLP-MBP. Die Extrazelluläre Domäne des TSLP-Rezeptors (exo-mTSLPR-Domäne) wurde zudem als kompetitiver Inhibitor produziert und zur Generierung von monoklonalen anti-murin-TSLPR-Antikörpern zur Detektion des zellulären TSLPRs genutzt. Diese Werkzeuge wurden erfolgreich mit den vorgenannten „Readout"-Systemen getestet. Der mTSLPR zeigte eine effiziente Blockierung der durch mTSLP induzierten Signalübertragung. Der generierte monoklonale Maus-mTSLPR-Antikörper wies eine positive Bindung an den zellulären TSLPR auf und zeigte keine inhibitorischen Effekte auf die Signalübertragung.Mit der Generierung der inhibitorisch wirksamen TSLP-Proteine konnten neue Strategien zur Analyse sowie spezifischen Inhibierung der TSLP-induzierten Immunreaktion entwickelt werden. Die Ergebnisse aus den Zellmodell-basierenden Studien der vorliegenden Arbeit stimmen mit vergangenen Studien der Arbeitsgruppe überein, in welchen ähnliche Moleküle konstruiert wurden, um das humane TSLP/TSLPR-System zu untersuchen. Insgesamt beweisen diese Ergebnisse, dass eine erfolgreiche Blockade des humanen/murinen TSLP/TSLPR-Systems möglich ist. Zudem gibt die vorliegende Arbeit einen Einblick in die vielseitige Rolle von TSLP und könnte möglicherweise den Weg in die therapeutische Manipulierung im Rahmen von allergischen Erkrankungen ebnen.

1. Introduction

1.1. Overview

Thymic stromal lymphopoetin (TSLP) has emerged as a central player in the pathogenesis of allergic Asthma (West et al., 2012). Produced by various allergen-challenged cell types, amongst them epithelial cells, fibroblasts and mast cells, it instructs dendritic cells to favor a T helper 2 (Th2) type immunological response which is crucial in the development of Asthma (Al Shami, et al., 2005). The essential functions of TSLP in this context are as yet only vaguely understood and need to be studied thoroughly in order to unveil their pharmacological potential.

Murine TSLP (mTSLP) was first recognized as a bioactive component in the conditioned medium supernatants from a mouse thymic stromal cell line cell Z210R.1 (Friend et al., 1994). This supernatant was observed to support growth and proliferation of a pre-B cell line. mTSLP behaved similar to IL-7 and could stimulate thymocytes and promote B-cell lymphopoiesis and was initially studied as a B-cell growth factor (Levin et al., 1999). Subsequently, expression and cloning lead to the revelation that the mTSLP is a member of the hematopoietic cytokine family (Sims et al., 2000). mTSLP consists of 140 amino acids (121 correspond to the mature murine TSLP and 19 correspond to signal peptides) (Sims et al., 2000) and is a 15 kDa protein coded by gene located on chromosome 18 (search data from NCBI Gene). mTSLP consists of seven cysteine residues and three sites for N-linked glycosylation.

A human homolog, human TSLP (hTSLP), was later identified using database search methods (Quentmeier et al., 2001, Reche et al., 2001). Sequence prediction revealed a similar four-helix structured cytokine with two N-glycosylation sites and six cysteine residues. hTSLP gene is located on chromosome 5q22, interestingly close to a gene cluster encoding Th2-related cytokines such as Inerleukin-4, 5, 9 and 13 (IL-4, IL-5, IL-9, and IL-13) (Loots et al., 2000). hTSLP and mTSLP exhibit poor homology with only 43% amino acid identity (Sims et al., 2000). TSLP is expressed mainly in the lungs, skin, and gut (Reche et al., 2001). The human TSLP sequence is 740 bp long, and encodes a protein of 159 amino acids. The mature human TSLP protein and the signal sequence are respectively 131 and 28 amino acid long (Sims et al., 2000). Human TSLP contains two sites for N-linked glycosylation, which are not conserved between mouse and humans. While human TSLP molecular weight (MW) is predicted at 14.9 kDa, practically, it resolves at 23 kDa, suggesting that it is indeed glycosylated. The 6 cysteines present in the murine TSLP are conserved in the human TSLP sequence. Disulfide bonds between cysteine pairs are also conserved between man and mouse (Quentmeier, 2001, Reche et al., 2001) As a reason, human and murine TSLP share a significant degree of functional homology (Reche et al., 2001, Sims et al., 2000).

TSLP receptor (TSLPR) is a heterodimeric receptor complex comprising of TSLPR and the IL-7α (Park et al., 2000, Pandey et al., 2000). The TSLPR chain is a member of the hematopoietin receptor

family and binds to TSLP at low affinity. A combination of TSLPR and IL-7α chain results not only in high-affinity binding but also in STAT1, STAT3 and STAT5 activation (Pandey et al., 2000, Park et al., 2000, Reche et al., 2001, Wohlmann et al., 2010) (see Fig. 1.1.). TSLPR alias Cytokine receptor like factor-2 (CRLF2) is expressed in heart, skeletal muscle, kidney and liver, as well as in asthma-inducing dendritic cells (Reche et al., 2001, Liu et al., 2007).

Asthma bronchiale is a globally prevalent major health concern (Vercelli, 2008, Concepts, 2006). It is a chronic inflammatory disorder characterized by variable and recurring symptoms like airway obstruction, hyper-responsiveness, goblet cell hyperplasia and airway remodeling (Umetsu et al., 2006, Kim et al., 2010). Asthma is associated with genetic susceptibility in combination with environmental factors and has been linked to a dysregulated Th2 immune response (Humbert et al., 1999, Cookson, 2000). A dysregulated Th2 polarization and expansion has been implicated to play a critical role in the development of airway hyperresponsiveness during asthma (Kim et. al., 2013) and various mechanisms which are responsible for it are being investigated upon. During atopic Asthma, TSLP is produced by epithelial and smooth muscle cells and is involved in the induction of an inflammatory Th2 response. (Soumelis et al., 2002, Watanabe et al., 2004). Exposure to allergens (Agrawal et al., 2012, Leyva-Castillo et al., 2013) or viruses (Fontenot et al., 2009) triggers mucosal epithelial cells or skin cells to produce TSLP (Shikotra et al., 2011). TSLP initiates the innate phase of allergic immune responses by activating the immature dendritic cells (DCs) to produce chemokines IL-8 and eotaxin-2, as well Th2-attracting chemokines. It also co-stimulates mast cells to produce IL-5 and IL-13 as well as Granulocyte macrophage colony-stimulating factor (GM-CSF) and IL-6 (Ito et al., 2005, Gilliet et al., 2003, Ito et al., 2012). TSLP-activated DCs mature and migrate into the draining lymph nodes to initiate the adaptive phase of allergic immune response. TSLP-activated DCs express the OX40 ligand (OX40L), which triggers the differentiation of allergen-specific naive T cells into inflammatory Th2 cells (Chen et al., 1999, Miura et al., 2005, Siddiqui et al., 2010, Kaur et al., 2012). The cytokines produced by the inflammatory Th2 cells (IL-4, IL-5, IL-13, and TNF-α) initiate allergic inflammation by triggering IgE and mucus production as well as eosinophilia (Reche et al., 2001, Soumelis et al., 2002, Liu et al., 2007). Notably, it has been shown that the local blockade of TSLP receptor alleviated allergic disease by regulating the airway dendritic cells (Shi et al., 2008). Nguyen et al. have shown that activated pulmonary regulatory T cells (Treg) express the TSLP receptor and respond to TSLP stimulation by activation of STAT5 (Nguyen et al, 2010). TSLP inhibits Treg suppressive activity by impairing IL-10 production. They demonstrated that in human allergic asthmatic subjects, pulmonary Treg exhibited a significant decrease in suppressive activity and IL-10 production compared to healthy control and non-allergic asthmatic counterparts. These functional aberrations were attributed to the elevated TSLP expression in bronchoaveolar lavage (BAL) fluid of allergic asthmatic subjects. From these findings it can be concluded that TSLP has a possible role in the regulation of suppressive activities of Treg. Strong evidence has been provided for the protective functions of Tregs and tolerogenic dendritic cell (DC)

subsets during allergic airway inflammation. Inhibition of Treg function by TSLP may provide a novel pathologic mechanism for dampening tolerogenic immune responses in inflamed asthmatic airways.TSLP signalling relies on the activation of signal transducer and activator of transcription (STAT) proteins. It has been shown that the TSLPR utilizes both STAT5 and STAT3 to regulate signals for the expression of target genes (Isaksen et al., 2002, Reche et al., 2001, Pandey et al., 2000). It has also been found that TSLP activates STAT1 in murine pro B cells (Wohlmann et al., 2010). Both STAT3 and STAT5 have been shown to be the regulators of IL-17 expression and Th17 cell development (Yang et al., 2011). Since TSLP is involved in the pathophysiology of inflammatory diseases and is related to regulatory T cells (Treg) via STAT signalling, it appears an interesting option to block STAT function to interfere with TSLP activity.

1.2. Murine Thymic Stromal Lymphopoietin (mTSLP): mode of action

mTSLP is an mIL-7-like cytokine and belongs to the IL-2 cytokine family. mTSLP was characterized as a 121-amino acid containing 4-helix bundle (Verstraete et al., 2014). This cytokine was originally discovered in murine thymic stromal cell line supernatants, which supported B-cell development in the absence of IL-7 (Sims et al., 2000). Polymorphisms of the TSLP gene have been associated with allergic asthma in humans (Sims et al., 2000). mTSLP and the other members of the IL-2 family member signal via the JAK-STAT pathway involving STAT1, 3 and 5 (Wohlmann et al., 2010, Isaksen et al., 2002) as shown in the Fig.1.1 below.

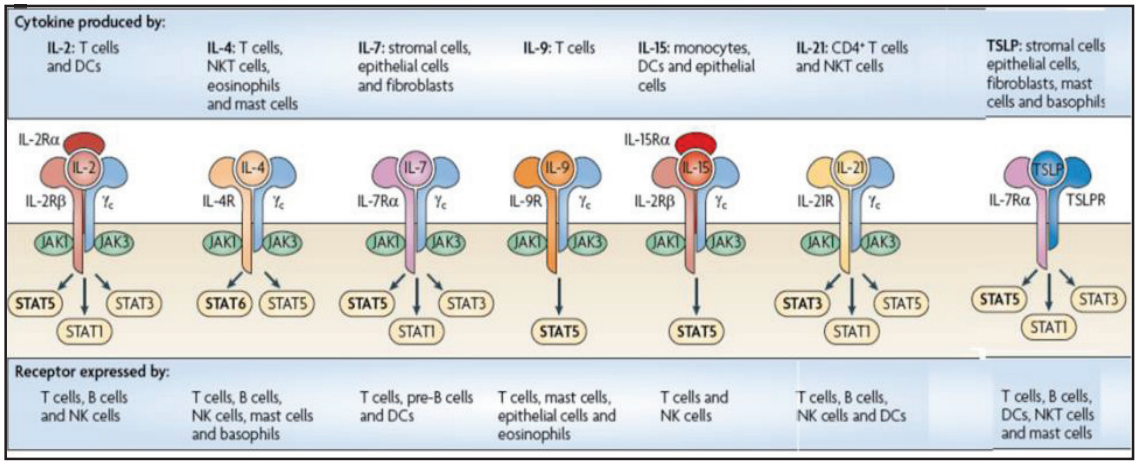

Fig. 1.1. Receptors for $\gamma_c$family cytokines and TSLP. The figure shows the receptors for Interleukin-2 (IL-2), IL-4, IL-7, IL-9, IL-15, IL-21 and thymic stromal lymphopoietin (TSLP). Only IL-2 and IL-15 have three receptor chains. The receptors for these receptors share the γ_c-chain. The IL-7 and TSLP share the IL-7Rα chain, thus only TSLP does not signal via γ_c. The receptor for each γ_c family cytokine activates the Janus kinase 1 (JAK1) and JAK3 and further STATs. The receptor for TSLP has been reported to activate STAT 1, 3 and 5. (Modified from: Rochman et al., 2009)

The mechanism of TSLP action involves the activation of the dendritic cells upon challenge with allergens on the mucosal surface leading to the secretion of TSLP from the basal epithelium (Lu et al., 2009, Ziegler et al., 2006), see Fig. 1.2.

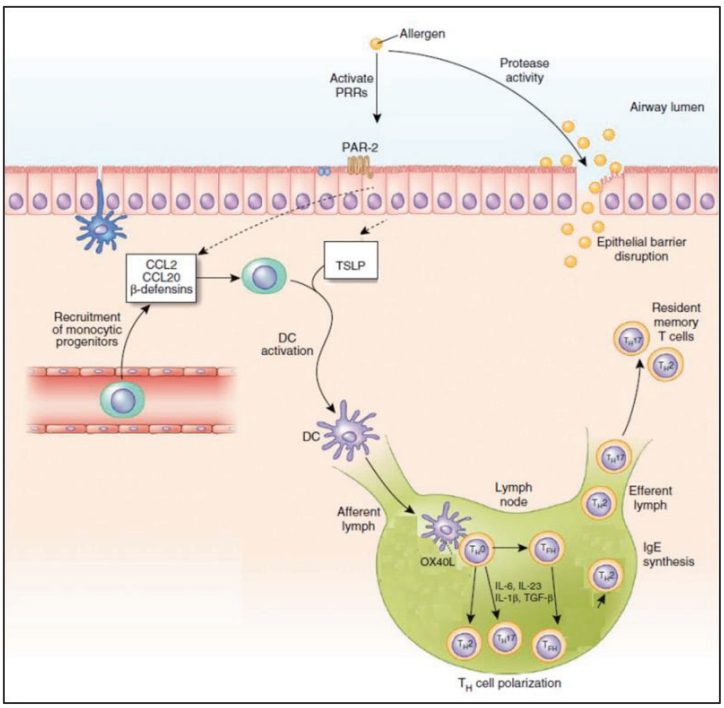

Fig.1.2. A cellular scheme showing mechanism of TSLP action. The pollens/allergens activate the secretion of TSLP from the basal epithelial layer. TSLP activates the dendritic cell maturation i.e. production of OX40L on the cell surface. The receptors for these ligands are present on the naive T cells. The dendritic cells migrate to the lymph nodes and activate the naive T cells to transform into Th2 cytokine producing cells.This occurs via OX40L-OX40R interactions between dendritic cells and T cells respectively. The mature T cells reach the site of inflammation and secrete Th2 cytokine. Modified from: (Lambrecht et al., 2012)

The dendritic cells which have been activated differ from the naive ones in the expression of surface OX40L. The OX40L has critical role in the activation of the naive T cells in the lymph nodes (Chen et al., 1999). The dendritic cells migrate to the lymph node and activate the naive T cell via OX40L-receptor interaction thus transformin the naive T cells into Th2 cytokine secreting cells (Ito et al., 2005).

1.3. Effects of TSLP on various immune cells

Several cells have been found to respond to TSLP because of the presence of TSLP receptor on them or because of an indirect response created by chemokines/receptor expression leading to activation or suppression. The table 1.1 below summarizes various cellular responses and salient effects on the functions of the immune cells activated by autocrine or epithelial TSLP secretion.

Table 1.1. Effect of TSLP on various immune cells.

Cells	Effects
Myeloid dendritic cells	$CD4^+$ T-cell homeostasis in co-culture (T-cell proliferation but no differentiation) (Watanabe et al., 2005). TSLP-stimulated DCs primed $CD4^+$ T cells in an antigen-specific manner which lead to the differentiation of T cells to Th2 cells (produced IL-4, IL-5, IL-13, and tumor necrosis factor TNF-α, without IL-10 production) (Soumelis et al., 2002). Leads to an enhanced levels of MHC class II, CD40, CD86, CD54, CD80, CD83, IL-8, eotaxin-2, Thymus and activation-regulated chemokine, C-C motif chemokine 17 (TARC) /CCL17), Macrophage derived chemokine (MDC/CCL22), Chemokine (C-C motif) ligand (I-309/CCL1) (Li et al., 2010). In the absence of IL-12, TSLP induced OX40 ligand (CD134) (Ito et al., 2005).
$CD4^+$ and $CD8^+$ T cells	Increased proliferation of T and B cells in γc /TSLPR double deficient mice (Al-Shami et al., 2004). Proliferation and Th2 differentiation of naive $CD4^+$ T cells by IL-4 gene transcription and feedback loop (Omori et al., 2007, Astrakhan et al., 2007, Rochman et al., 2007). Upregulation of TSLPR on Th 17, $CD4^+$ T (Th2) cells and human $CD8^+$ T cells (Tanaka et al., 2010, Akamatsu et al., 2008, Shane et al., 2014). STAT5 dependent upregulation of survival protein B-cell lymphoma 2 (Bcl-2) in both $CD4^+$ and $CD8^+$ T cells (Kitajima et al., 2011, Y. Rochman et al., 2010). Increased proliferation of $CD8^+$ cells (Akamatsu et al., 2008).
B cells	B-cell lymphopoiesis (Friend et al., 1994, Levin et al., 1999), pre-B cells proliferate in response to TSLP (Vosshenrich et al., 2003). Aberrant TSLP signaling leads to significant impact on B cells, as defined by association of TSLPR mutations with a subtype of B cell leukemia (Chapiro et al., 2010, Reuther, 2010, Tasian & Loh, 2011). Increased systemic TSLP leads to aberrant B-cell development and function, leading to autoimmune hemolytic anemia (Astrakhan et al., 2007, Iseki et al., 2012)
Mast cells	Increased IL-5,6,8,10,13, GM-CSF, Chemokine ligand 1 (CCL1) and decreased TGF-β levels (Allakhverdi et al., 2007, Gilfillan et al, 2006).IL-1 and TSLP secretion from epithelial cells activated Th2 cytokine production from mast cells (Nagarkar et al., 2011)

Natural killer T cells (NKT cells)	Enhanced cytokine production from NKTcells e.g. increased IL-4 and 13 (C. C. Hui et al., 2011, Allakhverdi et al., 2007, Nagata et al., 2007, Wong et al., 2009, Wu et al., 2010). TSLP induced IL-10 production and NK cell expansion in BALB/c x C57BL/6 mouse model (Lin et al., 2008).
Monocytes/ macrophages	Increased TARC (Ying et al., 2012) and CD80 surface expression (Hirano et al., 2011).
T regulatory cells	TSLP generated tolerogenic DCs lead to the differentiation of regulatory T cells (Tregs) (Besin et al., 2008, Iliev et al., 2009, Watanabe et al., 2005) while in certain diseases, it hindered the production and maintenance of forkhead box P3 ($FOXP3^+$), Tregs *in vivo* (Duan et al., 2010, Lei et al., 2011, Nguyen et al., 2010).
$CD34^+$ progenitor cells	Increased eosinophilpoiesis and basophilopoiesis (Siracusa et al., 2013). Increased cytokine and chemokines levels of IL-5, IL-13, GM-CSF, and chemokines (CCL22, CCL17, CXCL8, CCL1) (Allakhverdi et al., 2009), Increased IL-5Rα expression (C. C. Hui et al., 2011).
Basophils	Enhanced CD69, CD62L, CD11b, CD123, IL-33R, IL-18R surface expression (Siracusa et al., 2011, Tsai et al., 2012). Enhanced development of an IL-3-independent subset of basophils which plays a role in promoting Th2-type responses (Siracusa et al., 2011, Sokol et al., 2009). Leads to haemotopoesis (Siracusa, et al., 2013). Increased TNF α (Hui, et al., 2014).
Eosinophils	Increased survival and adhesion, increased surface expression of CD18, and increased secretion of ICAM-1, CXCL1, CCL2, CXCL8, IL-6 and decreased L-selectin (Wong et al., 2010). Induction of eosinophil extracellular traps and extrusions of mitochondrial DNA toxic granule molecules released in response to infections (Morshed et al., 2012).
Airway smooth muscle cells	Increased secretion of IL-6, CXCL8, CCL11 (Smelter et al., 2010) and increased migration, actin and cellular polarization (Redhu et al., 2013).

1.4. Molecular structure of murine TSLP/TSLPR complex

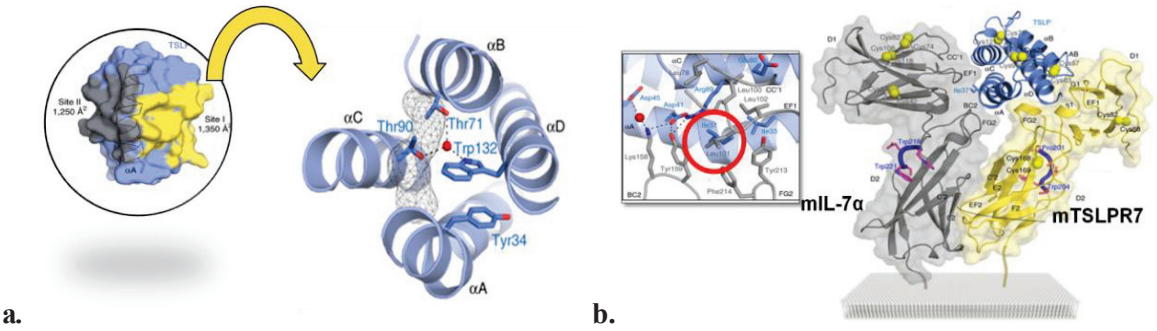

a. b.

Fig.1.3. a. The structure of mTSLP and b. mTSLP-mTSLPR interactions. The murine TSLP comprises of 4 helices α-A, α-B; α-C and α-D. The cytokine interacts with the mTSLP receptor at various hot spots. An important hot spot identified on the interactive interface is mediated by Ile37 (see Fig 1.3 b. encircles red) (modified from Verstraete et al., 2014)

The X ray crystallographic structure of murine TSLP and TSLPR interactions was revealed by Verstraete et al., 2014. They used HEK293S *MGAT1*−/− cells to coexpress mouse TSLP (mTSLP)-TSLPR (mTSLPR) binary complexes with homogeneous N-linked $GlcNAc_2Man_5$ glycan trees. (Verstraete et al., 2014). They produced the mouse IL-7Rα (mIL-7Rα) in *Escherichia coli* coupled to refolding *in vitro* and then post purification they assembled the mouse TSLP–TSLPR–IL-7Rα ternary complex by mixing purified TSLP–TSLPR complex with a molar excess of purified recombinant IL-7Rα. The accessible N-linked glycans were removed by endoglycosidase H (EndoH) treatment. The ternary TSLP-TSLPR complex showed binding similar to other members of the IL-2 family. The cytokine interacts with the two receptors chains with the cytokine-binding epitopes available at the D1-D2 junctions of each receptor (see Fig.1.3.b). TSLP binds between the TSLPR and IL-7Rα on surfaces, in a T shaped assembly. TSLP exhibits a short-chain four-helix bundle fold resembling IL-7, despite the low sequence homology between the two cytokines, and has an extended helix A at the N terminus and markedly shorter B and C helices (Fig. 1.3 a). The core residues and cysteines involved in the disulfide bonds (Cys25-Cys98, Cys57-Cys63 and Cys78-Cys121) are strongly conserved and this suggests that the observed fold can be generalized to all mammalian TSLPs. An ordered water molecule is located in the in the TSLP core and is coordinated by a conserved triad of residues (Thr71, Thr90 and Trp132). Unlike other IL-2 family cytokines which possess conformational plasticity, TSLP core remains largely invariable.TSLPR bears a structural and evolutionary resemblance to the common cytokine receptor γ chain (γc) and IL-13Rα1. TSLPR carries a conserved PSxW(S/T) sequence cassette instead of the WSxWS sequence fingerprint in other type I cytokine receptors. TSLPR also showed a disulfide-bridge network, with a *cis* peptide bond between Cys168 and Cys169. A single well-conserved N-linked glycosylation site in mammalian TSLPR, *N*-acetylglucosamine (GlcNAc) glycan moiety at Asn53 was located in TSLPR crystal form. This GlcNAc residue is involved in the interaction of the with residues located in strands D and E leading to the stabilization of the regional structure.The kinked helix A in TSLP contributes

to both the TSLP–TSLPR interface (site I) and the TSLP–IL-7Rα interface (site II). The TSLP–TSLPR interface was characterized by the presence of several polar interactions which indicate a highly specific interaction. This is perhaps the reason for the poor conservation of site I interacting residues in mouse and human TSLP and TSLPR orthologs and the lack of species cross-reactivity among TSLP orthologs. An important hot spot identified on the interactive interface is mediated by Ile37 (see Fig. 1.3 b. encircled red) protruding from the π-helical turn on helix A of TSLP into a conserved hydrophobic pocket in the D1-D2 junction of IL-7Rα and is defined by the residues Leu101, Ile102, Tyr159, Tyr213 and Phe214.

1.5. Role of TSLP in diseases

Since several different types of cells are associated with various responses to TSLP, it can cause Th2 type inflammation through numerous pathways. The various studies in mouse models and humans have lead to the implication of TSLP in several disorders (see Fig.1.4) including allergic inflammation, infection, cancer and autoimmunity. The various disorders associated with TSLP and its role in these diseases has been described below.

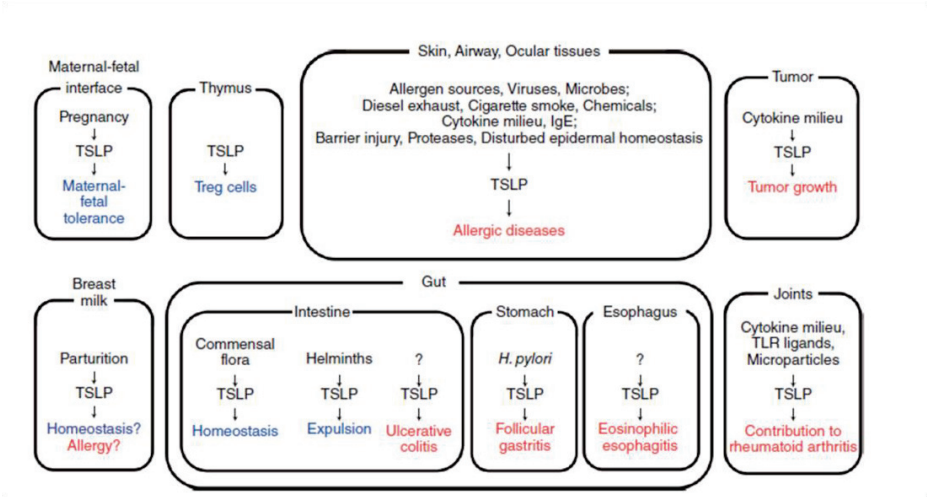

Fig. 1.4. Diseases in which TSLP has a direct or suspected role. TSLP is involved in several diseases and in some its role is being probed. (Takai, 2012)

Atopic Dermatitis: Atopic dermatitis (AD) is a chronic inflammatory skin disease affecting approximately 20% infants and young children in the USA (Boguniewicz et al., 2011). TSLP was found to be highly expressed in acute and chronic lesional AD patients while its level were undetectable in non lesional AD patients (Soumelis et al., 2002). The migration and activation of the Langerhans cell (LC) was observed in human AD lesions and TSLP was implicated for the increased proliferation and induced migratory behavior in LC cultures. These LCs could prime co-cultured naive $CD4^+$ T cells and transform them to inflammatory Th2 cells (Ebner et al., 2007). The over expression

of TSLP in mice skin induced the phenotypic features of AD (Yoo et al., 2005). Single nucleotide polymorphisms (SNPs) in the TSLP gene in AD suggested an evident linkage between them. It was reported that the subjects with AD were more sensitive to Th2-polarized diseases and had a background patient history of asthma, food allergy, or both (Gao et al., 2010). TSLP was also over expressed in the skin of patients suffering from Netherton syndrome (NS), which is characterized by lesions and allergic symptoms resulting from mutations in the serine peptidase inhibitor Kazal-type 5 (SPINK5) gene, that encodes the serine protease inhibitor lymphoepithelial Kazal type-related inhibitor (LEKTI) (Briot et al., 2009). In a model of NS, SPINK5 knockout (SPINK5 −/−) mouse, the absence of LEKTI lead to uncontrolled activity of the serine protease kallikrein 5, resulting in activation of activated protease-activated receptor 2 (PAR-2) and stimulation of nuclear factor κB (NF-κB)-mediated TSLP overexpression (Kouzaki, et al., 2009). TSLP expression was reduced though inflammation still occurred in the SPINK5/PAR-2 double-knockout mice (Briot et al., 2010). It has been reported that during steady state in the skin, TSLP expression is negatively regulated by retinoid X receptors.(RXRs) which is supported by the fact that keratinocyte-specific extirpation of the RXR isotypes (RXRα and RXRβ) lead to an upregulation of TSLP and therefore an AD-like skin inflammation (M. Li et al., 2006). The RXRs heterodimerize with several nuclear receptors including the vitamin D receptors. The administration of vitamin D/analogs lead to an upregulation of TSLP leading to dermatitis (M. Li et al., 2006, Mei Li et al., 2009). The tendency of the patients suffering from AD of developing allergic rhinitis (AR) and asthma later in life is known as atopic march and TSLP has been implicated in this event (Bieber, 2010, Tang, et al, 2012). TSLP is thought to be a key factor causing the progression from AD to AR and then further to asthma. This has been shown by various AD mouse models that induced TSLP expression in keratinocytes resulted in subsequent allergic airway inflammation following intranasal challenges (Demehri et al., 2009, Jiang et al., 2012, Leyva-Castillo et al., 2013, Zhang et al., 2009). It has been also observed that even in absence of systemic TSLP, the intradermal administration of TSLP initiates AD to asthma transition (Han et al., 2012). It was also reported that IL-13 in conjunction with TSLP lead to skin fibrosis via stimulation of fibrocyte collagen production.in atopic dermatitis (Oh et al., 2011).

Asthma, Chronic Obstructive Pulmonary Disease (COPD) and other lung related diseases: The initial findings showing elevated TSLP in AD and the initiation of inflammatory Th2 responses by TSLP suggested a potential hypothetical role for TSLP also in allergic airway disease (Soumelis et al., 2002). This hypothesis was strongly supported with the reports of presence of TSLP mRNA in human lung fibroblasts, bronchial epithelial and smooth muscle cells (Soumelis et al., 2002) and the aberrant expression of TSLP in several respiratory disorder (Kamekura et al., 2009, Kimura et al., 2011, Semlali et al., 2010, Shikotra et al., 2011, Xu et al., 2010, Ying et al., 2012). Ying et al used *in situ* hybridization and immuno-histochemistry to examine the expression of TSLP mRNA, Th2 and Th1-attracting chemokines and their receptors in the bronchial biopsies of asthmatic patients as compared to the healthy individuals. The results

from this study indicated a significant increase in the number of $CD4^+$ chemokine receptor ($CCR4^+$) T cells within the submucosa, TSLP mRNA expression, enhanced levels of Th2-attracting chemokines CCL17, CCL22 and Th1-attracting chemokine C-X-C motif chemokine 10 (CXCL10), in asthmatic subjects as compared with the controls. Similarily, TSLP mRNA expression in the epithelial macrophages, as well as submucosal endothelial cells and neutrophils was also significantly higher in the asthmatics as compared to the healthy controls. The expiratory volume in one second (FEV1) showed an inverse correlation with the expression of TSLP, thereby proving that TSLP is responsible for the pathophysiology of asthma and deteoration in lung volume functions. The lung epithelium and submucosal patient samples from other diseases such as chronic obstructive pulmonary disease (COPD) patients also contained a higher number of TSLP mRNA positive cells and TSLP levels in the bronchoalveolar lavage (BAL) samples as compared to healthy individuals (Semlali et al., 2010, Shikotra et al., 2011, Ying et al., 2012). The TSLP expression levels can vary from one patient to another but a direct correlation between the levels of Th2 cytokine and the chemokine expression and an inverse relation with the lung function has been established (Shikotra et al., 2011, Ying et al., 2008). The biopsies in the patients suffering from atopic rhinitis have shown enhanced TSLP levels in the nasal epithelium which has been has also linked with the infiltration of the epithelial tissue with the eosinophils and production of Th2 cytokine (Kamekura et al., 2009, Kimura et al., 2011, Mou et al., 2009 , Xu et al., 2010). The genetic studies have also shown that single nucleotide polymorphisms at the TSLP genomic locus in several ethnic populations were linked with atopy and vulnerability to asthma (Bunyavanich et al., 2011, 2015, Harada et al., 2009, 2011, Hunninghake et al., 2010, Torgerson et al., 2011). For example, Harada et al. showed in their studies that such a SNP present at TSLP genomic locus leads to a new binding site for activator protein 1 (AP-1) transcription factor-binding and possibly enhanced transcription of TSLP. There are other genes that may also be linked to TSLP activity in asthma. It has been observed that epistasis between SPINK5 and TSLP may contribute to childhood asthma. The study by Myers et al. has a clinical relevance that the therapeutic effects of anti-TSLP therapy in asthmatic patients might be dependent on SPINK5 genotype due to epistasis between SPINK5 and TSLP, which contributes to childhood asthma (Myers et al., 2014). The role of TSLP in disease is also established in several mouse models. The surfactant protein C (SPC)-TSLP mouse model has also supported the fact that TSLP is involved in asthma. In such a mice, constitutive TSLP expression occurs in the lung epithelium under control of the SPC promoter (Zhou et al., 2005, Headley et al., 2011) . These mice developed asthma-like symptoms such as eosinophil and Th2 $CD4^+$ T infiltrated lungs, remodeling of the airway pathway and airway hyper-responsiveness with enhanced levels of IL-4 and IL-13 (Headley et al., 2009, Zhou et al., 2008). The BAL fluid and the lungs of the OVA/alum allergic airway inflammation mice models contain significant level of TSLP post ovalbumin (OVA) challenge. The disease symptoms could be restricted by blocking the TSLP activity by the use of anti TSLP or anti TSLPR antibody (Al Shami et al., 2005, Shi et al., 2008, Borowski et al., 2013). Similar effects were noticed in an OVA-mouse model of allergic rhinitis where blocking TSLP activity lead to repressed asthma symptoms (Miyata et al., 2008). Several studies have shown that the TSLP related inflammation is mediated by

dendritic cells which prime the naive Th2 cells to Th2 cytokine producing cells. This is in orchesrated by expression of a costimulatory molecule OX40L on the surface of mature dendritic cells and secretion of chemokines such as CCL17 and CCL21. (Allakhverdi et al., 2007, Bleck et al., 2010, Soumelis et al., 2002, Li et al., 2010, Seshasayee et al., 2007; Shi et al., 2008; Zhang et al., 2011, Zhou et al., 2005). TSLP also promotes the development of thymic Tregs *in vitro* (Hanabuchi et al., 2012, R. Mazzucchelli et al., 2008 , 2012). In allergic airway disease, TSLP has been shown to inhibit IL-10 mediated Treg function and formation of inducible Tregs against exogenous antigens (Nguyen et al., 2010). A TSLP-dependent inhibition of pulmonary Treg activity was shown in the BAL fluid from asthmatics (Nguyen et al., 2010). An interfering role of TSLP in tolerance was observed in an OVA allergen model where it inhibited the generation of allergen-specific Tregs (Lei et al., 2011). In similar model, nucleotide-binding oligomerization domain-containing protein (Nod1 and Nod2) stimulation lead to curtailed tolerance towards OVA intranasal challenge correlating to TSLP- and OX40L levels (Duan et al., 2010). Also post Nod2 stimulation, the loss of TSLP signaling was found to be correlated with an enhanced antigen-specific $FOXP3^+$ T cells (Duan et al., 2010). Several different kind of allergic stimuli like IL-4, IL-13, TNF-α, IL-1, bacterial peptidoglycan, lipoteichoic acid, dsRNA, respiratory viruses, air pollutants and allergens induce NF-κB-dependent expression of TSLP (Lee et al., 2007), by lung-derived parenchymal cells and immune cells (Allakhverdi et al., 2007, Bleck et al., 2015, Lee et al., 2008, Kashyap et al., 2011, Kato et al., 2007, Kouzaki et al., 2009, Smelter et al., 2010, Soumelis et al., 2002; Zhang et al., 2007). A negative regulation of TSLP transcription by 9-cis-retinoic acid via retinoid X receptor (RXR) has been shown in the lung cells (Lee, et al., 2012).

Sepsis: High mortality and morbidity has been observed in sepsis related multiorgan system failure. In a cecal ligation and puncture (CLP) murine model for sepsis cohorts were treated with neutralizing anti TSLP antibodies or isotype controls pre- CLP to ascertain the changes in mortality and survival, bacterial loads, cytokine levels, and neutrophil inflammatory functions. This study lead to the observations that the TSLP levels were at their peak after 6 h and could be detected uptil 48 h post CLP. The mice which were pretreated with neutralizing TSLP showed decreased death rate and bacterial load post CLP. An enhanced level of tumor necrosis factor α and oxidative burst as well as increased interleukin 17 and increased neutrophil numbers were noticed in .the septic mice pretreated with the anti-TSLP antibody as compared to their counterparts treated with the isotype controls. This study leads to a speculation that TSLP numbs the neutrophil response resulting in increased bacterial load and mortality (Kuethe et al., 2014).

Intestinal Inflammation: TSLP has been found to be expressed in the gastrointestinal tract of the mouse and human. Its expression has been found to be affected by cytokines or microbial inducers (He et al., 2007, Humphreys et al., 2008, Tanaka et al., 2010, Taylor et al., 2009, Zaph et al., 2007, Zeuthen,et al., 2008). Knockout mouse models with epithelial-specific Dicer gene (involved in microRNA

biosynthesis) (Biton et al., 2011) or IκB kinase-β gene deletions (Zaph et al., 2007) affect the gut mucosa with low expression of TSLP mRNA. These mouse models exhibited enhanced vulnerability to *Trichuris muris* worm infections. TSLP expression was reduced in a mucin gene (Muc2) missense mutation mice and lead to an epithelial defect and spontaneous colitis (Eri et al., 2011). Polymorphisms in genes locus of TSLP and TSLPR have been found to be associated with the disorder eosinophilic esophagitis (EoE) (Rothenberg et al., 2010, Sherrill et al., 2010) . In disparity to the enhanced TSLP expression in EoE, decreased TSLP expression was observed seen in noninflamed colonic tissue the two differenct conditions of inflammatory bowel disease (IBD), Crohn's disease (CD) and ulcerative colitis (UC) (Noble et al., 2008, 2010, Iliev et al., 2009, Spadoni et al., 2012; (Rimoldi et al., 2005). However, in the inflamed UC tissues from patients an upregulation of TSLP as compared to the noninflamed tissue from UC patients or normal controls was observed (Noble et al., 2008, Tanaka et al., 2010).

Cancer: Recent studies have suggested a possible role of fibroblast secreted TSLP in the metastasis and growth of breast and pancreatic cancer tissues which also show Th2 infiltration and upregulation of Th2 cytokines (De Monte et al., 2011, Olkhanud et al., 2012, Bodegom et al., 2012, Pedroza-Gonzalez et al., 2011). The shRNA knockdown of TSLP in these cancer cells lead to clones which showed reduced growth or metastasis (Olkhanud et al., 2011). Tumor progression and metastasis was also diminished in TSLPR-deficient mice with an injected breast cancer cell line as compared to the wild-type mice (Olkhanud et al., 2011). TSLP linked enhancement of Th2 cytokines can promote an increased survival of cancer cells, macrophage (M2) differentiation, and fibrosis (Aspord et al., 2007), (Joyce et al., 2009, Balkwill et al., 2012, Mantovani et al., 2008, Wynn, 2004). TSLP can alter the immunoregulatory environment by influx of Treg cells by migration caused due to CCL22 production in human breast cancer cells (Gobert et al., 2009, Menetrier-Caux et al., 2009). It has been observed that TSLPR is overexpressed in 5-10% patients suffering from childhood B-cell progenitor acute lymphoblastic leukemia (ALL) and approximately 60% of ALL cases in children with Down's Syndrome (Ensor et al., 2011, Russell et al., 2009, Mullighan et al., 2009, Tasian & Loh, 2011, Roll et al., 2010) thus suggesting the role of TSLP-TSLPR system in these disorders.

Autoimmune Diseases: An inducible overexpression mice models of TSLP show that it can be associated with autoimmune diseases The inflammation driven cryoglobulinemic glomerulonephritis in these mice was associated with enhanced systemic polyclonal IgM and IgG production and deposition via a monocyte/macrophage dependent mechanism in the kidneys (Astrakhan et al., 2007, Taneda et al., 2001). Autoantibodies against red blood cells and autoimmune hemolytic anemia depending on $CD4^+$ T cell and IL-4 was observed (Iseki, et al., 2012). The TSLP signaling ablation in a mouse model of autoimmune gastritis increased the severity of the disease (Nishiura et al., 2012). TSLP was found to be active in Th1/Th17-associated autoimmune diseases such as rheumatoid arthritis (RA) and multiple sclerosis (MS). In RA mouse model, TSLPR-deficiency reduced the disease associated immunopathology

with reduced IL-17, IL-1β, and IL-6 cytokine levels but enhanced IFN-γ and IL-10 (Hartgring et al., 2011). The role of TSLP in diabetes is evident as introduction of TSLP-treated bone marrow-derived DCs into a nonobese diabetic mice abrogated the development of diabetes (Besin et al., 2008). TSLP is produced and secreted by first semester trophoblasts and and has been linked with immune tolerance in maternal-fetal tolerance during pregnancy (Li et al., 2009). The tissue from normal pregnancies demonstrated a Th2 prejudice and had elevated levels of TSLP expression than the samples from miscarriages (Wu et al., 2010, Guo et al., 2010, Pu et al., 2012).

1.6. Specific targeting of mTSLP/mTSLPR system

Recent advances in deciphering the cellular and molecular mechanisms of Asthma have led to the recognition of novel targets for therapeutic strategies. (Seshasayee et al., 2007) provided direct *in vivo* evidence that TSLP and OX40 have critical roles in allergic inflammation. The blockade of interactions between OX40 surface-expressed on Th2 cells and OX40 ligand (OX40L) presented by TSLP-activated DCs using an OX40L-specific monoclonal antibody has been shown to inhibit Th2 cell mediated immune responses in allergic inflammation models of nonhuman primate and mouse. These results in conjunction with various reports on the involvement of TSLP in allergic asthma (Shi et al., 2008, Borowski et al., 2013) serve as an encouragement to further explore the potential of TSLP signal transduction as a target for therapeutic approaches to ameliorate Asthma symptoms. In mouse, several strategies such as receptor targeted antibody approach have been used in the OVA/HDM model of asthma and transgenic TSLP receptor knockout models. The various studies have been summarized in table 1.2. It can be noticed that blocking TSLP activity leads to the reduction in levels of various allergic inflammatory markers and parameters suggesting tha TSLP is an important protein in the development of pathophysiology of these diseases.

Table 1.2. Specific targeting of mTSLP pathway in mice (adapted from Watson et al., 2014)

Intervention type	Effects
Lung-specific TSLP transgenic with and without OVA challenge	TSLP overexpression in lungs, increased AHR, BAL eosinophils, lymphocytes, neutrophils, serum IgE, expression of co-stimulatory molecules in bone marrow DC, airway remodeling, subepithelial fibrosis, goblet cell hyperplasia, T helper type 2 cell-attracting chemokine CCL17, fully differentiated Th2 effector cells. (Zhou et al., 2005)

TSLP receptor knock out monoclonal antibody (mAb) in OVA challenge mouse model	Lack of TSLPR expression decreased these factors: Airway inflammation, goblet cell hyperplasia, AHR, BAL T-cell activation, eosinophils, lymphocytes, and monocytes neutrophils, BAL IL-4, IL-5, IL-10, IL-13, IFN-γ, IL-12 and serum IgE. (Dolgachev et al., 2009)
TSLP receptor mAb in OVA challenge mouse model	TSLP receptor blocking antibody lead to reduction in the following parameters: BAL TSLP, IL-5, IL-4, IFN-γ levels, BAL total cell count, eosinophils, lymphocytes, macrophages, DC co-stimulatory marker expression and serum IgE, mucus hypersecretion, peribronchiolar and perivascular connective tissue eosinophils (Shami et al., 2005, Zhou et al., 2005, Shi et al., 2008).
OX40L mAb in OVA challenge mouse model	OX40L blocking antibody reduced BAL eosinophils and lymphocytes, BAL IL-4, IL-5, IL-14, serum IgE and IgG1 (Seshasayee et al., 2007)
TSLP mAb in house dust mice (HDM) mouse model	TSLP blocking antibody reduced airway hyperresponsiveness (AHR), lung tissue TSLP protein and mRNA, BAL total cell count, eosinophils, lymphocytes,macrophages, neutrophils, airway remodeling, goblet cell hyperplasia, mucus hypersecretion, peribronchial collagen deposition, BAL IL-4, IL-13, IFN-g, Transforming growth factor (TGF-β1) and $CD11c^+$ co-stimulatory marker expression (Chen et al., 2013)

2. Aims of the study

1. To generate an effective Ba/F3 cell based luciferase assay readout system for analyzing and characterization of murine TSLP (mTSLP) signaling activities.

2. To clone, express, purifiy and characterize the exo-domain of the TSLP receptor chain in the soluble form.

3. To characterize the ligand binding properties of exo-mTSLPR-domain and the biological activity of the exo-mTSLPR-domain in a Ba/F3 cell luciferase assay.

4. To produce and characterize the specific binding properties of a rat anti mouse-TSLPR antibody.

5. To clone, express, produce and characterize mTSLP

6. To identify, produce and characterize a potentially antagonistic TSLP variant.

7. To confirm these antagonistic properties in the context of artificial cell based models and primary TSLP responsive dendritic cells to prove that the interference in the TSLP based communication mimics cellular model context. This shall be the last step before testing the molecules in the mouse model.

3. Materials and Methods

3.1. Materials

3.1.1. Equipment and accessories

Table 3.1. List of used laboratory equipment

Equipment	Model	Manufacturer
Amaxa Nucleofactor	Amaxa Nucleofactor I	Lonza
Bacterial incubator	Incu-Line	VWR
Benchtop centrifuges	Rotina 380R Rotina 420R MF48 Centrifuge 5415R	HettichLab Awel Eppendorf
Cell incubator	Nuaire	IBS Integra Biosciences
Chromaotgraphy (Purification)	Äkta Purifier	Roche
Chemiluminescence detection system	G box Syngene	VWR
Clean bench	Nuaire	IBS Integra Biosciences
Dry block heater	QBD2	Grant
Electrophoretic chamber	Mini-PROTEAN Tetra system	Bio-Rad
Flow cytometer	Partec/BD Diva	Partec/BD
Incubator shaker	Ecotron	Infors HAT
Inverted microscope	AE21 Routine	Motic
Luminometer	Glo Max	Promega
Magnetic stirrer	MR3001	Heidloph
Mini centrifuge	Sprout™	Biozym Scientific
pH-meter	761 Calimatic	Knick
Platform shaker	Titramax 100	Heidolph
Precisions balance	MC1 Analytik AC120S	Sartorius
Spectral photometer	NanoDrop 2000c	Thermo Scientific
Plate reader	Sunrise	Tecan
Thermocyler	AB2720	Applied Biosystems
Vortex shaker	-	VWR
Water bath	Julabo 208	Julabo
Western blot system	Trans-Blot™ Cell	Bio-Rad

Table 3.2. List of used laboratory consumables

Equipment	Manufacturer
Cell culture plates (10cm)	Greiner
Combitips (1ml, 2.5ml, 5ml and 10ml)	Eppendorf
Nunc™ cell scrapers	Thermo Scientific
PCR plates ABgene® (96-Well)	Thermo Scientific
PCR tubes (0.2 ml)	Biozym
Plates (6-, 12-, 24- and 96-well)	Greiner
Plastic pipettes (2 ml, 5 ml, 10 ml, 25 ml)	Greiner
Nitrocellulose membrane	Amersham/ Millipore
Reaction tubes (0.5ml, 1.5ml and 2-ml)	Eppendorf; Sarstedt
Sterile filters Minisart® (pore size 0.2µm)	Sartorius
Syringes Injekt® (1ml,5ml,10ml and 20ml)	Braun/ BD Bioscience
Syringes Plastipak™ (50ml)	BD Bioscience
Test tubes Cellstar® (15ml and 50ml)	Greiner
Whatman® chromatography paper (3mm)	Biometra

3.1.2. Chemicals and reagents

Table 3.3. List of chemicals and reagents used

Chemical	Manufacturer	Storage	Usage
Agar	Carl Roth	Room Temp. (RT)	LB growth medium
Agarose Seakem® LE	Biozym	RT	Agarose gel formation
Dulbecco's Modified Eagle Medium (DMEM)	PAA	2-8°C	Cell culture growth medium
Dimethyl sulfoxide (DMSO)	Carl Roth	-20°C	Dissolving of compounds and control substance; freezing medium
Fetal calf serum (FCS)	Biochrom	-20°C	Additive to the cell culture medium
Peptone-casein	Roth	RT	LB growth medium
TurboFect™ Transfection reagent	Thermo Scientific	2-8°C	Transfecting eukaryotic cells
Yeast extract	Roth	RT	LB growth medium

Table 3.4. List of other chemicals and reagents

Chemical	Manufacturer	Storage	Usage
Ammonium persulfate (APS)	Serva	RT	Polyacrylamide gel
β-mercaptoethanol	Roth	2-8°C	SDS sample buffer
Bromphenolblue	Merck	RT	SDS sample buffer
Calcium chloride ($CaCl_2$)	Roth	RT	Production of competent cells
Sucrose	Serva	RT	Lysis Buffer A
Ethanol	Echter-Nordhäuser Spirituosen	RT	Tankblot Buffer
Ethylenediaminetetraacetic acid (EDTA)	Roth	RT	TE buffer
Ethylene glycol tetraacetic acid (EGTA)	Serva	RT	Lysis Buffer A
Glycerol	Roth	RT	SDS sample buffer
Glycin	Roth	RT	SDS running buffer and Tankblot buffer
Potassium chloride (KCl)	Merck	RT	Lysis Buffer A
Potassium phosphate tribasic (K_3PO_4)	Sigma	RT	PPBT lysis buffer
Luminol	Roth	RT	Enhanced chemiluminescence solution (ECL)
$MgCl_2$ x 4 H_2O	Roth	RT	Lysis Buffer A
Manganese (II) chloride ($MnCl_2$)	Roth	RT	Production of competent cells
Methanol	Roth	RT	Cell fixation
3-(N-morpholino) propanesulfonic acid (MOPS)	Serva	RT	Production of competent cells
Polysorbate 20 (Tween 20)	Roth	2-8°C	Polyacrylamide gel electrophoresis and wash buffer for various assays.

Potassium acetate	Roth	RT	Production of competent cells
Potassium chloride (KCl)	Merck	RT	Production of competent cells
Rotiphorese® 40	Roth	2-8°C	Polyacrylamide gel
Sodium chloride (NaCl)	Roth	RT	Buffers
Sodium dodecyl sulfate (SDS)	Roth	RT	Ingredient in the some buffers
Sodium fluoride (NaF)	VEB Fluorwerke Dohna	RT	Lysis Buffer A
Sodium orthovandate (Na_3VO_4)	Sigma	RT	Lysis Buffer A
Na_2MbO_4	Sigma	RT	Lysis Buffer A
Tetramethylethylenediamine (TEMED)	Roth	2-8°C	Polyacrylamide gel
Tris(hydroxymethyl)-aminomethane (Tris)	Roth	RT	Ingredient in some buffers
Triton X-100	Merck	RT	PPBT lysis buffer

3.1.3. Buffers/solutions

Table 3.5: List of commercial buffers

Buffers	Manufacturer	Storage	Usage
Dulbecco's Phosphate Buffered Saline (PBS) with Ca & Mg	PAA	4°C	Washing adherent cells and maintaining their normal osmotic pressure
Detection solution ECL I + ECL II (1:1)	Roche	4°C	WB detection

Table 3.6: List of self-made buffers

Buffers	Content	Storage	Usage
SDS running buffer	25mM Tris,19.2mM Glycin, 0.01% (w/v) SDS	RT	Running of SDS-PAGE
Tris-buffered saline + Tween 20 (TBS-T buffer)	50 mM Tris 150 mM NaCl 0.1% (v/v) Tween 20	RT	Blocking and washing the PVDF membrane; dilution of primary and secondary antibodies
Potassium phosphate buffer + Triton-x100 (PPBT buffer)	100mM K_3PO_4 0.2% Triton-x100	2-8°C	Cell lysis
Solution 1 Luciferase assay (pH 7.8)	200 mM Tris-HCl 15 mM $MgSO_4$ 100 µM EDTA 1M ATP 25 mM DTT 200 µM Coenzym A 200 µM D-Luciferin	-80°C	Detection substrate in reporter gene assay
Standard transformation buffer (TFB I) (pH 5.8)	30mM $CH_3COO^-K^+$ 50mM $MnCl_2$ 100mM KCl 15% (v/v) Glycerin	2-8°C	Production of competent cells
Standard transformation buffer (TFB II)	10 mM MOPS NaOH (pH 7) 75 mM $CaCl_2$ 10 mM KCl 15% (v/v) Glycerin	2-8°C	Production of competent cells
0.1x Tris-EDTA buffer (TE buffer)	10 mM Tris pH 8 0.1 mM EDTA	RT	Dilution and preservation of DNA plasmids
LB medium	1% Peptone-casein 0.5% Yeast extract 85.6 mM NaCl, 7.5 pH	RT	Growth medium for bacterial cultures

LB agar	1% Peptone-casein 0.5% Yeast extract 85.6 mM NaCl 1.5% Agar	RT	Growth medium for bacterial cultures
Blocking buffer	5 % milk powder in TBST	4°C	Blocking western blot membranes
Electrophores buffer (10x)	2.5 mM Tris, 19.2 mM glycine, 3.5 mM SDS	RT	Electrophoresis
Haematoxylin	0.5 g Haematoxylin, 0.1 g NaI, 25 g KOH solution, 25 g chloral hydrate, 0.5 g citric acid in 500 ml H_2O	RT	Staining dye
(4-(2-hydroxyethyl)-1-piperazineethanesulfonic acid (HEPES)	10 mM HEPES, 145 mM NaCl, 5 mM KCl, 1mM $MgSO_4$,10 mM D-Glucose	RT	Staining procedure
Loading-buffer (6x)	1.3 mM bromophenol blue,1.6 mM xylene cyanol,60 % Glycerol (v/v), 60 mM EDTA	RT (in use) stock at -20°C	Staining DNA samples
Phosphate buffered saline (PBS)	680 mM NaCl, 13.5 mM KCl, 9 mM KH_2PO_4, 50 mM Na_2HPO_4 x 12 H_2O, pH 7.4	RT	Buffer (washing)
Ponceau-S-Mix	1 % Ponceau S (w/v), 0.1 M trichloroacetic acid, 1.3 M sulfosalicylic acid	RT	Staining and visualization of proteins on WB membrane
Sample buffer (5x)	0.3 mM bromophenol blue, 500 mg SDS, 2 ml H_2O, 1.5 ml 1 M Tris/HCl pH 6.8, 1.5 ml glycerol, 550 µl mercaptoethanol	-20°C	Denaturation and Staining of protein samples

Strip buffer	60 mM Tris/HCl pH 6.7, 2 % SDS (w/v), 0.4 % 2 ß-mercaptoethanol	RT	Western blot antibody stripping
Tris, Acetic acid EDTA (TAE) buffer (50x)	2 M Tris/HCl pH 8.0, 50 mM EDTA, 5.7% acetic acid (v/v)	RT	Agarose gel electrophoresis
Transfer buffer	25 mM Tris/HCl pH 7.5, 190 mM glycine, 20 % methanol(v/v)	4°C	Western blot transferring of proteins to membranes
Trypan buffer solution	4 % trypan blue in PBS	RT	Cell counting stain
PBST	680 mM NaCl, 13.5 mM KCl, 9 mM KH_2PO_4, 50 mM Na_2HPO_4. 12 H_2O, pH 7.4 0.05 % Tween 20	RT	Washing
Developer	12 gm of Na_2CO_3 (w/v), 80 µl 0.1% of NaS_2O_3 x $5H_2O$ (0.1 gm in 100 ml) 100 µl formalin, 200 ml dd H_2O	RT	Silver Gel
Fixer	100 ml methanol (v/v), 24 ml acetic acid,100 µl formalin, 76 ml ddH_2O	RT (fresh)	Silver Gel
Silver nitrate	100 mg $AgNO_3$, 50 ml ddH_2O, 37 µl formalin	RT (fresh)	Silver Gel
Coomassie staining solution	0.25% Coomassie; 45% Methanol(v/v), 45% H_2O (v/v), 10% Essigsäure (v/v)	RT	Staining proteins on gel
Separating gel buffer	2.5 M Tris/HCl, pH 8.0	4°C	Western blot
Stacking gel buffer	620 mM Tris/HCl, pH 6.8	4°C	Western blot
Lysis buffer	40 mM Tris/HCl, 100 mM NaCl, pH 8.0	4°C	Protein production
Elution buffer	20 mM Tris/HCl, 20 mM Maltose, pH 8.0	4°C	Protein production

3.1.4. Enzymes

Table 3.7. List of enzymes

Enzymes	Manufacturer	Stock conc.	Storage	Usage
Trypsin-EDTA	PAA	1x	4°C	Facilitates detachment of cells from the bottom of the culture plate
FastDigest® restriction endonuclease: EcoRI, Xba1, BamH1, Xho1	Fermentas	1x	-20°C	Restriction digestion in cloning
Buffer solution FastDigest® endonuclease	Fermentas	10x	-20°C	Cloning
T4 DNA ligase, buffer solution for T4 DNA ligase	Fermentas	1x	-20°C	Cloning
Taq polymerase	Fermentas	1x	-20°C	PCR
Phusion polymerase	Fermentas	1x	-20°C	PCR

3.1.5. Antibiotics

Table 3.8. List of antibiotics

Antibiotic	Manufacturer	Stock concentration	Storage	Usage
Penicillin/ Streptomycin	PAA	100x	-20°C	Additive to the cell culture medium, prevents fungal and bacterial contamination
G 418 – BC (Neomycin)	Biochrome AG	30000U/ml(50mg/ml)	2-8°C	Selection pressure agent
Ampicillin	Carl Roth	1 mg/ml	-20°C	Selection pressure agent
Zeocin	Invitrogen	1 mg/ml	-20°C	Selection pressure agent

3.1.6. Kits

Table 3.9: List of commercial kits

Kit	Manufacturer	Storage	Usage
Plasmid DNA purification	Macherey-Nagel	RT	Isolation and purification of plasmid DNA
Agarose DNA extraction	Macherey-Nagel	RT	Isolation and purification of total RNA
CloneJET™ PCR Cloning Kit	Fermentas	-20ºC	pJET1.2 cloning system
5-Prime MasterMix	Fermentas	-20ºC	Used in PCR
Phusion® Hot Start High-Fidelity Polymerase	Thermo	-20ºC	Used in PCR

3.1.7. Antibodies

All the antibodies were stored at 4ºC. Lab made antibodies were preserved with 0.1% sodium azide and all unlabelled stocks were frozen at -20ºC.

Table 3.10: List of antibodies

Antibody	Epitope	Manufacturer	Species	Used dilution
Goat anti-mouse IgG- HRP/FITC/PE (Secondary Ab)	Mouse-IgG	Santa Cruz	Goat	1:10000
Anti-P5D4	P5D4	Lab made	Mouse	1 µg/ml
Anti-His	His Tag	Qiagen	Mouse	1 µg/ml
Anti mouse $CD11c^+$ PE	$CD11c^+$	BD	Rat	0.1 µg/ml
Anti mouse CD86 FITC	CD86	BD	Rat	0.1 µg/ml
Anti mouse CD80 FITC	CD80	BD	Rat	0.1 µg/ml
Anti mouse OX 40 PE	OX40	Ebiosciences	Hamster	0.1 µg/ml
Anti MBP	MBP	Lab made	Mouse	0.5 µg/ml
Goat anti rat IgG-PE	Rat IgG	Santa Cruz	Goat	0.4 µg/ml

3.1.8. Eukaryotic cells/Cell lines

a. Primary cells

Table 3.11. List of primary cell

Cells	Bone marrow derived dendritic cells (BMDC)
Source	Isolated from thigh bone marrow of C57BL/6mice
Splitting	3 days
Medium	RPMI with L-Glutamine, 10% of FCS, 1% Penicillin/Streptomycin, 20 ng/ml m GM-CSF
Description	Mouse bone marrow derived dendritic cells (BMDCs) are obtained from femur of freshly sacrificed mice (BALB/c or C57BL/6J) (see method 3.3.1. for details). These are spherical adherent cells initially at time of seeding on day 0 but change morphology to show dendrites within a week.

b. Cell Lines

All the cells were grown at 37 ºC at 5% CO_2 under aseptic conditions.

Table 3.12. List of eukaryotic cell lines

Cell line	Source	Splitting	Medium	Description
KCMH-1	Prof. Hirano Tohoku Univ.	1:10 3-4 days	α- MEM, with L-Glutamine, 10% of FCS, 1% Penicillin/streptomycin	Spindle shaped adherent mouse skin epithelial carcinoma cell line. It secretes mTSLP on stimulation.
Ba/F3	Lab	1:5 3 days	RPMI 1640 with L-Glutamine, 10% of FCS, 50µg/ml Gentamycin, 20 ng/ml of mIL-3	Spheroid shaped, murine IL -3 dependent pro- B cell line established from the bone marrow of BALB/c mouse. (Palacios & Steinmetz, 1985). Grow in suspension culture with a doubling time of about 20 h.

Ba/F3-hTSLPR and Ba/F3-IL-4	Lab	1:5 3-4 days	RPMI 1640, with L-Glutamine, 10% of FCS, 1% Gentamycin, hTSLP 20ng/ml	Stable cell line made in the lab dependent on mIL-3 but responsive to hTSLP & hIL-4 respectively. Used for control experiments.
HEK 293-exo-mTSLPR-His8x-TraN stable cells line	Lab	$1x10^6$ cells/ml 5-6 days	DMEM, with L-Glutamine 10% of FCS 1% Penicillin Streptomycin Zeocin 100 µg/ml	HEK293T are spindle shaped adherent human embryonic kidney cell line with sheared adenovirus 5 DNA. The cells were transfected with a plasmid expressing stable soluble exo-mTSLPR domain to make a stable soluble protein secreting cell line.

3.1.9. Bacterial strains

Table 3.13. List of bacterial strains

Bacterial strain	Source	Medium	Genotype	Usage
E. coli- strain Top 10	Invitrogen	LB medium	F- mcrA Δ(mrr-hsdRMS-mcrBC) φ80lacZΔM15 ΔlacX74 nupG recA1 araD139 Δ(ara-leu)7697 galE15 galK16 rpsL(Str^R) endA1 λ^-	Cloning and plasmid amplification
E.coli- BL21 (DE 3)	Novagen (Obtained from Invigate)	LB medium	$F^–$ ompT gal dcm lon $hsdS_B(r_B^- m_B^-)$ λ(DE3 [lacI lacUV5-T7 gene 1 ind1 sam7 nin5])	Used as an expression vector for production of proteins.

3.1.10. Plasmids

i. Expression vector pcDNA3.1 + neo/zeo

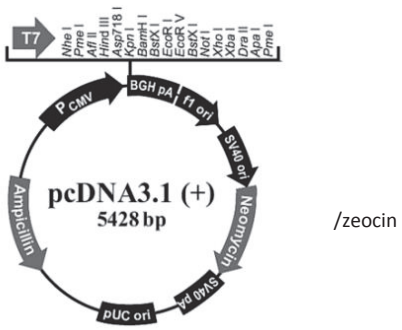

Fig.3.1. Plasmid map of the vector pcDNA3.1 (+) Neo. The vector is derived from Invitrogen and is suitable for the expression of recombinant proteins in eukaryotic system (Product information from Invitrogen).

This plasmid is suitable for transient and stable expression of recombinant proteins in eukaryotic cells. CMV promoter can lead to very high expression levels of the target protein (Boshart et al., 1985). The bovine growth hormone (BGH) polyadenylation signal is responsible for efficient termination of transcription and for polyadenylation of the mRNA. This signal is located behind a polylinker in which the cDNA to be expressed can be inserted (Goodwin et al., 1992). The Simian virus 40 (SV-40) origin in cells expresses the large T antigen and causes the replication of the vector in order to maintain a high plasmid copy number in the proliferating cells (Gluzman, 1981). Ampicillin and G418 resistance genes offer the possibility of selection in bacteria or animal cells.

Table 3.14. pcDNA3.1 + (Neo/Zeo) -derived receptor expression constructs (see Appendix for maps) (Wohlmann et al., 2010).

Plasmid	Description
pcDNA3.1 mTSLPR	carrying cDNA of complete murine TSLPR receptor chain, G418 resistance and a P5D4 epitope
pcDNA3.1 mIL-7Rα	carrying cDNA of complete murine. IL-7Rα-chain receptor, G418-resistance as well as a P5D4 epitope tag
pcDNA3.1exo-mTSLPR-intra hTSLPR Hybrid	carrying cDNA of exo-murine TSLPRα receptor chain and inner hTSLPR chain, G418 resistance and a P5D4 epitope tag
pcDNA3.1exo-mIL-7Rα-intra hIL-7 Rα Hybrid	carrying cDNA of exo-murine IL7α receptor chain and inner IL-7 Rα chain, G418 Resistance and a P5D4 epitope tag.
pcDNA3.1 exo-mTSLPR-His 8xTraN/pcDNA3.1 exo-mTSLPR-His6x	carrying cDNA of exo-murine TSLPRα receptor chain, a zeocin-resistance as well as hIL-4Rα signal peptide , a TraN His8x tag and a P5D4 epitope tag. A version with His6x tag was also prepared which had all other components same.

ii) Expression vector pMAL-2 series

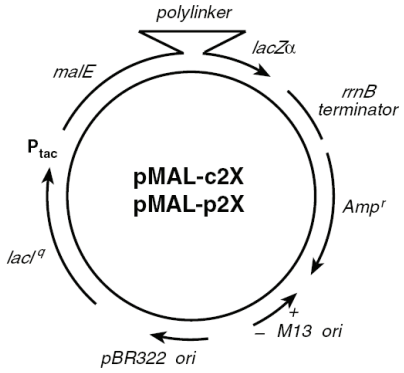

Fig.3.2 The pMAL-2 vectors expression system for production of mTSLP. pMAL-c2X (6646 base pairs) has its malE signal sequence deleted. pMAL-p2X (6721 bp) includes the malE signal sequence. The arrows indicate the transcription direction of the gene (product information from New England Biolabs).

Table 3.15. pMAL-c2X derived expression constructs (see Appendix for maps)

Plasmid	Description
pMAL-c2X	Empty vector to produce MBP
pMAL-c2X-mTSLP-MBP(wild type)	carrying cDNA of the fusion protein mTSLP-MBP(wild type)
pMAL-c2X-I37EmTSLP-MBP (mutant)	carrying cDNA of the fusion protein I37E mTSLP-MBP (mutant)

This method produces a high level of expression of the cloned gene sequence by using the strong "tac" promoter and the malE translation initiation signals, combining it with a one-step purification of the fusion protein using MBP's affinity for amylose The vectors can express the malE gene (with or without its signal sequence) fused to the lacZα gene. The restriction sites in between malE and lacZα are available for insertion of the coding sequence of interest.

In the pMAL-c2X vector, the malE gene on these vectors has a deletion of the signal sequence, leading to cytoplasmic expression of the fusion protein. The advantage of the c2X vector is that it generally expresses more fusion protein than the pMAL-p2X series. The fusion proteins that cannot be exported to the periplasm are more stable in pMAL-c2X vectors.The $lacI^q$ gene present in both the vectors codes for the Lac repressor. This gene minimizes the P_{tac} expression low in the absence of IPTG induction. The pMAL-2 series vectors also have specifically coded recognitions site for a specific protease, located just 5´ to the polylinker insertion sites. This allows MBP to be cleaved from the protein of interest after purification.The pMAL-c2X and pMAL-p2X vectors that are used for the production of mTSLP encode the site for Factor Xa (Ile-Glu-Gly-Arg). Factor Xa cleaves after these

four amino acid recognition sequence so as to leave few or no vector-derived residues attached to the protein of interest. This is dependent on the cloning site used for the purpose.The pMAL-2 vectors also include the origin of DNA replication site of the *E. coli* bacteriophage M13, which allows the production of single-stranded DNA by infection of cells bearing a pMAL-2 plasmid with a helper phage.

iii) Reporter gene plasmid pGL3-basic

The reporter gene pGL3-basic is derived from Promega and offers the possibility for quantitative analysis of eukaryotic factors regulating gene expression. These include promoters and transcription factors. They are encoded with the gene for plasmid firefly luciferase (*Photinus pyralis*) whose expression occurs upon active binding of transcription factors to the promoter region of the reporter gene. The receptor specific cell ligand/stimulus thus leads to activation of transcription factors in cell signaling, which could thus be quantified as a measure of transcriptional activity in the eukaryotic cells.

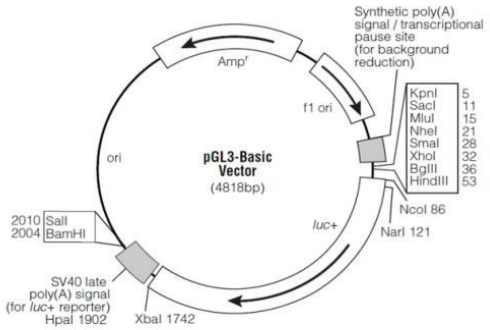

Fig.3.3 Plasmid map of the vector pGL3-basic. The vector is well suited for quantifying transcriptional activity of promoter sequences in eukaryotic cells (product information from Promega).

Table 3.16. pGL3-basic derived expression constructs (see Appendix.)

Plasmid	Description
pGL3-basic IRF Luc	Contains the human IRF STAT1 promoter, which serves as a sensitive readout of the cytokine response by pSTAT1 activation and binding and further transcription of the luciferase gene.

iv) pEGFP

pEGFP containing the cDNA of eGFP (enhanced green fluorescent protein), a CMV promoter and is from the company "Clontech" (Cormack et al., 1996).

3.1.11. Oligonucleotides

All oligonucleotides were synthesized by the company Eurofins.

Table 3.17. Oligonucleotide sequence

Name	Sequence 5´- 3´
exo-mTSLPR-TraN-8x His For (Forward)	GCCGGGTCCACTCGAGGCGGCGGCGGTGACGTC
exo-mTSLPR-His 6x For	GGTACCGAGCTCGGATCCATGGCATGGGCACTC G
exo-mTSLPR- Rev (Reverse)	GATCCAGATGCGGCCGCGAGGGGCGGGGCCAGG GCCG
mTSLP-MBP For (p2X)	TTTCAGAATTCTACAACTTTTCTAACTGC
mTSLP-MBP Rev (p2x)	GTGCCAAGCTTATTCTGGAGATTGCATGAAGG
I37E mTSLP-MBP For (c2X/p2X)	ATTCAGGAATTCTACAACTTTTCTAACCTGCAAC TTCACGTCAATTACGAAAATATATTGTAACGAA AATTTTTCATGACC
I37E mTSLP-MBP Rev (c2x)	CTAGAGGATCCTTATTCTGGAGATTGCATGA
I37E mTSLP-MBP Rev (p2x)	GTGCCAAGCTTATTCTGGAGATTGCATGAAGG
exo-mIL-7Rα-hybrid For	GGTCCAGCGGCCGCGGAAAGTGGAAATGCCCAG G
exo-mIL-7Rα-hybrid Rev	ATAGGCTCGAGATCCCATCCTCCTTGATTC
exo-mTSLPR-hybrid For	GTCCAGCGGCCGCGGCGGCGGCGGTGACG
exo-mTSLPR-hybrid Rev	ATAGGCTCGAGGAGGGGCGGGGCCAGGGCC
Oligonucleotides for the mycoplasma test	
Myc For	AGCAAACAGGATTAGATACC
Myc Rev	CATCTGTCACTCTGTTAACCT

3.1.12. Cytokine and factors

Table 3.18. Cytokines and factors used

Cytokine	Company
mTSLP	R&D Systems GmbH
mTSLP-MBP	Lab made
mI37E mTSLP-MBP	Lab made
mIL-3	Immunotools
mGMCSF	Immunotools

3.1.13. Software

Table 3.19. Software

Name	Company
Graphpad prism	GraphPad Software, Inc.
Flowjo	Flowjo LLC
ApE Plasmid editor	M. Wayne Davis
Cyflogic	CyFlo Ltd.
Microsoft Office	Microsoft
Paint	Microsoft
Snap Gene	GSL Biotech LLC

3.2. Molecular biological methods

3.2.1. Preparation of competent *E. coli* Top 10/ BL-21 DE3 cells

A modified version of the protocol from Hanahan (Hanahan, 1983) for the preparation of competent *E. coli* cells was used. Top10/ BL-21 DE3 cells were grown in 5 ml LB medium overnight at 37°C, 5 % CO_2 and 95 % humidity. Of these 10 µl pre-culture was used to inoculate 200 ml LB medium and then shaken up to an OD_{600} of 0.15-0.3 at 37°C in 1 litre shaker incubation flasks. Subsequently, the cells were harvested. All work had to be done on ice maintaining sterile conditions. These solutions and equipment were pre-cooled. The culture was divided into tubes (50 ml) and centrifuged for 5 min at 4000 rpm, the supernatant was discarded. The pellet was resuspended in 20 ml of transformation buffer TFB I, and incubated for 30 min on ice. After another centrifugation for 4 min at 4000 rpm, the pellet was taken up in ice cold 4 ml TFB II and mixed well. The batch was then aliquoted into Eppendorf tubes to make 30 µl aliquots and snap frozen in liquid nitrogen.The cells were stored at -80 ° C until further use. (For components of TFB see 3.1.3 Table 6).

3.2.2. Chemical transformation and plasmid amplification in *E. coli*

For the amplification of plasmids one aliquot of 30 µl of the prepared competent Top10 strains were thawed on ice. 50-100 ng of DNA to be amplified was added to the cells. The cells were first conditioned for 20 min on ice, and were then heat shocked at 42°C for 90 s after which they were immediately put back on ice. Then 1000 µl of LB medium was added and the samples were shaken for 30-45 min in the incubator at 37°C and 180 rpm. During this period, the transformed cells should express the ampicillin resistance gene. The cells were spun down at 4000 rpm for 5 min. Thereafter, 40 µl of a mixture was evenly distributed an LB-ampicillin agar plate by a sterile L shaped glass spreader and incubated at 37°C overnight. Only the transformed cells formed colonies which were visible the next day. From the several colonies a single colony was picked up and used to inoculate a 200 ml suspension culture with appropriate antibiotic resistance (Ampicillin). This culture was then shaken overnight at 37°C until an OD_{600} of 2-3 was reached. Subsequently, the plasmids from *E. coli* were isolated.

3.2.3. Isolation and purification of plasmid DNA from *E. coli*

The purification of the plasmid DNA was achieved from *E.coli* cultures by using commercial kits, based on the amount of DNA requierd. For small bacterial cultures, the plasmids were isolated with Miniprep DNA kit (Machery and Nagel) and for larger DNA yield the NucleoBond® Extra Midi (Machery-Nagel) kit was used according to the appropriate protocol for large scale plasmid isolation. For longer use, plasmids are stored at -20ºC dissolved in TE buffer or water.

3.2.4. Measurement of DNA concentration

The DNA concentration was measured as absorbance on Nano Drop at 280 nm wavelength by using 2 µl of the DNA sample and a similar amount of water as blank.

3.2.5. Restriction digestion of plasmid DNA

The DNA digestion with restriction enzymes was always carried out using the series FastDigest® (Fermentas Life Sciences) according to the manufacturer's protocol. For analytical approaches, DNA constructs always contained 0.5 µg of DNA digested for 15 min. The preparative approaches leading to the production of new DNA constructs always contained 3 µg of DNA digested for 1 hr.The insert was excised out of the plasmid by incubation with fast digestion enzymes for 1 hr at 37°C as follows:

Table 3.20. Components of a plasmid digestion reaction

Ingredients	**Volume in µl**
ddH_2O	add to reach 20
Plasmid DNA	1 µg
Restriction enzymes (e.g.EcoR I, Hind III)	each 1
Restricition buffer (10x FD green buffer)	2
Total	**20 µl**

The PCR product was also treated with the restriction enzymes for cleaving off blunt ends for 1 hr at 37°C.

3.2.6. Agarose gel electrophoresis

For the agarose gel electrophoresis, the corresponding amount of agarose was dissolved (as the percentage of required gel) in 1 x TAE buffer by heating in a microwave followed by cooling to about 50°C. Red-safe was added in a ratio of 1: 40000. The gel was casted by pouring the mixture into an electrophoresis chamber. After polymerization of the gel, the chamber was filled with 1X TAE buffer. About 0.5 µg of the DNA to be analyzed was mixed with the loading buffer (6x) and pipetted into the wells of the gel. The gel was run for about 20-30 min under a voltage of 100 V. The bands on the gel were then viewed as compared to a molecular weight marker, the desired fragments were identified and documented in a transillumination UV light chamber (analyzer VWR) or cut out on a UV light plate.

3.2.7. DNA extraction from agarose gels

The extraction of DNA from agarose gels was mainly used for PCR products and digested plasmids, which should be used later for the cloning of novel DNA constructs. After the DNA was electrophoretically isolated, 80% of the gel bands were cut out vertically, and put aside. The remaining gel was observed under ultraviolet light and target bands marked with a scalpel. Thereafter, the excised gel bands were loaded again, and the target product can be isolated without the use of UV light on the basis of the markings. The extraction of the DNA was then carried out with a gel extraction kit (Machery and Nagel).

3.2.8. Ligation

100 ng of restricted plasmid and 350 ng of restricted insert DNA were mixed with 1 U of T4 ligase in a buffered reaction volume of 20 µl. The mixture was incubated at RT for 1 hr or overnight at 4°C for ligation and then transformed into *E. coli*.

3.2.9. DNA Sequencing

In order to verify a successful progess of cloning process, the plasmid DNA was sequenced. Cloned constructs were sent to either GATC Biotech or Eurofins MWG Operon to be sequenced by modified chain termination method. The sequences were analysed by ApE software.

3.2.10. Polymerase chain reaction (PCR)

Polymerase chain reaction (Saiki et al., 1985) is a molecular biological method used to amplify a particular DNA sequence. PCR relies on primer- dependent DNA polymerase replication of a double stranded DNA template and depends on an order of distinct steps, which make up a so called cycle of reaction. These different steps are performed by a thermocycler. The principle of this method and the reaction components are illustrated in the following tables. Denaturation to elongation comprised of a cycle and was repeated approximately 25 times for DNA inserts cloned in this project.

Table 3.21. Principle of PCR (*Steps repeated during the PCR cycle)

PCR steps	Description
Initialisation step (98°C for 10 min	Heat activation of polymerases
Denaturation* (96°C for 30 s)	Separation of DNA strands by H-bonds disruption
Annealing* (for 30 s, primer dependent)	Attachment of primer to DNA strand

Elongation*(72°C for 45 s)	Synthesis of new complementary DNA srand by DNA polymerase (polymerase speed dependent)
Final elongation (72°C for 7 min)	Extension of any remaining single-stranded DNA

Table 3.22. Reaction mixture

Component	Quantity	Component	Quantity
cDNA template	1 µl	DMSO	20 µl
Primer fwd	1 µl	ddH_2O	1 µl
Primer rev	6 µl	Phusion polymerase	0.25 µl
Buffer GC	1 µl	**Total**	**30.75 µl**
dNTPs	0.5 µl		

In this thesis, this method was used to generate DNA sequences out of cDNA, generate new restriction sites, and introduce point mutations in a DNA sequence. PCR site directed mutagenesis creates a defined site in a DNA molecule by using primers that contain the desired mutation. The site next to the recognition site for restriction enzyme was the target for site-directed mutagenesis. This was accomplished by using mutagenic primers (with non-matching bases) with flanking primers ends to generate intermediate PCR products that are overlapping fragments of the entire product. Intermediate products are used as template DNA for the second cycle of PCR; strands of each product hybridize at their overlapping, complementary regions that also contain the desired mutation. Amplification of mutated product in second PCR cycle is driven by flanking primers. The final product possesses the desired mutation and can be inserted into an expression vector to generate larger quantities of DNA, which need to be sequenced to ensure the presence of the desired mutation. Analytical PCR was also used for screening transformed cells. After the transformation of the ligation products the resulting colonies were grown in a 24 well plate till an OD_{600} of 1 and 0.2 µl from it was examined by a PCR using specific primers. PCR was performed using a 5-Prime ready mix containing Taq DNA polymerase. The corresponding PCR protocol was carried out according to manufacturer's instructions. As negative and positive controls were PCR reactions without DNA or a DNA template that contained the corresponding nucleotide sequence of the insert. The positive transformed cells produced a band while no bands were observed in untransformed colonies.

3.3. Cellular biological methods

3.3.1. Cell culturing and passaging

The cultivation of all primary cells and cell lines was carried out under sterile condition in an incubator at 37°C, 95% humidity and 5% CO_2.Cell line passages and transfers were performed cultivation was performed under sterile conditions in a tissue culture hood.

The cultivation of Ba/F3 cells (non adherent), KCMH-1 and HEK293T (adherent) cells was initiated in 25 cm^2 flask from frozen cells and is up-scaled to be normally carried out in 75cm^2 cell culture flasks with the characteristic medium (see Table 3.12 subsection 3.1.8). The dendritic cells (non adherent) were cultured in a petri dish. At 90% confluence; the cells adherent cells were split.

In case of adherent cells, after washing the cells with PBS, 2-3 ml Trypsin /EDTA (0.05%/0.02%, w/v) was added for 3-5 min in an incubator and then cells detached by knocking on the sides of the flask. The HEK293T cells could be also detached directly by tapping without the use of Trypsin/ EDTA. The action of trypsin was stopped by the addition of media containing 10 % FCS. After centrifugation of the detached cells at 300g for 5 min, the culture flask was seeded with approximately 0.5 x 10^6 cells. In case of the experiments, only 10 cell passages were used for the adherent cell lines. The cultivation of the Ba/F3, Ba/F3-mTSLPR cells was carried out in RFG medium supplemented with 20 ng/ml mIL-3 or 5% mIL-3 culture supernatant and 10ng/ml rmTSLP respectively as growth factors. A cell density of 1 x 10^6 cells/ml was maintained and cells were split in the ratio 1:5 of cell: medium, during passage. For experiments, not more than 25 passages were made. The primary dendritic cells survived only for 4-5 days of culturing and were supplemented with GM-CSF to support growth and proliferations.

Mouse Bone marrow cells (BMCs) are obtained from femur of freshly sacrificed mice (BALB/c or C57BL/6J) (see Fig.3.4) (Madaan et al., 2014). These are round in shape and behave like suspension cells at time of seeding on day 0 and are transformed in the presence of GM-CSF to dendritic cells displaying extracellular processes on day 6 when they are harvested. The transformation was confirmed by testing the expression of CD11c surface marker on the surface of the dendritic cell surface using FACS analysis. (see subsection 4.4.2, Fig. 4.2.9) .The medium was replaced on day 3 and comprised of RPMI 1640, 10% FCS (v/v), 1% Penicillin/Streptomycin and 20 ng/ml of GM-CSF.

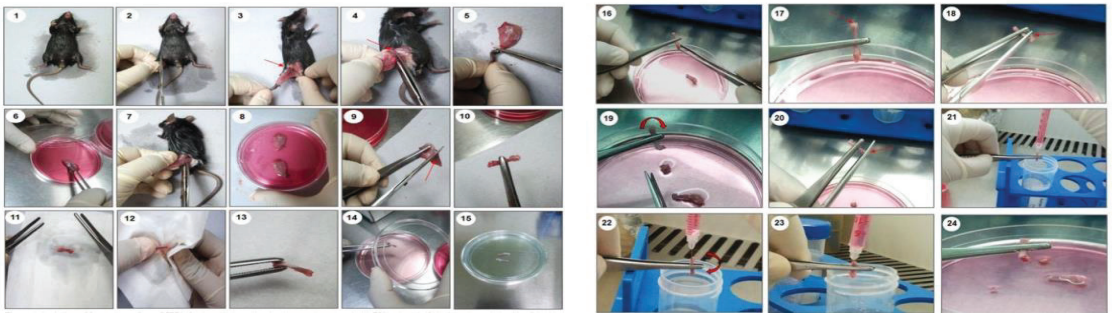

a. b.

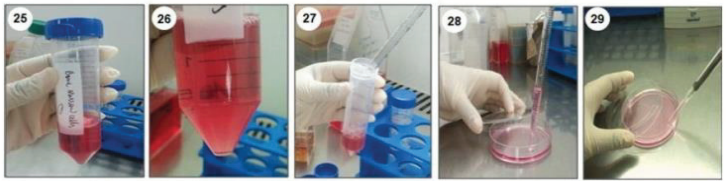

c.

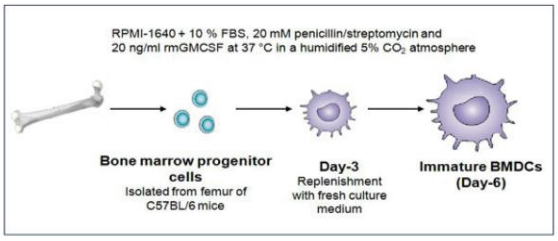

d.

Fig. 3.4. Steps involved in the generation of the dendritic cells from the bone marrow cells from C57BL/6J mice. a.1-18 shows the isolation of femur bone from the C57BL/6J mice. b. 16-24 show isolation of cells from the femur by passing medium though the bone shaft by a needle.c.25-29 show the seeding of the cells and addition of GMCSF in pic 29 on day 0.(Madaan et al., 2014).

The cells were used for migratory studies and surface marker studies.

3.3.2. Cryopreservation and thawing of cells

To store the cells, they needed to be cryopreserved. Approximately 6 ml ($2x10^6$ cells/ml) from a cell line with low passages and confluence between 80-90% was taken. The cells were washed with 10 ml PBS and detached by incubation in 3 ml trypsin-EDTA mixture at 37°C. The action of trypsin was stopped by an addition of 5 ml medium. The entire suspension was then centrifuged at 1000 rpm for 5 min and supernatant discarded. The pellet was re-suspended in a mixture of 70% medium, 10% FCS and 10% DMSO and the cell suspension stored at 80°C in a cryovial for a short time prior to the storage in liquid nitrogen.The cryopreserved cells stored in liquid nitrogen (-196°C) were thawed by warming in a water bath at 37°C. Subsequently, cells were washed to remove the DMSO and then transferred to a 25 cm^2 flask with 6 ml media (10% FCS). After 3-4 days, cells could be passaged into a 75 cm^2 flask depending on the state of growth and cells counted.

3.3.3. Cell counting

The various assays like the Luciferase reporter gene mono assay required a defined amount of cells. Cell concentration was determined by the *Neubauer*-counting chamber. Cells pellet were suspended in 1 ml PBS. A defined volume of this cell suspension was mixed with trypan blue, which stains only dead cells. The trypan blue/cell mix was pipetted at the edge of the cover-slip of the *Neubauer*-counting chamber. Using a microscope, all cells in 4 large squares of the grid were counted. The final number of cells was calculated as: Cell count (as 10^4 /ml) = Dilution factor x Average count of four chambers.

3.3.4. Extraction of mIL-3-containing supernatants

The untransfected Ba/F3 cells required a constant growth factor dependence of mIL -3. mIL -3 was produced by the cultivation of the cell line X63Ag8-653BPV-mIL-3 in (RPMI-1640, FCS and gentamycin) RFG medium and was secreted into the supernatant. The cells were cultured at a cell density of 2 x 10^5/ml and grown for 4 days. Subsequently, the supernatant was removed by centrifugation of the cells, sterile filtered and stored at -20°C.

3.3.5. Cultivation and isolation of hybridomas

The production of the hybridoma cells was done by collaboration partner Dr. Michael Küpper, University Hospital Rostock. The rats were immunized with the extracellular domain of mTSLPR chain and the fusion of the spleen cells from the immunized rat was performed with a myeloma cell line (X-63). From the clonal mixtures, hybridoma cells were selected in HAT medium on 96-well plates and grown on RFG medium after about 3 weeks with 20 ng/ml rhIL-6. The clonal mixtures that survived were grown in at a cell density of approximately 5x10^4 cells per well on 24-well plates, and further cultured on 6-well plates. Depending on the growth rate, the cells were split every 2-4 days in a ratio of 1: 5 and fed with fresh medium. The isolation of clonal mixtures was carried out in a 96-well plate. 6x10^4 cells were seeded in well A1 and then were serially diluted 1:1 vertically from wells B1-H1. A horizontal dilution in 1: 1.ratio was performed starting from the first well A1 of each horizontal row. The clones that showed proliferation were considered and isolated in this way and viewed from the bottom right of this separation, only for the first clones. In this way, one could expect to have obtained monotype clones.

The cultivation of the individual monotype clones recovered for the production of supernatants was carried out on 6-well plates. In order to obtain large amounts of supernatants the cultivation was carried out in 175 cm^2 cell culture flasks with RFG-medium and 20 ng/ml rhIL-6. Medium was harvested every 3-4 days depending on the growth of the cells and replaced by fresh medium. The cells were

split in the ratio of 1:5. The supernatants thus obtained were cleared of the debris by centrifugation at 1000 rpm for 5 min. The supernatant was frozen at -20°C.

3.3.6. Mycoplasma test

The cells were screened for mycoplasma infection every 2 weeks.2µl of cell free supernatant were checked for possible contamination by a PCR-based Mycoplasma detection kit (Biochrom AG). Infected cultures were immediately discarded and destroyed.

3.3.7. Transfection by electroporation

Electroporation is a mechanical transfection method which allows cellular introduction of large highly charged DNA molecules. This method utilises an electric pulse to rearrange the hydrophobic bilayer resulting in small pores across the membrane. These pores serve as an entrance for DNA molecules. Transient transfection of the HEK293T cells/Ba/F3 was performed using the device Nucleofector®-Lonza (Maasho et al., 2004). For this, the cells were detached at reaching 80% confluence by trypsinization or by tapping the cell culture flask and and washed with PBS. The cells were starved to about 6-8 h (by removing the growth factor mIL-3 in Ba/F3 cells and FCS in HEK cells). 1 x 10^6 cells with 100 µl transfection solution V and 2µg plasmid was added. The transfection was carried out as electroporation with the program A-23 for HEK293T cells and T-16 for Ba/F3 cells. The cells were then seeded in the corresponding medium (see 3.1.8) in the desired numbers, stimulated or unstimulated as design of the experiment and grown in cell culture flasks/plates incubated at 5% CO_2 for 72 h at 37°C.

3.3.8. Lipofection

Stable transfection of HEK293T cells was carried out with Turbofect® (Lonza) by lipofection. This technique utilises liposomes to transfer genetic material into a cell. Liposomes are vesicles that can easily merge with cell membranes since they are both made of phospholipid bilayer. Lipofection has high efficiency, ease of use, reproducibility, low toxicity and its ability to transfect a wide range of cell types. TurboFect™ *in vitro* transfection reagent is a sterile solution of a proprietary cationic polymer in water. The polymer forms compact, stable, positively charged complexes with DNA. These protect DNA from degradation and facilitate gene delivery into eukaryotic cells.The complexes are endocytosed via lysosomes or endosomes and provoke a massive chloride influx. Due to a rapid osmotic swelling, endosomal rupture occurs, allowing a translocation of DNA to the nucleus.Initially, 250,000 cells per well were seeded into a 12-well-plate and settled at 37°C over night. The next day, 2 to 5 µg of plasmid DNA was mixed with 200 µl of appropriate medium and 2 µl of TurboFect Reagent, and incubated at room temperature for 20 min. Subsequently the suspension was added dropwise to the adherent cells. Transfection results were examined after 24 to 48 h.

3.3.9. Luciferase reporter gene assay

Reporter gene assays are widely used to determine eukaryotic gene expression and cellular physiology. By using this system receptor activity, transcription factors, intracellular signalling, mRNA processing and protein folding can be investigated. In this thesis, luciferase reporter gene assay was used to determine the relative upregulation of the cytokine (mTSLP) induced activity by using the luciferase reporter gene construct with a promoter responding to a downstream STAT1 transcription factor (IRF-1-Luc). For this purpose the 'Luciferase Assay System' was used from Promega. The monoassays were used in the experiments with transiently transfected Ba/F3 mTSLPR cells. In the mono-assay all transfected cells were pooled and divided into identical aliquots and then stimulated by cytokine treatment except for the negative control. At the end of each stimulation period, cells were lysed for 15 min and the amount of expressed firefly luciferase was measured by adding Luciferase assay substrate-I in the luminometer. Here, the luciferin contained in the added buffer coverts to oxyluciferin in the cells which expressed luciferase, thus producing a chemiluminiscence signal which can be recorded by the luminometer. (Sherf, B.A et al., 1996).

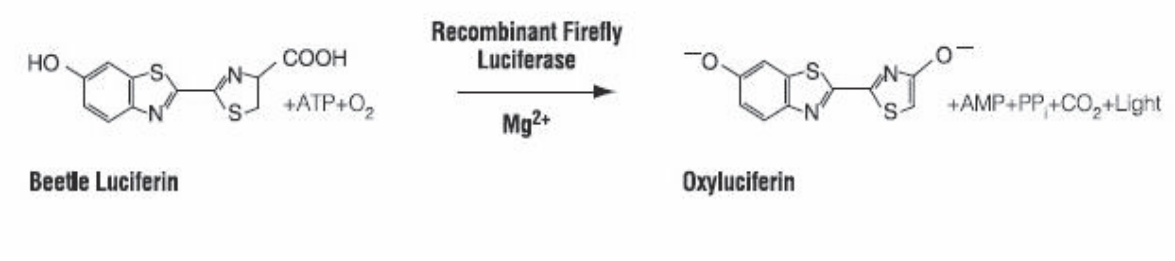

Fig.3.5. A schematic overview of the chemical reactions underlying the Promega Luciferase® Reporter Assay.

All measurements were carried out in a luminometer GloMax® Promega. This device allows very sensitive measurement and the automated pipetting of each buffer in order to obtain consistent and comparable values. The following settings were used: sample to be measured per well 25 µl, luciferase assay substrate I 30 µl measurement time per well 5 s.The intensity of the luminescence (LU) is proportional to the expressed luciferase and so that it allows accurate quantification of the relative cytokine activity (Wood et al., 1984). A comparison of the measured intensities from the unstimulated cells to that of the cytokine stimulated cells provides a measure of the relative stimulation of a reporter gene construct.

3.3.10. Flow cytometry

Flow cytometry is a method which can be used to analyze various parameters of an individual cell in a homogenous or heterogenous population. This technique involves the passage of thousands of cells per second across a laser beam. The cells suspended in PBS are sucked and passed through a

capillary in the fluidic chamber such that one cell individually moves past a laser beam. The incident light is deflected in different directions based upon the size and granularity of the cell. Forward scattered light (forward scatter or FSC) provides information on the relative size of the cell, lateral scattered light (sideward scatter or SSC) is a measure of the surface quality/granularity of the cell. The data gathered can be analyzed statistically by flow cytometry software to report cellular characteristics such as size, complexity, phenotype, and health of the cell.

In this thesis, flow cytometry was used to study the expression of receptor chains on the surface of Ba/F3 cells and the surface markers on the dendritic cells. The cells were initially washed and treated with Fc bockers (IgG) containing PBS if needed for 20 min. The markers were stained by using 1 µg of antibodies directed against the target (P5D4 tag in recptor cells and anti-CDs in dendritic cells). The cells were incubated for 30-60 min and twice washed with PBS and analysed on the cytometer as per the protocol. If a secondary antibody was used then another incubation of 30 min was given for incubation with secondary antibody. GFP expression was analyzed by direct measurement of the cells. For GFP and FITC FL-1 channel was used for detection while FL-2 channel was used for detection of PE based signals. Data analysis was performed with Cyflogic BD FACS diva and Flow Jo data analysis software.

3.3.11. Staining of dendritic cell carrying well-inserts during migration assays

Well-inserts were washed in HEPES and fixed in 4% PFA (ice cold) for 10 min on the outer side. The inserts were washed 3 times with distilled water. The inserts were stained in Haematoxylin stain (1 ml in a 6 well plate and 0.5 ml in the insert). The inserts were washed 3 times in tap water and kept for 10 min in warm water so that the water turns blue. The inserts were cleared on the inner surface using cotton buds and kept on the plate and left overnight for drying.Next day the membranes were cut and fixed on slides in Etellan and dried.

3.4. Protein biochemical methods

3.4.1. Sodium dodecyl sulfate-polyacrylamide gel electrophoresis (SDS-PAGE)

Protein separation by SDS-PAGE was used in this thesis to estimate approximate relative molecular mass, to determine the relative abundance of major proteins in a sample, and to determine the distribution of proteins among fractions obtained during chromatographic separation. This technique separates proteins according to their electrophoretic mobility. For this purpose, a polyacrylamide gel as a support medium and SDS to denature the proteins are used. SDS is a detergent that induces denaturation of the protein and creates negative charge around the polypeptide chain. The negative charges on SDS destroy most of the complex structure of proteins and are attracted strongly towards the anode in an electric field. The monomers of acrylamide are cross-linked to a polymeric matrix and the reaction is initiated by APS (ammonium persulfate), which produces free radicals. TEMED (tetramethylethylenediamine) stabilizes the free radicals as a catalyst in this process. The molecular mass of the determined protein defines the porosity of the gel used. The bigger the molecular mass of a protein, the smaller is the percentage of acrylamide in the separating gel. The following table shows composition of reagents used in a 12.5% polyacrylamide gel which was frequently used in this thesis.

Table 3.23. Composition of 12.5% gels

Component (for 2 gels)	Volume for Seperating gel	Volume for Stacking gel
Distilled water	2.1 ml	2.0 ml
Seperating gel buffer (2 M Tris HCl) pH 8.0	2 ml	X
Stacking gel buffer (0.5 M Tris HCl) pH 6.8	X	1.3 ml
Acrylamide (40%)	3.7 ml	700µl
Glycerine (40%)	4 ml	1.0 ml
SDS (20%)	50 µl	25 µl
APS (10%)	50 µl	40 µl
TEMED	10 µl	10 µl

During SDS-PAGE electrophoresis, gel assembly was used to create 1 mm thick gels by using appropriate seperators (Bio-Rad): The seperating or resolving gel was first poured (about 4/5 of the gel height) and covered with isopropanol layer to avoid distortion due to drying of the gel. After approximately an hr (polymerization of the separating gel), isopropanol was dried and the stacking gel was poured in between the plates and the corresponding combs were inserted depending on the

number of samples. Each sample (approx. 15-80 µg protein in 15-20 µl total volume) was added with 5 µl of 5x protein sample buffer and denatured at 95°C for 5 min. The sample buffer denatures the proteins. After filling the electrophoresis chamber of the mini PROTEAN® system from Bio-Rad with electrophoresis buffer solution, the prepared samples and a molecular weight marker were loaded onto the gel in different lanes as per the loading scheme. The molecular weight marker "Pager Ruler Plus" (Fermentas Life Sciences) serves as a size standard. An initial electric field of 100 V and 0.25 A was used for 20 min until each sample was within the stacking gel. For the separating gel electrophoresis, a voltage of 180 V and 0.5 A was used for approximately for 90 min. The proteins were thus separated and could be visualized by different staining methods, or can be blotted on a membrane using western blot. Coomassie staining was used for the visualization of the proteins produced by bacterial cloning in this thesis. The mTSLPR protein production was visualized by silver staining and western blotting.

3.4.2. Coomassie staining

The gels were stained in Coomassie stain for 30 min and then de-stained using de-stainer solution (for composition of solution see 3.1.3) .The protein bands were stained in blue color.

3.4.3. Silver staining

The SDS page gels were incubated in the fixer solution for 60 min. The gels were washed in 50% ethanol for 15 min followed by 30% ethanol for another 15 min. The gels were then shaken in sodium thiosulphate solution for 1 min and washed 3 times in water quickly within 30 seconds. The gels were then incubated in silver nitrate solution for 20 min and then washed 3 times with water. The gels were then incubated in developer solution, which was often changed to reduce background. The development of the gels was stopped by shaking the gels in 5% acetic acid solution. The gels were finally washed for 10 min twice in water to remove the acid. The developer, silver nitrate solution and sodium thiosulphate solutions are always prepared fresh for silver staining (For composition of solutions, see 3.1.3).

3.4.4. Western blotting

Western blotting is an analytical technique which allows the detection of specific proteins in a given sample. In this technique, after the SDS-PAGE, the proteins which have been separated on the gel are transfered from the electrophoresis gel to the membrane, either nitrocellulose or polyvinylidene difluoride (PVDF), by applying a lateral electric field across the gel and the membrane. The proteins of interest can be detected by using specific antibodies.

The western blot was performed in a Bio-Rad Western Blot apparatus. The assembly was organized in the order: sponge filter, gel, membrane, filter, sponge. The gel was placed on the cathode side to ensure the transfer of the proteins in the right direction. The blot chamber was then filled up with transfer solution buffer and protein transferred to a membrane at 0.3 A and 100 V at room temperature for 1.5-2 h. Due to their negative charge, proteins in the gel move to the positive pole on to the membrane. To check whether the blotting process was successful, the membrane was stained with Ponceau S solution. This sodium diazo- dye stains reversibly stains the protein bands red on the membranes. The nitrocellulose membrane was incubated for 15 min with Ponceau S solution and then rinsed with tap water until the proteins were visible as bands. In this way, it was possible to check the protein transfer as well as a uniform protein loading of different tracks.

The membrane was then blocked with milk protein solution for 1 hr to prevent any non-specific antibody binding. Milk powder contains a mixture of proteins, which bind to non-protein areas on the membrane, and thus allows specific immunological detection of the target proteins.

After incubation in milk protein solution the membranes were washed with TBS-T and incubated with a primary antibody solution at room temperature for 1 h or at 4°C over night. The primary antibody solution comprised of the specific dilution of primary antibody dissolved in 1x TBS, 0.1% Tween-20 (v/v); 5% BSA (w/v); 0.02% NaN_3 (w/v). BSA was added to the solution in order to block non-specific binding and sodium azide as a preservative. After primary antibody incubation, unbound antibodies were removed by washing with TBS-T three times. The membrane was then incubated with a secondary antibody solution (1 x TBS; 0.1% Tween-20 (v/v), secondary antibody 1:10000) for 1 hr. The secondary antibody was coupled to horseradish peroxidase. The choice of species of secondary antibody depended on the primary antibody.

Subsequently, Lumi-light western blot substrate 1 and 2 were mixed 1:1, added to the membrane and incubated for 5 min. This solution contains peroxide which is a substrate for horseradish peroxidase.This enzyme catalyses the oxidation of luminol to 3-aminophthalate by formation of several intermediate products. From this reaction, light is emitted at 428 nm, which then was used for detection of the specific protein by chemo-luminescence chamber (analyzer VWR). The membrane was then stored at -20 ºC.

3.4.5. Chromatographic protein purification of His tagged proteins

The histidine tagged receptor exo domain receptor protein purification was performed with the Fast protein liquid chromatography (FPLC), Äkta purifier® (GE Healthcare). A FPLC system allows automated and consistently reproducible protein purification process. To purify the exo-mTSLPR-domain 8x-His tagged protein, a 2 ml nickel Sepharose column (GE Healtcare) was used. The proteins containing supernatant as obtained from the HEK-exo-mTSLPR-cell line was filtered and dialysed overnight in 20 mM sodium phosphate buffer pH 7.5. The supernatants were then pumped

over the nickel column and then washed with buffer in next cycle. The bound protein was eluted with an increasing step gradient of Imidazole. The eluted fractions were collected in the fraction collector and then analysed for the presence of protein using western blotting and silver gel. The manufacturer's specifications for flow rate and purification steps of the matrices were followed. Once a program has been obtained, it can be used for further purification cycles. The proteins were dialysed in a membrane bad in required buffers overnight at 4ºC.

3.4.6. Expression and purification of MBP-fusion proteins

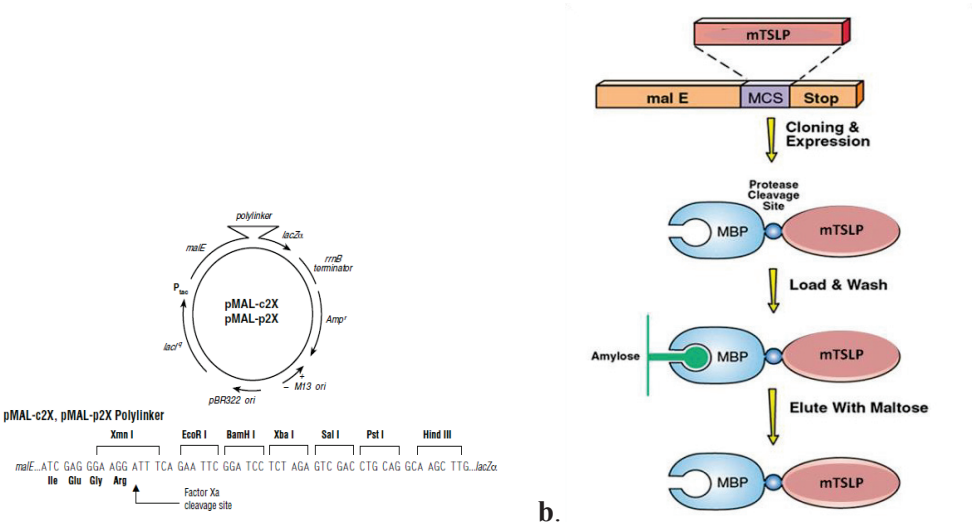

Fig.3.6. The pMAL-2 vectors expression system for production of mTSLP. a. pMAL-c2X (6646 base pairs) has its malE signal sequence deleted.pMAL-p2X(6721 bp) includes the male signal sequence. The arrows indicate the transcription direction of the gene. The unique sites for restriction are shown. b. Scheme showing the cloning and purification steps using the pMAL system via affinity chromatography on amylase column.

The pMAL™-2 vectors (Fig. 3.6) express the target protein quickly and efficiently as a fusion protein along with maltose-binding protein (MBP) separated by a cleavage site. The gene of interest (mTSLP/I37E mutant mTSLP) was cloned downstream from the malE gene of *E. coli*, encoding the maltose-binding protein (MBP), resulting in the expression of an MBP fusion protein.

It was decided initially to try the p2X and the c2X series and to choose the better one. In p2X series vectors, the protein is produced in the periplasmic space. The signal peptide, on pre-MBP guides the fusion proteins the periplasm. If the mTSLP fusion protein could be successfully exported, this would allow the folding and disulfide bond formation to successfully take place in the periplasm of *E. coli*, so as to allow the purification of the proteins from the periplasmic space.

The pMAL-c2X and pMAL-p2X vectors that are used for the production of mTSLP encode the site for Factor Xa (Ile-Glu-Gly-Arg). Factor Xa cleaves after these four amino acid recognition sequence so as to leave few or no vector-derived residues attached to the protein of interest. This is dependent on the cloning site used for the purpose.

An overnight culture was produced by growing a colony from the respective plates produced above in 100 ml of LB medium with glucose (1%) + Ampicillin (1:1000) in two respective conical flasks. 20 ml of overnight culture was used from each flask to inoculate total 1 litre of respective cultures (LB medium with glucose (1%) + Ampicillin (1:1000)) in 2 ml flasks. The bacteria were grown at 190 rpm and 37°C for approximately 3 h when an O.D. of 0.5 was reached. At an O.D. of 0.5 cells were induced with a molecular mimic of allolactose, a lactose metabolite that triggers transcription of the lac operon, 1M Isopropyl β-D-1-thiogalactopyranoside (IPTG), before which some uninduced sample was collected for Coomassie gel analysis. The flasks were shaken for another 6-8 h at 190 rpm and 37°C for production of adequate protein.

Purification by affinity chromatography from the periplasmic extract: The protein laden cells obtained above were harvested by spinning on the centrifuge them at 4000 rpm for 20 min. The pelleted bacterial cells were resuspended in 400 ml of 30 mM Tris-HCl; 20% sucrose; pH 8.0. EDTA was added to the mixture (0.15 g in 400 ml). The mixture thus obtained is incubated for 5 – 10 min at room temperature on a shaker. Now the mixture was centrifuged at 8000x rcf for 20 min at 4°C. All the supernatant was removed. The pellet was resuspended in 400 ml of 5 mM $MgSO_4$. The mixture is then incubated on an ice bath on a shaker for 10 min. The mixture is again centrifuged at 8000x rcf for 20 min at 4°C. Now to the supernatant was added 8 ml of 1 M Tris-HCl; pH 7.4 (osmotic shock fluid). After this equilibration of the amylose resin column with Lysis buffer (2x – 3x column volumes) was performed. The sample was loaded on the column. The column was washed with 2x – 3x column volumes Lysis buffer. The fusion protein was eluted with elution buffer. The eluted fractions were collected as volume of 500 µl each (around 5 ml of elution buffer was used so as to produce 10 fractions of eluted solution). The protein samples could be dialysed in Dialysis buffer (10 mM Tris-HCl; 50 mM NaCl; pH 8.0).The proteins samples were run over a 12.5% SDS gel and a Commassie staining was performed (see section.4.3). The concentration of the protein was determined by measuring the concentration on the Nanodrop spectrophotometer or a Bradford assay. Prot Param tool was used to get the actual concentration by dividing it with the extinction coefficient. For the samples shown in figure the concentration of protein was 2.5 mg/ml. Additional bands were seen in Coommassie perhaps point out that the protein undergoes degradation or half trancribed protein fractions are produced.

Purification by affinity chromatography from the cytoplasmic extract: The protein laden cells obtained above were harvested by spinning on the centrifuge them at 4000 rpm for 20 min. The cells pellets obtained were resuspended in 3 ml of Lysis buffer (protease inhibitors were added). The cells were sonicated at 3x 40 cycles. The cells lysate thus obtained was centrifuged at max.speed for 30 min at 4°C. The amylose resin columns were equilibrated with Lysis buffer (2x – 3x column volumes). The supernatant from the centrifuged lysate was loaded on the column. The column was washed with 2x – 3x column volumes with Lysis buffer. The protein was eluted with the elution buffer. Fractions of 500

µl were collected (around 5 ml of elution buffer was used so that means 10 fractions of eluted solution were obtained). The protein samples could be dialysed in dialysis buffer (10 mM Tris-HCl; 50 mM NaCl; pH 8.0). The proteins samples were run over a 12.5% SDS gel and a Commassie staining was performed. The protein concentration was determined by measuring by Nanodrop or doing a Bradford assay and dividing it with extinction coefficient calculated from the Prot Param tool online.

3.4.7. Enzyme-linked immunosorbent assay (ELISA)

The binding activity characterization of the cytokine and their receptors was done by an ELISA. An immunoabsorbent 96 well ELISA plate was coated with wild type mTSLP-MBP fusion or commercial TSLP for overnight mixed with PBS. The plate was then treated with exo-mTSLPR - His8x TraN in increasing concentrations (Fig. 4.12,4.13) and the binding quantified by detecting the His Tag via anti His primary and HRP conjugated secondary antibodies and 3,3',5,5'– Tetramethylbenzidine (TMB)-Citrate Buffer substrate reaction. The reaction was stopped using 2N H_2SO_4 and the absorbance from the plate was read in an ELISA plate reader at measurement wavelength 450 nm and reference wavelength used was 570 nm. (see Fig. 4.12 for scheme of ELISA)

4. Results

4.1. Generation of an effective readout system for characterizing and analyzing murine TSLP (mTSLP) signaling activities

4.1.1. Improvisation of the Ba/F3 system to generate a novel readout system for the quantification of the relative bioactivity of murine TSLP (mTSLP)

The cytokine mTSLP activates the cell signaling via the JAK Stat pathway (Wohlmann et al., 2010). An artificial system was designed to quantify the activation of the STAT signaling cascade inside the cells in the form of a relative readout. This system could be used for comparing the luciferase reporter gene activity of mTSLP receptor expressing Ba/F3 cells treated with cytokine to that of the cells without any cytokine treatments. The readout system expressing the native chains on the cell surface was designed as follows:

Ba/F3 cells which are murine pro B cells were transfected with the receptor chain expressing plasmids: pcDNA3.1 mTSLPR, pcDNA3.1 mIL-7Rα and reporter gene pGL3-basic IRF1 Luc using T-16 program on the Amaxa Nucleofactor device (refer protocol in subsection 3.3.7). The transfected plasmids expressed chains similar in structure to the native mIL-7Rα and mTSLPR chains in approximately 12 h and the activity of the reporter gene was best observed between 16-18 h after transfection.

To check the status of the expression of the chains on the surface of the cells, cytometric analysis was performed after transfecting 1 million cells with 5µg plasmid of only one DNA receptor chain thereby expressing only single chain of the receptor on the surface of the cell. Both the chains expressed a tag P5D4 after 12 h of transfection, which could be detected via flow cytometric analysis using a primary antibody directed against P5D4 tag and a secondary fluorophore conjugated antibody anti mouse IgG-FITC (visible in FL-1 channel) (see Fig. 4.1. a-j). 50000 cells were analysed on CyFlogic software. This anti- P5D4 signal readout serves as a direct estimated measure of the expression of mIL-7α and TSLPR chains. The overlay plots between empty vector transfected cells and cells transfected with vector expressing receptor chains (see Fig 4.1 e), showed a low signal shift which indicates that the mIL-7Rα chains were expressed but in a low amount. The mTSLPR chains were expressed in moderate amounts (see Fig 4.1 j).

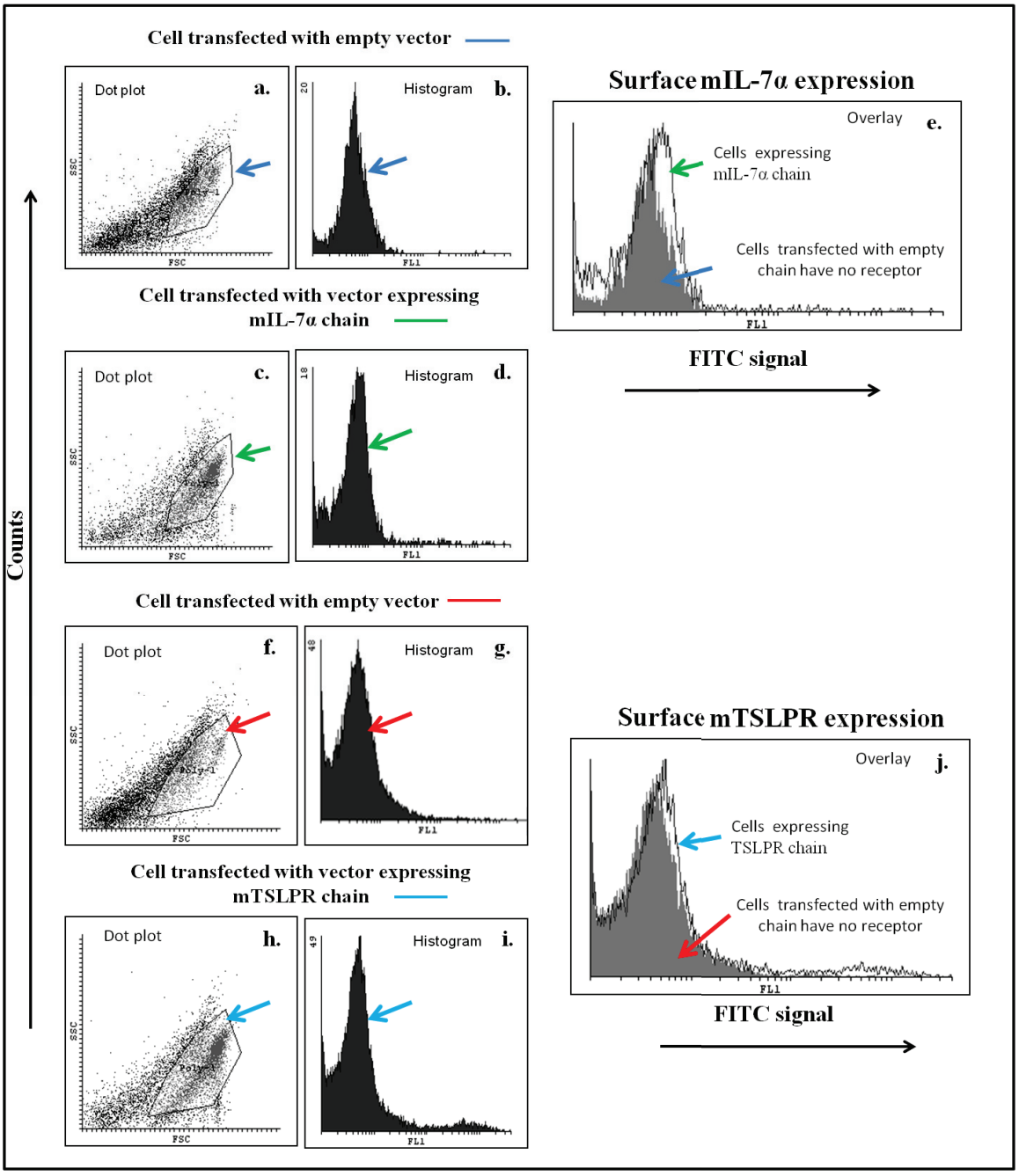

Fig.4.1 Flow cytometric analysis of mIL-7α and mTSLPR receptor chain expression on the surface of the transfected Ba/F3 cell line. Anti- P5D4 Tag Ab treated Ba/F3 cells showing the expression level of murine IL-7/TSLPR chain on the surface of the Ba/F3 cells. The Ba/F3 cells transfected with the empty vector plasmid pcDNA3.1, pcDNA3.1 mIL-7Rα or pcDNA3.1 mTSLPR and then analysed by flow cytometry after staining with the anti- P5D4 tag and a secondary fluorophore conjugated anti mouse IgG-FITC antibodies after 12 h. a. cells transfected with empty vector pcDNA 3.1, b. Histogram for transfected cells with empty vector pcDNA 3.1, c. cells transfected with vector pcDNA3.1 mIL-7Rα, d. Histogram of mIL-7Rα expressing transfected Ba/F3 cells, e. An overlay of the histograms in b and d showing the expression levels of the mIL-7Rα chain, f. cells transfected with empty vector pcDNA3.1, g. histogram for transfected cells with empty vector pcDNA3.1, h. cells transfected with vector pcDNA3.1 mTSLPR, i. histogram of cells transfected with vector pcDNA3.1 mTSLPR, j. An overlay of the histograms in g and i showing the expression levels of the mTSLPR.

Further, in order to check whether the receptors expressed on the cell surface are biologically functional, a luciferase reporter gene assay was performed. The activity of the transient Ba/F3 reporter cell line was tested by treating the reporter gene construct pGL3-basic IRF1 Luc transfected cells with a series of various dosages of mTSLP. mIL-3 serves as a positive control for the reporter gene (see Fig 4.2).

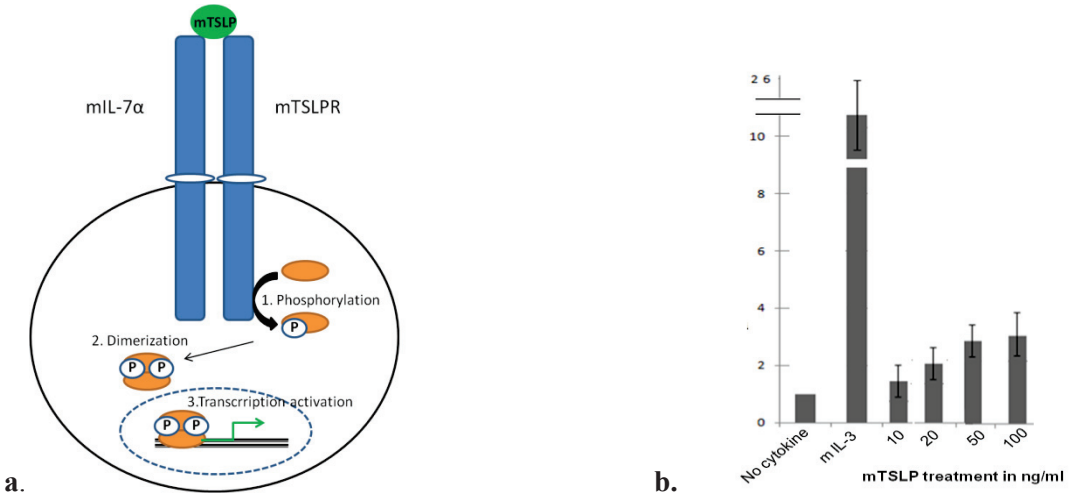

Fig.4.2. Luminometric analysis of the dosage response exhibited by the Ba/F3 luciferase gene readout system.
a. Ba/F3 cell luciferase reporter gene system setup (see text for details) b. relative luciferase activity readout on luminometer. The plasmids for expressing the native chains mTSLPR/IL-7α and IRF Luc reporter gene were transfected in the Ba/F3 cells (T-16 Amaxa program). The cells were given various treatments with cytokine mTSLP in ng/ml as shown, lysed after 16 h and luciferase gene activity evaluated on a luminometer. mIL-3 (20 ng/ml) serves as a positive control for the reporter gene. SD is derived from duplicate samples and shown as error bars. Shown are representative data from three independent experiments.

The relative luciferase reporter gene readout yielded a low comparative luciferase signal mith maximum value as 3 fold. This value of comparative luciferase signal was not sufficient enough for sensitive evaluation of ligand activity. The low amplification magnitude factor 3 of the luciferase assay readout is in line with the findings of the results obtained from flow cytometry which indicated the low expression of the mIL-7Rα receptor chain (see Fig. 4.2.b.).

4.1.2. Ba/F3 cells system expressing hybrid exo-mouse – intra-human receptor chains on cell surface

It has been shown in the previous section 4.1.1 that the readout based on the native receptor chains is unsatisfactory. It demanded further improvisation so as to get a better evaluation on the readout system. To make this system better we created the exo-mouse – intra-human chain hybrid chains as

described in next section. It was observed by Andreas Wohlmann that the hybrid receptors are providing better amplification of luciferase signals when used together with human intra domain receptor chains (Wohlmann, 2014). Based on this observation it was decided to combine the exo-domains of mouse into already existing human TSLP receptor chains.The hybrid receptors were generated by constructing the expression plasmids pcDNA3.1 exo-mTSLPR-intra-hTSLPR hybrid and pcDNA3.1 exo-mIL-7Rα-intra-hIL-7Rα hybrid. These hybrid genes were amplified by generating the DNA sequences encoding the murine exo domains by PCR using primers: 1. exo-mIL-7Rα-hybrid-For/Rev and 2. exo-mTSLPR-hybrid-For/Rev. These inserts were then ligated into the pJET vector. These pJET vectors carrying inserts were then verified by colony PCR followed by a sequencing of the positive colony, to confirm the presence of the target insert. These were then excised and ligated in the excised plasmids pcDNA3.1 intra-hTSLPR and pcDNA 3.1intra-hIL-7Rα. (see Fig. 4.3). Finally pcDNA3.1 exo-mTSLPR-intra-hTSLPR hybrid and pcDNA3.1 exo-mIL-7Rα-intra-hIL-7Rα hybrid were obtained as a result.

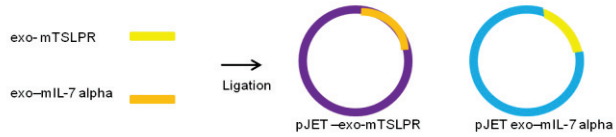

Step1. exo-mTSLPR and exo-mIL-7 alpha DNA inserts was amplified using Phusion PCR from mouse cDNA, cloned in pJET and the sequence verified by colony PCR followed by sequencing for the positive colonies

Step 2. pcDNA 3.1 hTSLPR and pcDNA 3.1 hIL-7 alpha were excised using enzymes Bgl-II and Bam-HI

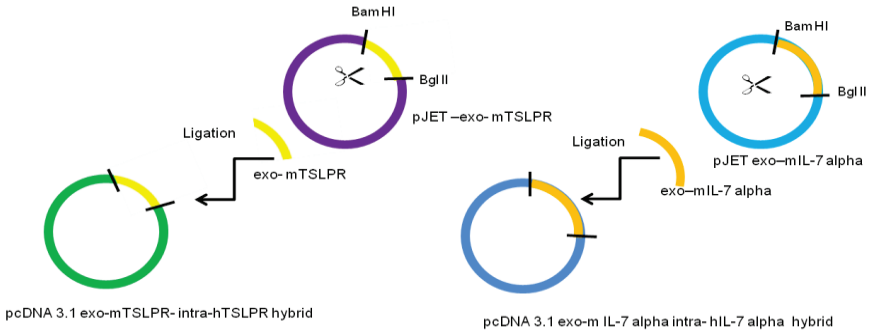

Step 3. pcDNA 3.1 exo-mTSLPR- intra-hTSLPR hybrid and pcDNA 3.1 exo-m IL-7 alpha intra- hIL-7 alpha hybrid were generated by excising the desired inserts from pJET using enzymes Bgl-II and Bam-HI and ligating them in the plasmids obtained from step 2

Fig.4.3. A schematic representation of cloning performed for generating the hybrid chain expressing plasmids. The DNA inserts which express exo-domains of murine TSLP receptor were cloned in already existing hTSLP receptor chain expressing plasmid DNA. The cloning was carried out in three steps as shown above. For details see text.

To evaluate functional properties, 1 million Ba/F3 cells were taken and transfected with 5 microgram of the receptor chains expressing plasmids: pcDNA3.1 exo-mTSLPR-intra-hTSLPR hybrid and pcDNA3.1 exo-mIL-7Rα-intra-hIL-7Rα hybrid as cloned above and reporter gene pGL3-basic IRF1-Luc using T-16 program on the Amaxa Nucleofactor device (Refer protocol Nucleofaction (Section 3).

The transfected plasmids expressed chains exo-mTSLPR-intra-hTSLPR hybrid and pcDNA3.1 exo-mIL-7Rα-intra-hIL-7Rα hybrid on the surface of the cells in approximately 12 h and the activity of the reporter gene was best observed between 16-18 h after transfection. To check the status of the expression of the chains on the surface of the cells, flow cytometric analysis was performed after transfecting the cells with only one plasmid DNA thereby expressing only single chain of the receptor. Both the chains expressed a tag P5D4, which could be detected by using a primary antibody directed against P5D4 tag and a secondary fluorophore conjugated antibody anti mouse IgG-FITC on FACS after 12 h of transfection (see Fig Results 4.4). This Anti- P5D4 readout serves as a direct estimated measure of the expression of mIL-7 and mTSLPR chains.

The overlay plots showed a stronger signal shift which indicates that the pcDNA3.1 exo-mTSLPR-intra-hTSLPR hybrid and pcDNA3.1 exo-mIL-7Rα-intra-hIL-7Rα hybrid chains were expressed in a higher amount as compared to the wild type native chains as described in 4.1.1.

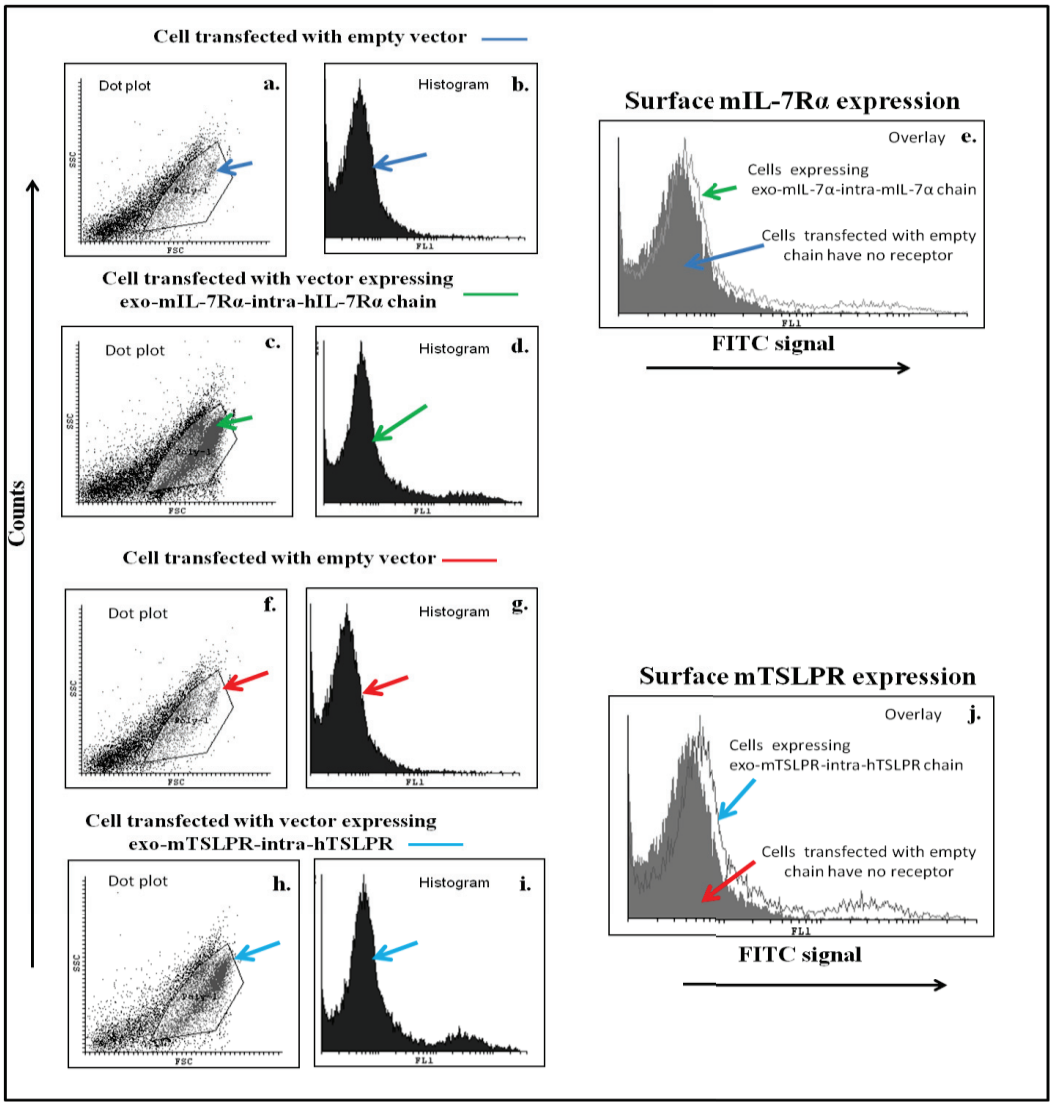

Fig.4.4. Flow cytometric analysis of hybrid receptor chain expression on the surface of the transfected Ba/F3 cell line. Analysis of exo-mIL-7Rα-intra-hIL-7Rα receptor expression on the surface of the Ba/F3 cell line using flow cytometer: a-e. Anti- P5D4 Tag expression readout showing the expression level of the pcDNA3.1 exo-mIL-7Rα-intra-hIL-7Rα to produce exo-mIL-7Rα-intra-hIL-7Rα chain on the surface of the Ba/F3 cells. The cells were transfected with the plasmids and then readout after staining with the anti- P5D4 tag and a secondary flurophore conjugated anti mouse IgG-FITC antibodies on FACS after 12 h. a. cells transfected with empty vector b. histogram of cells transfected with empty vector c. cells transfected with the plasmid pcDNA3.1 exo-mIL-7Rα-intra-hIL-7Rα d. histogram of cells transfected with pcDNA3.1 exo-mIL-7Rα-intra-hIL-7Rα e. overlay of histograms b and d.

Analysis of hybrid chains pcDNA3.1 exo-mTSLPR-intra-hTSLPR receptor expression on the surface of the Ba/F3 cell line using flow cytometer f-j.: Anti- P5D4 Tag expression readout showing the expression level of the exo-mTSLPR-intra-hIL-7Rα to produce exo-mTSLPR-intra-hIL-7Rα chain on the surface of the Ba/F3 cells. The cells were transfected with the plasmid and detected as above 12 h. f. cells transfected with empty vector g. histogram of cells transfected with empty vector h. cells transfected with the plasmid pcDNA3.1 exo-mTSLPR-intra-hIL-7Rα i. histogram of cells transfected with pcDNA3.1 exo-mTSLPR-intra-hIL-7Rα, j. overlay of histograms b and d. Shown are representative data from three independent experiments.

A receptor activity control test was performed so as to make sure that the single receptor chains transfected in the Ba/F3cells do not give false positive signals with some native receptor present on the cell surface. Also the specificity of the transient Ba/F3 readout can be tested by treating the system with another cytokine except mTSLP. Here we used hIL-4 (see Fig. 4.5 c.). It was observed that there was only a signal when all the three chains were transfected together and treated with mTSLP. This indicates that the system is highly specific for induction with mTSLP.

As already described above for the native receptors, the activity of the transient Ba/F3 reporter cell line was further tested in a luciferase reporter gene assay by treating the transfected cells with a gradient of various dosages of mTSLP. mIL-3 serves as a positive control for the reporter gene (see Fig 4.5 b).

The receptor chains show improved expression levels. This is improved luciferase reporter gene readout as compared to the one described in 4.1.1. This system with hybrid chains yields an improved evaluation of the quantified data to the order of 6 fold signals as compared to the untreated sample. This is in line with the obtained observations through flow cytometry which show that the hybrid chains are expressed well on the surface of the cells.

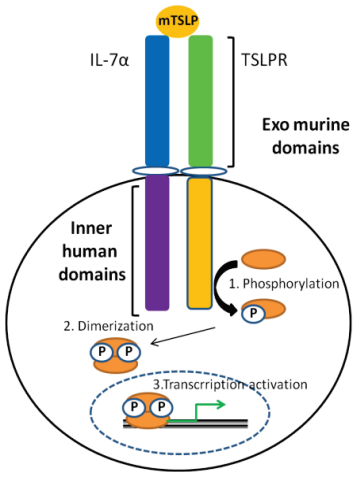

a.

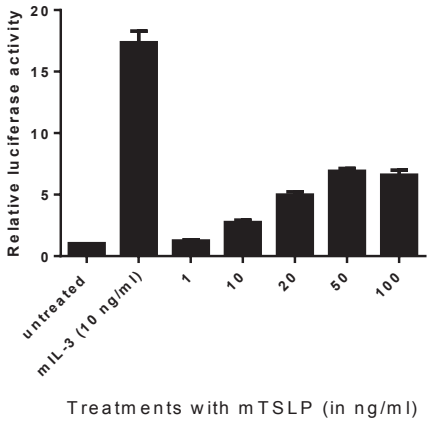

b.

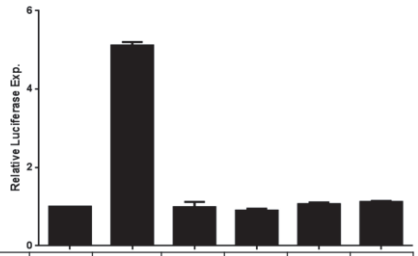

exo-mIL-7Rα-intra-hIL-7Rα hybrid (Hyb1)	+	+	+	-	-	+
exo-mTSLPR-intra-hTSLPR hybrid (Hyb2)	+	+	-	+	-	+
IRF-Luc Reporter	+	+	+	+	+	+
Cytokine	No mTSLP	50 ng/ml mTSLP	50 ng/ml mTSLP	50 ng/ml mTSLP	50 ng/ml mTSLP	50 ng/ml Human IL4

c.

Fig 4.5. Analysis of signalling activity of the murine TSLP hybrid receptor chains with Ba/F3 luciferase gene readout system Ba/F3 Luciferase readout with hybrid chains **b).** Ba/F3 cell-hybrid chain luciferase reporter gene readout on Glomax. The hybrid chains exo-mTSLPR-intra-hTSLPR hybrid/exo-mIL-7Rα-intra-hIL-7Rα hybrid and IRF-Luc reporter gene were transfected in the Ba/F3 cells (T-16 Amaxa program). The cells were given various treatments with cytokine mTSLP in ng/ml. mIL-3 (10 ng/ml) serves as a positive control for the reporter gene. SD is derived from duplicate samples and shown as error bars. Shown are representative data from three independent experiments.

4.1.3. Probing the effects of relative rotation of TSLP receptor chain domains on induced reporter gene activation

There was further scope of improvising the Ba/F3 luciferase readout system by relative rotation of the transmembrane domains (Bell et al., 2000) of the inner hybrid human chains as shown by Wohlmann (Wohlmann, 2014) in case of human TSLP chains. To test the possibility that the signal intensity of the Ba/F3 system could be further enhanced, the clones were prepared by Wolhlman by introducing internal human chains which had 1-4 amino acid extra in the transmembrane domain. One amino acid twisted the chain by 110° changing the spatial confirmation in such a way to increase the final luciferase activity several folds higher (see Fig. 4.6). The effective rotations, compositions and various possible combinations of these chains are listed in the table 4.1.

Table 4.1(a). Composition of chains with rotated domains (b) combination of chains

Domain combination	**Name**	**Rotation (in degrees)**
exo-mTSLPR-intra hTSLP + 4AA	T5	+440
exo-mTSLPR-intra hTSLP + 3AA	T6	+330
exo-mTSLPR-intra hTSLP + 2AA	T7	+220
exo-mTSLPR-intra hTSLP + 1AA	T8	+110
Domain combination	**Name**	**Rotation**
exo-mIL-7-intra hIL-7+ 4AA	71	+440
exo-mIL-7-intra hIL-7– native	72	+ 0
exo-mIL-7-intra hIL-7+ 2AA	73	+220
exo-mIL-7-intra hIL-7+ 1AA	74	+110

	IL-7_0	**IL-7_0+4AA or 71**	**IL-7_0 native or 72**	**IL-7_0+2AA or 73**	**IL-7_0+1AA or 74**
T_0	$T_0/7_0$	-	-	-	-
T_0+1AA or T5	-	T5/71	T5/72	T5/73	T5/74
T_0+2AA or T6	-	T6/71	T6/72	T6/73	T6/74
T_0+3AA or T7	-	T7/71	T7/72	T7/73	T7/74
T_0+4AA or T8	-	T8/71	T8/72	T8/73	T8/74

For studying the functional properties of these chains, the various combinations of the plasmids expressing these chains (5 microgram) were transfected separately into 1 million/ml Ba/F3 cells using Amaxa T-16 program. The various combinations are listed in the table 4.1 b above.

All the combinations of cells were treated with 20ng/ml of mTSLP. After 16 h they were lysed and the relative luciferase activity was determined through a luminometric analysis. The results obtained are shown in Fig 4.6 b.

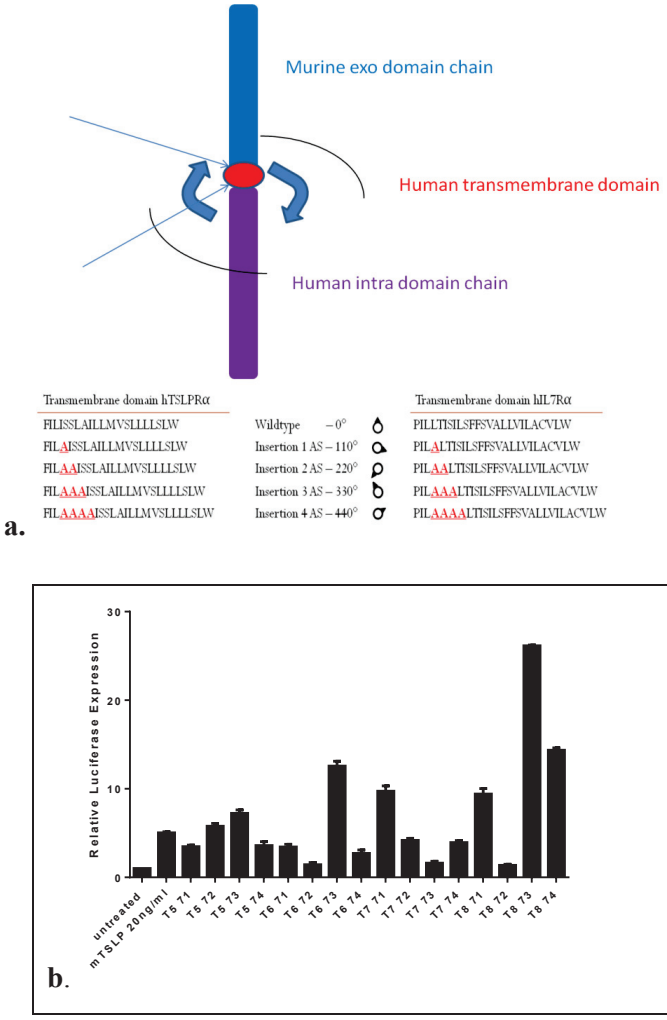

Fig.4.6. Effects of relative domain rotations in the transmembrane region. a. Schematic representation of the domain rotated hybrid chains. b. Luminometric analysis of relative luciferase activity on Ba/F3 readout (for experimental details see text). SD is derived from duplicate samples and shown as error bars. Shown are representative data from three independent experiments.

The combination T8/73 gave signals 5 fold higher as compared to the native chains without insertion of amino acids. The possible combination thus obtained can provide better resolution of signaling activity in the luciferase assay and used for further studies.

4.2. Cloning, expression, purification and characterization of the exo-domain of the TSLPR chain and its use in producing an anti-mouse TSLPR antibody

4.2.1. The purpose of production and cloning of mTSLPR exo-domain protein

Murine Thymic stromal lymphopoietin (mTSLP) is a cytokine produced by the epithelial cells at barrier surfaces. mTSLP acts as a pivotal axis of the inflammatory responses by immune cells in the development of chronic inflammatory disorders such as asthma and atopic dermatitis (see section 1.Introduction). TSLP establishes extensive interfaces with its cognate receptor (TSLPR) and the shared interleukin 7 receptor α (IL-7Rα) chain to induce a membrane-proximal receptor complex poised for intracellular signaling. TSLP binding to TSLPR is a mechanistic prerequisite for the recruitment of the IL-7Rα chain to the high-affinity ternary complex, which is coupled to a structural signaling switch in TSLP at the crossroads of the cytokine-receptor interfaces. Further functional studies of the TSLP-receptor interfaces can lead to putative interaction hotspots which could be exploited for designing antagonists.

The purpose of cloning exo-mTSLPR domain was to use it as an antigen for immunizing rats for the generation of anti murine TSLPR antibodies, as an active inhibitor for blocking mTSLP signaling and for testing the bioactivity of mTSLP-MBP wild and mutant I37E mTSLP-MBP fusion proteins.

Cloning: The cDNA sequence to the exo-mTSLPR-domains was obtained from NCBI Gene database. The expression vector pcDNA3.1 exo-mTSLPR was designed using program Ape editor. The gene was amplified using Phusion polymerase PCR reaction from the plasmid pcDNA3.1 mTSLPR (containing code for murine native TSLPR chain), spleen and liver gDNA (see Fig. 4.7).The primers used were: exo-mTSLPR-His8xTraN For , exo-mTSLPR-His6x For and RP exo mTSLPR Rev (see 3.1.11).

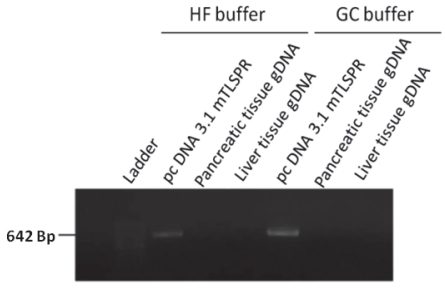

Fig.4.7. Production of insert exo-mTSLPR by Phusion PCR. An agarose gel showing the products obtained via a Phusion polymerase chain reaction (PCR) using primers as described above in a PCR program (see materials and methods section 3.2.10. for conditions). The desired product is visible as a band at 642 Bp in length.

The exo-domain insert thus obtained was cloned into the pJet plasmid, verified by colony PCR and sequencing for the accuracy of the sequence and then cloned into pcDNA 3.1-hTSLPR by excising the inserts by Xho1 and Not 1. The constructs thus obtained from this cloning appeared as shown in Fig 4.8 a and b. This cloning was performed by Simone. The expression plasmids contain the signal sequence and tags as shown in Fig 4.8 a. and b. see appendix for maps.

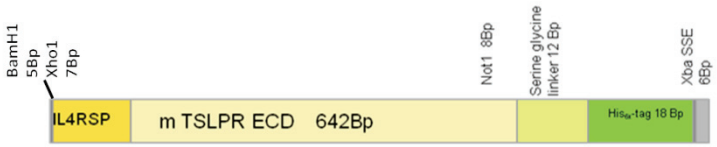

Fig.4.8 a. Schematic linear illustration of exo-mTSLPR His6x plasmid gene sequence including restriction sites. The DNA segment was arranged in the order: BamH1 (5Bp), Xho 1(7 Bp), signal peptide (74 Bp), mTSLPR ectodomain 642 bp. Not1 (8Bp), Serine Glycine Linker SGL, His6x (18 Bp) and Xba SSE enzyme (68Bp). The His6x-tag to could be used for the detection and purification of the ectodomain protein. The sequence was cloned in pcDNA3.1 expression vector.

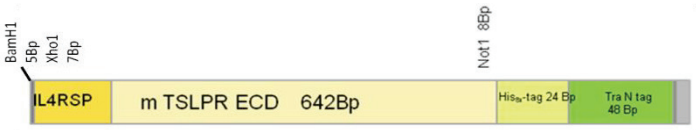

Fig.4.8 b. Schematic illustration of exo-mTSLPR-8x His TraN sequence including restriction sites. The DNA segment was arranged in the order: BamH1 (5 Bp), Xho1(7 Bp) signal peptide74 Bp, mTSLPR ectodomain 642 Bp. Not1 (8 Bp); His8x (24 Bp) TraN (48 Bp) Xba SSE enzyme (68 Bp).The TraN and His8x-tag could be used in the detection and purification of the ectodomain protein. The sequence is cloned in pcDNA3.1 expression vector.

4.2.2. Expression of mTSLR exo-domain protein

A stable cell line was prepared by transfecting the recombinant plasmid thus obtained into HEK 293T cells by using a. Amaxa Nucleofactor and b. Turbofect. The program used was A-23. For transfection protocols refer to section 3.3.7. The stable cells were selected via resistance against antibiotic zeocin in DMEM medium for a week. Cells which were successfully transfected survived in zeocin containing medium and these were frozen at -80°C in 10% DMSO, 20% FCS and 70% DMEM. A few aliquots were taken and grown (1 million/ml cells) in medium DMEM 10% FCS, 1% Gentamycin in 75 sq m flasks till confluence. The supernatant was harvested every 4th day (yellow in appearance). The cells were split 1:10 and reused. Relative protein production as an indicator for the transfection efficiency was checked by SDS PAGE (see Fig 4.9).

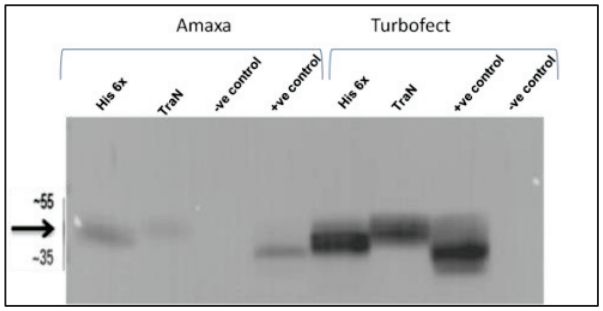

Fig.4.9. Western blot analysis showing comparative expression of mTSLPR in HEK 293T cells transfected with pcDNA3.1 exo-mTSLPR-His 8xTraN by Amaxa and Turbofect. The western blot shows the expression of mTSLPR in supernatants from stably transfected HEK293T cells with pcDNA3.1-mTSLPR-His8xTraN. The transfection methods used were a. Amaxa Nucleofactor and b. Turbofect. Anti-Histidine antibody (Qiagen) was used as primary and goat anti mouse Ab (Santa Cruz) was the secondary Ab used for detection of the bands. Positive control: hTSLPR-His Tag Negative control: Loading buffer. The cells transfected with Turbofect showed better expression of protein.

The western blot analysis shows that the cells transfected via amaxa showed lesser expression of protein as compared to those transfected by Turbofect transfection medium. This shows that the transfection method is critical to the production of the proteins. Therefore, the scaling up of production of exo-mTSLPR was done with cells transfected with Turbofect®.

4.2.3. Production and purification of mTSLPR exo-domain protein

The stable HEK 293-exo-mTSLPR-His8x-TraN cells obtained as above were grown (1 million/ml cells) in 175 sq. cm flasks in DMEM medium with 10% FCS and 1% gentamycin till confluence. The antibiotic resistance was maintained by adding zeocin in 1 microgram per ml. The supernatant was harvested every 4th day (yellow in appearance). The supernatants were spun in centrifuge at 4500 rpm for 15 min, filtered and stored at minus 20°C in 1 litre bottles till purification via affinity chromatography through the His8x tag-nickel fast flow column interactions.

The supernatant was then dialyzed at 4°C overnight inside the dialysing bags in Na-Phosphate Buffer (pH 8.0) and proceed for further purification on ÄKTA explorer purification system via Ni-Affinity chromatography and a western blot was run to detect the protein in the eluted fractions. It was observed that the protein was eluted in the range from 25% to 70% of the Imidazol gradient elution (see Fig. 4.10). The purity of the sample was assessed via a silver gel (see Fig. 4.11). For dialysis and silver gel protocols, please refer to sections 3.4.3 and 3.4.5.

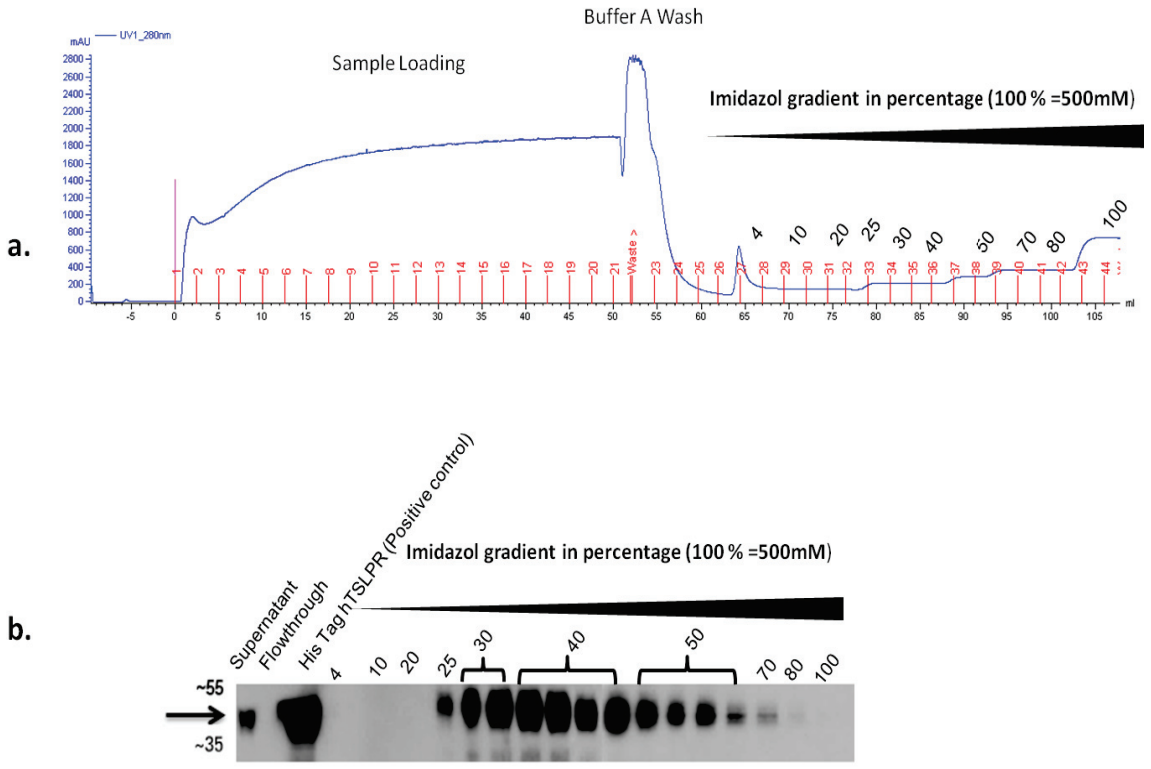

Fig.4.10. **Purification of exo-mTSLPR-His8xTraN protein on ÄKTA explorer purifiction system.**

a. A chromatogram showing the loading and gradient elution of exo-mTSLPR-His8xTraN protein based on the affinity of the protein´s His tag towards nickel coated matrix on the fast flow separation column. The various phases of loading and elution of the protein are indicated in the diagram. The supernatant obtained from HEK 293-exo-mTSLPR-His8x-TraN cells was loaded over a Ni-Fast flow column, washed and then the protein eluted. The elution was made by step gradient increase of Imidazol concentration percentage in the Na-Phosphate buffer. (pH 8.0).

b. A western blot showing the elution performed via a stepwise increasing gradient of Imidazol (expressed in percentage where 100% equals to 500mM). The eluted fractions were analysed by staining with anti His tag antibodies. His tagged human TSLPR serves as a positive control.

The fractions thus obtained were mixed to obtain final 3 fractions. The proteins were further dialysed (for protocol see materials and methods section 3.4.4) in PBS by putting them in dialysis bags overnight at 4 ºC. The proteins were further concentrated by spinning them on Millipore concentrator tubes (cutoff 30000 daltons). The concentrated proteins thus obtained were frozen at -20 ºC.

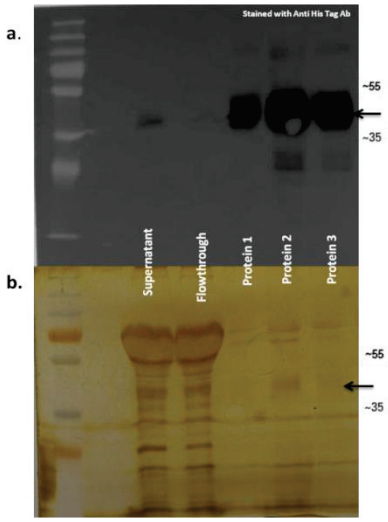

Sample	Conc. (mg/ml)	Volume (in ml)	Final amount (mg)
Protein 1	0.0805	7	0.5635
Protein 2	0.2265	2	0.453
Protein 3	0.1645	5	0.8225
Total	-		**1.8 mg**

Fig.4.11. Analysis of mTSLPR production via western blot and silver gel analysis. a. Western blot (stained with anti-His tag antibody) showing the purified and concentrated exo-mTSLPR-His8xTraN fractions as obtained via purification in 4.10. b. silver gels showing purified murine TSLP receptor protein (indicated by the arrows). Silver gels were run to assess purity of the sample. Approximately 1.5 litres of supernatant was used for this purification.

4.2.4. Characterization of the ligand binding properties of exo-mTSLPR protein

The exo-mTSLPR protein which is obtained as purified above is characterized for its binding properties towards the mTSLP-MBP fusion protein (see production and purification in results section 4.3) by an ELISA. The scheme for ELISA is illustrated in Fig 4.12. An immunoabsorbent 96 well ELISA plate was coated with wild type mTSLP-MBP fusion or commercial TSLP mixed with PBS overnight. The plate was then treated with exo-mTSLPR in increasing concentrations (Fig 4.13) and the binding quantified by detecting the His tag via anti His and HRP conjugated secondary antibodies and substrate (TMB-Citrate buffer) reaction.

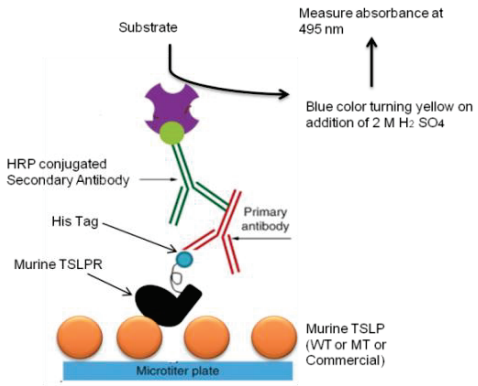

Fig.4.12. Schematic representation of ELISA to detect the binding activity of exo-mTSLPR His8xTraN to its ligand murine TSLP-MBP/commercial TSLP. The plate was coated with mTSLP (fusion or commercial). The His tag was detected via primary anti His tag antibody and secondary anti HRP conjugated antibody. TMB-citrate acid buffer was used as a substrate.

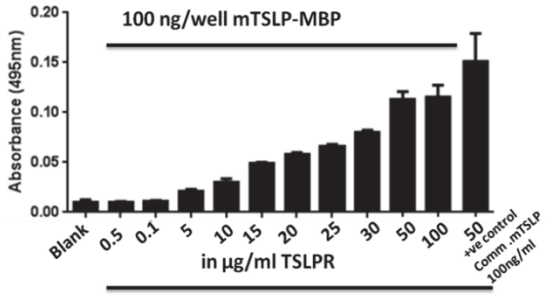

Fig.4.13. ELISA based analysis to detect the binding activity of exo-mTSLPR to its ligand murine mTSLP-MBP /commercial TSLP. The plate is coated with mTSLP-MBP (100ng/well) in PBS. The mTSLPR was added in different dosages as shown in the graph followed by washings with PBST. The mTSLP which binds to the cells is detected via primary anti His tag antibody and secondary anti HRP conjugated antibody. The TMB-citrate acid buffer was used as a substrate for HRP and produced a blue color which turned yellow on addition of 2M H_2SO_4. 50 ng/ml commercial TSLP coated well acts as a positive control. 100 µg/ml TSLPR is added to this well.

It is observed that mTSLPR-exo shows binding towards mTSLP-MBP and commercial mTSLP in a dosage response curve to reach saturation at 100µg/ml.

4.2.5. Characterization of the biological activity of the exo-mTSLPR in a Ba/F3 cell Luciferase assay

The mTSLPRexo-domain protein obtained was checked for biological activity by using it as a competitor against mTSLP which binds to the TSLPR receptor present on the Ba/F3 cells.

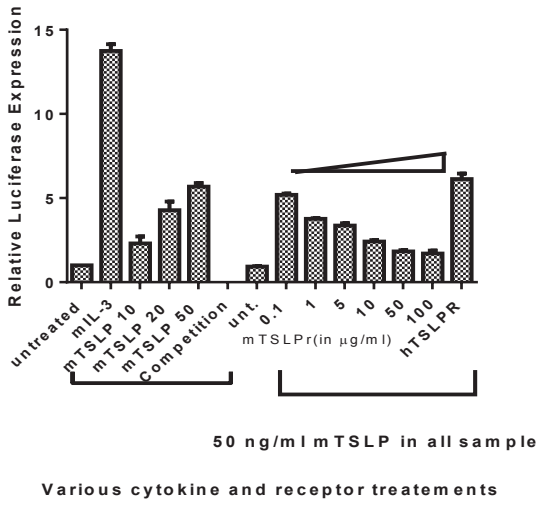

Fig.4.14. A Ba/F3 cell Luciferase assay to prove whether the exo-mTSLPR-His8xTraN is bioactive. The Ba/F3 reporter gene cells were treated with 50 ng/ml of commercial TSLP and then increasing dosages of exo-mTSLPR. hTSLPR (100µg/ml) treatments were given to ensure that mTSLPR-mTSLP interactions are specific.

It was observed that the luciferase signal is impeded as we increase the dosages of the mTSLPR. hTSLPR (100µg/ml) has no effect on the cells thus proving that the mTSLPR-mTSLP interactions are specific. This shows that the exo-mTSLPR domain is active and actively competes with mTSLP and prevents it from bindings to the TSLP receptors present on the cell.

4.2.6. Production and specific binding characterization of rat anti mouse-TSLPR antibody

Monoclonal antibodies against target receptors have been used as valuable therapeutics in recent times. An antibody that binds to the exo-mTSLPR domain could either be an inhibitory antibody or serve the purpose of being used as a detection antibody when coupled to a fluorophore. The exo-mTSLPR protein as produced above was used also to produce an antibody by outsourcing the entire immunization in rats and production strategy to our collaboration partners. The strategy applied for antibody generation is shown in Fig. 4.14.

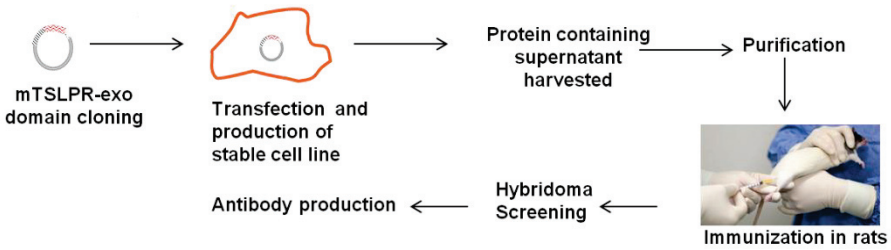

Fig.4.15. A schematic representation of production of rat anti exo-mTSLPR-His8x TraN. The protein after production from the stable cell line as described above was used to immunize rats. The resulting hybridomas were screened and antibody was produced by conventional methods defined.

The rat anti mouse mTSLPR antibody was produced and provided to us for testing. The antibody was provided in two forms, biotinylated and non biotinylated. The antibody was tested for binding by transfecting 1 million cells Ba/F3 cells with only mTSLPR chain expressing plasmid. These cells were allowed to grow for 16 h, washed and were treated with 1µg of anti mTSLPR antibody. The cells were then washed again and stained with goat anti rat IgG-PE secondary antibody. A control experiment was also done to ensure if the TSLPR chain was expressed by detection of the P5D4 tag on the surface of the transfected cells (a-c. The signals were detected by flow cytometry and analyzed using the Cyflogic software. The results obtained are shown in Fig. 4.16.

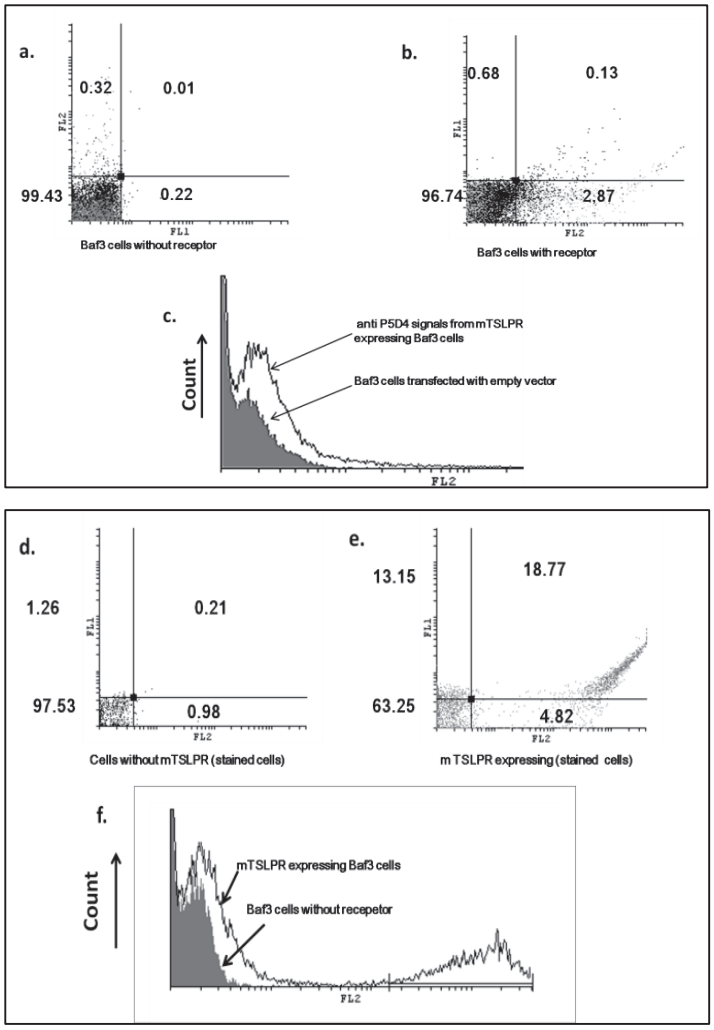

Fig.4.16. Flow cytometric analysis of specific binding characteristic of rat anti mTSLPR. Two sets of $1x10^6$ cells Ba/F3 cells were transfected with empty vector pcDNA3.1 and pcDNA3.1-mTSLPR and the cells were grown overnight for 16 h. 20000 cells were detected on flow cytometer. a-c. show control experiment for detection of mTSLPR expression. The detection was made withanti-P5D4- secondary goat anti mouse IgG-PE antibody. The P5D4 tag is expressed on the surface at the N terminal region of the chain and provides readout for detection of chain expression. d-f. show specific binding characterization of the rat anti-mTSLPR. After expression on the surface of Ba/F3 cells of mTSLPR was confirmed by checking the cells for P5D4 tag expression, the cells were then stained with rat anti-mTSLPR and then with secondary goat anti rat IgG-PE. The figure d- shows dot plot of cells which are transfected with empty vector and which don't express mTSLPR. The figure e represents dot plot from cells transfected with pcDNA 3.1- mTSLPR and which expressed mTSLPR. The figure f- shows the ovelay histogram from samples shown in d and e.

The dot plots and overly 4.16 a-c show that transfected Ba/F3 cells expressed mTSLPR after 16 h while the dot plots and overlay 4.16 d-e shows that the rat anti mouse anti mTSLPR could bind successfully to the mTSLPR chain. The overlay 4.16 c shows a strong shift in signal indicating the binding of antibody to the receptor chain. Thus, after confirming the binding properties, the antibody

was tested in a Ba/F3 Luciferase based mTSLP activity inhibition assay for inhibitory properties. It was found that it was non-inhibitory in nature (data not shown).

4.3. Cloning, expression, production and characterization of mTSLP and I37E mTSLP mutant using the pMAL system

mTSLP was needed to be produced so as to ensure an inexpensive and constant supply for *in vitro/in vivo* studies related to mTSLP signaling. It also had to be used during biological testing of binding studies related to mTSLPR. Therefore a need arose for this protein to be produced in the lab. The initial approaches to produce mTSLP were taken by Andreas Borowski (personal communication) were not successful. The bacterial expression of this protein yielded inclusion bodies and after their lysis, the protein produced using Sepharose G column was not active. The eukaryotic expression was tried in the HEK cells using vectors pcDNA3.1 mTSLP-CD14 signal peptide and pcDNA3.1 mTSLP, did not show any expression on Western blot (data not shown).

4.3.1. Cloning of pMALp2X/c2X-mTSLP constructs

Guan, C. et al. (1987) for the first time described a method for expression of proteins as fusion proteins attached to C terminus of MBP and purification by binding to cross linked amylose. The pMAL vector system is a convenient way of expressing proteins as fusion protein with MBP. The system has been described in materials and methods section 3.2.

In order to produce the mTSLP-MBP fusion protein in the pMAL-2 vectors, the mTSLP gene was inserted into the pMAL-2 vectors in a way that it is in the same translational reading frame as the vector's malE gene. Software Ape was used for the purpose. There were 2 different set of vectors which were used:

The pMAL-c2X was obtained from colleagues in from Experimental Animal Center, Institute of Genetics and Developmental Biology, Chinese Academy of Sciences, Beijing, PR China. The construct was ready to be used for production of mTSLP. The plasmid DNA was amplified via transformation into *E. coli Top* 10 (for detailed protocol, see material and methods 3.1) cells and a plasmid DNA mini prep was done. The sequence was obtained via sequencing of the plasmid DNA. The malE primer which initiates sequence near the 3´ end of malE, 78-81 bases upstream of the primary site in the polylinker, was used for sequencing the plasmid DNA. After ascertaining that the sequence matches to the sequence from NCBI, the plasmid DNA was then used to transform BL-21 DE3 strain (Novagen) cells. These transformed bacteria were directly used for the production of

mTSLP by IPTG induction as described in the materials and methods 3.4.6. This construct secretes the protein in cytoplasm.

The pMAL-p2X vector was obtained as pMAL-p2X-cMPL ectodomain construct from Sebastian Krause, Invigate. This construct secretes the protein in the periplasmic space. Since a comparison of protein secretion efficiency was desired between the cytoplasmic and periplasmic spaces, this vector was modified to insert the mTSLP gene as described below.The software Ape was used for designing the construct map for pMAL-p2X-mTSLP and the primers mTSLP-MBP For (p2X) and mTSLP-MBP-Rev (p2X). These primers were then used to amplify the mTSLP gene from pASKIEP-mTSLP construct as a template. These primers were used to initiate a Phusion Polymerase PCR reaction using the program as listed in materials and method. This construct pMAL-p2X-cMPL was modified by excising the cMPL ectodomain using restriction enzymes Eco RI and Hind III and inserting the mTSLP protein expressing gene (see Fig. 4.17). The cloning was performed by Karstern Letsch. The ligated plasmid thus obtained was transformed into *E. coli* Top 10 cells and the cloning effectiveness was verified by a colony PCR. The positive clones were selected and then their plasmids isolated by mini prep. The plasmid DNA was sent for sequencing to verify the sequence. The malE primer which initiates sequence near the 3´ end of malE, 78-81 bases upstream of the primary site in the polylinker, was used for sequencing the plasmid DNA. After making sure that the sequencing yielded no error, the plasmid DNA was used for protein production by transformation into BL-21 DE3 strain (see materials and methods 3.4.6 for details).

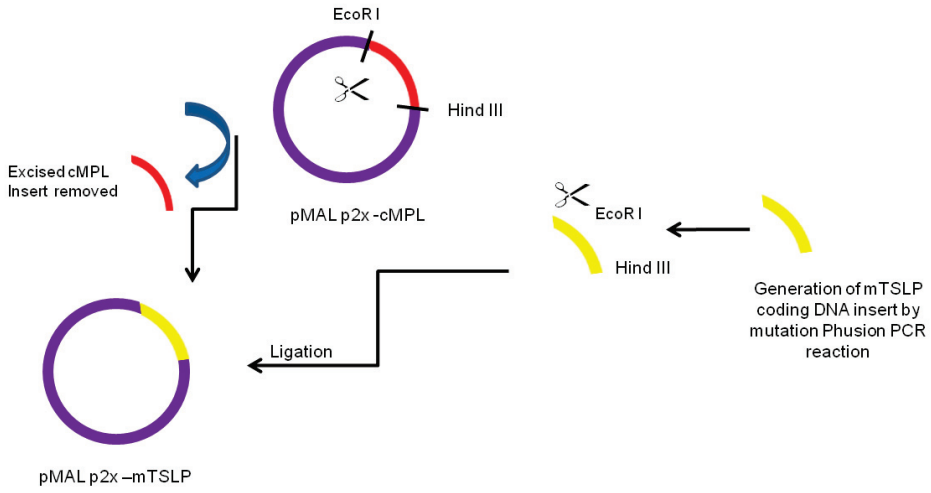

Fig.4.17. Schematic representation of cloning scheme showing the preparation of the pMALp2X-mTSLP vectors. The plasmids pMALp2X-cMPL was restricted with EcoRI and Hind III enzyme treatments. The inserts were generated by a PCR. The insert was ligated in the restricted pMALp2X vector. The end results of the cloning were final vectors pMALp2X-mTSLP.

4.3.2. Expression and purification of mTSLP-MBP fusion protein

The two construct as above: pMALp2X-mTSLP and pMAL-c2X-mTSLP from the Chinese colleagues, were transformed into BL-21 DE 3 (Novagen) competent bacterial cells and were plated on an Agar plate with Ampicillin resistance (100µg/ml Ampicillin resistance) and incubated at 37°C (for protocols see material and method 3.2.1 and 3.2.2).

The protein production was initiated by induction with IPTG 1M at an O.D. of 0.5, for 1 litre of the bacterial culture. 6 h later the cells were harvested by spinning the cells down at 4000 rpm for 20 min. A coomassie gel (for protocol see material and methods 3.4.2 was run with induced and uninduced samples of bacteria to check for the success of induction. The results are shown in Fig.4.18 below:

The weight of the MBP is 42.5 kDa and that of mTSLP is 15 kDa so together, the weight of the fusion protein shall be 57.5 kDa and we must expect a band in the coomassie blot at this level for the mTSLP-MBP fusion protein.

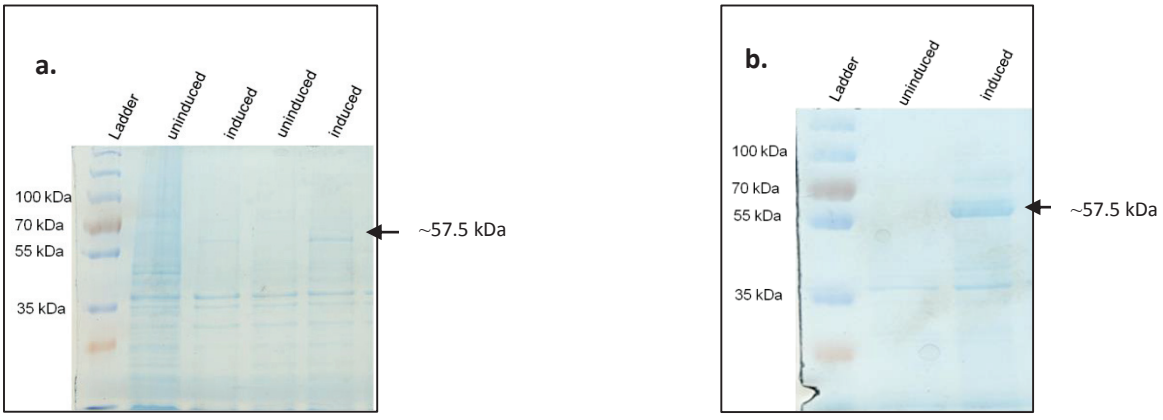

Fig.4.18. Coomassie blot analysis of IPTG induction of BL-21 DE3 cells carrying pMAL-2 series constructs with mTSLP insert.1 litre of bacterial culture was inoculated with 50 ml of the respective overnight bacterial culture and induced with 1M IPTG at OD 0.5 and shaken for 6 h after induction. a. Comparison of pMAL-p2X-mTSLP-BL21 DE3 bacteria samples (uninduced and induced) in different lanes b. Comparision of pMAL-c2X-mTSLP-BL21 DE3 bacteria samples (uninduced and induced) in different lanes. 20 µl of the bacterial culture was mixed in 50 µl of loading dye and out of this mixture 20 µl is loaded on the gel (Fig. from Karstern Letsch, unpublished results).

pMAL-p2X-mTSLP-BL21 DE3 and pMAL-c2X-mTSLP-BL21 DE3 both show induction as evident by the dark band on the Commassie gels at approximately 57.5 kDa.

Purification by affinity chromatography from the periplasmic/cytoplasmic extracts

The protein laden cells obtained above were harvested by spinning on the centrifuge them at 4000 rpm for 20 min and the samples prepared respectively as described in the materials and methods. The protein extraction was made via affinity chromatography on amylase columns. The fusion

protein mTSLP-MBP was eluted as fractions of volume of 500 µl each (around 5 ml of elution buffer was used so as to produce 10 fractions of eluted solution). The protein samples could be dialysed in the dialysis buffer (10 mM Tris-HCl; 50 mM NaCl; pH 8.0) depending upon the usage.

The proteins samples were run over a 12.5% SDS gel and a Coomassie staining was performed (see Fig.3.2.2). The concentration of the protein was determined by measuring the concentration on the Nanodrop spectrophotometer or a Bradford assay. Prot Param tool was used to get the actual concentration by dividing it with the extinction coefficient. The value of extinction coefficient is 1.4 for mTSLP-MBP protein.

For the periplasmic expressed protein samples shown in figure, the concentration of protein was 2.5 mg/ml. Therefore, the yield from 1 litre of bacterial culture was approximately 2.5x10= 25 mg. The coomassie gel showed additional bands and this perhaps point out that the protein undergoes degradation or half trancribed protein fractions are produced.

For the cytoplasmic expressed protein samples shown in figure, the concentration of protein was 7 mg/ml. Therefore, the yield from 1 litre of bacterial culture was approximately 7x10= 70 mg. The coomassie gel showed a distinct band at 57.5 kDa which is the desired protein size. Therefore the cytoplasmic expression of protein yields almost 3 times more protein.

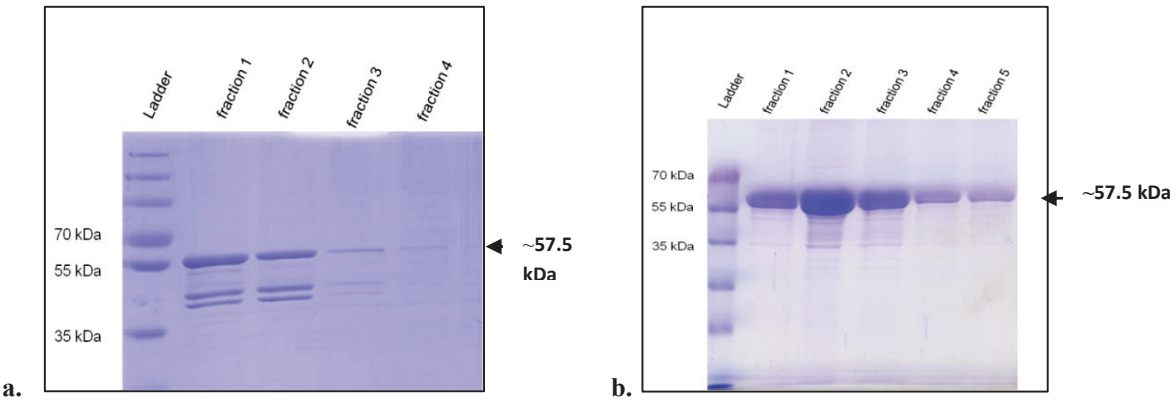

Fig.4.19. Coomassie blot analysis of purified elutes obtained from pMAL-2 series constructs with mTSLP insert. 1 litre of culture was inoculated with 50 ml of the respective overnight bacterial culture and induced with 1M IPTG at OD 0.5 and shaken for 6 h after induction. The cells lysates/periplasmic preparations were passed over amylose column and washed with lysis buffer. After this the protein mTSLP-MBP was eluted by Elution buffer a. pMAL-p2X-mTSLP-BL21 DE3 bacteria produced mTSLP-MBP from the periplasmic extract which are eluted in fractions of 500 µl each. b. pMAL-c2X-mTSLP-BL21 DE3 cell lysate extract also shows protein production in elutes of fractions of 500 µl. 10 µl of each sample was loaded on the gel.

4.3.3. Characterization of binding activity of mTSLP-MBP protein

The fusion protein thus produced above was tested for its binding activity. This was done by an ELISA in which the plate was coated with a fixed amount (500ng/well) of mTSLP-MBP. The various dosages of mTSLPR were then added in increasing dosages. The mTSLPR which binds to the mTSLP-MBP can be detected by antibodies against His tag on mTSLPR and secondary Ab Goat Anti mouse IgG-HRP conjugated. The results obtained are shown in Fig. 4.20.

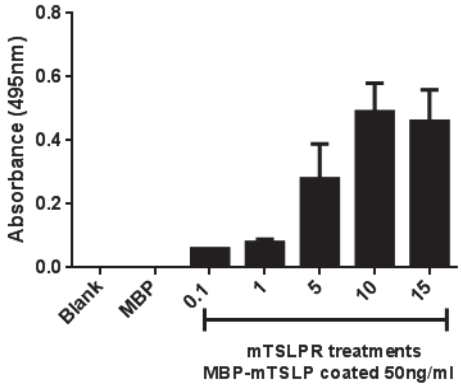

Fig.4.20. ELISA based analysis to detect the binding activity of exo-mTSLPR to its ligand mTSLP-MBP. The plate is coated with mTSLP-MBP (50ng/well) in PBS. The mTSLPR was added in different dosages as shown in the graph. The mTSLP which binds to the cells is detected via primary anti His tag antibody and secondary anti HRP conjugated antibody. The MBP amount is 50ng/well.

It was observed that the mTSLP-MBP protein binds to the mTSLPR in a dose dependent manner.

4.3.4. Activity assay on Ba/F3 cellular test system

After confirming the binding characteristics of the mTSLP-MBP protein with an ELISA, the bioactivity was determined by using a Luciferase gene based assay. Approximately 1 million cells starved Ba/F3 cells were transfected with plasmids expressing plasmids expressing hybrid chains exo-mTSLPR-intra-hTSLPR hybrid/exo-mIL-7Rα-intra-hIL-7Rα hybrid and IRF-Luc reporter gene. They were treated with mTSLP-MBP in various dosages as a gradient. The cells were grown for 12-16 h, lysed and reporter gene activity determined on a luminometer. The results obtained are shown in Fig 4.21.

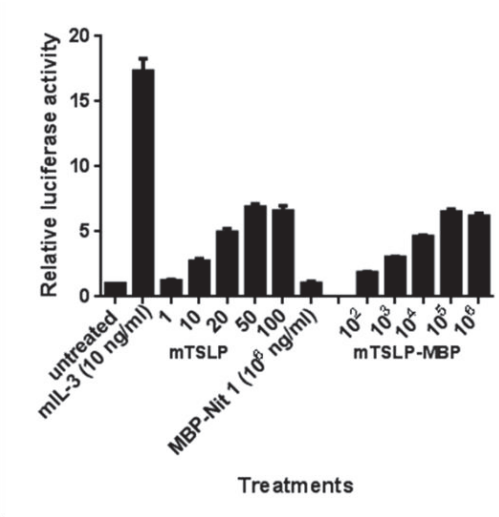

Fig.4.21. Analysis of Ba/F3 luciferase gene based readout to determine the relative bioactivity of mTSLP-MBP fusion protein. The plasmids expressing hybrid chains exo-mTSLPR-intra-hTSLPR hybrid/exo-mIL-7Rα-intra-hIL-7Rα hybrid and IRF-Luc reporter gene were transfected in the Ba/F3 cells using T-16 Amaxa program. The cells were given various treatments with cytokine mTSLP-MBP in ng/ml. The cells were grown for 16 h, lysed and luciferase activity determined on Luminometer. mIL-3 (10 ng/ml) serves as a positive control for the reporter gene. SD is derived from duplicate samples and shown as error bars. Shown are representative data from three independent experiments.

It was observed that mTSLP-MBP is bioactive and it produces a dosage dependent activity in the reporter gene system. A bioactive form of murine TSLP is obtained which does not have a high specific activity, but it could be used in relative studies aimed at designing antagonistic mutants.

4.3.5. Cloning of pMALp2X/c2X-I37EmTSLP construct for generation of a potentially antagonistic mutant

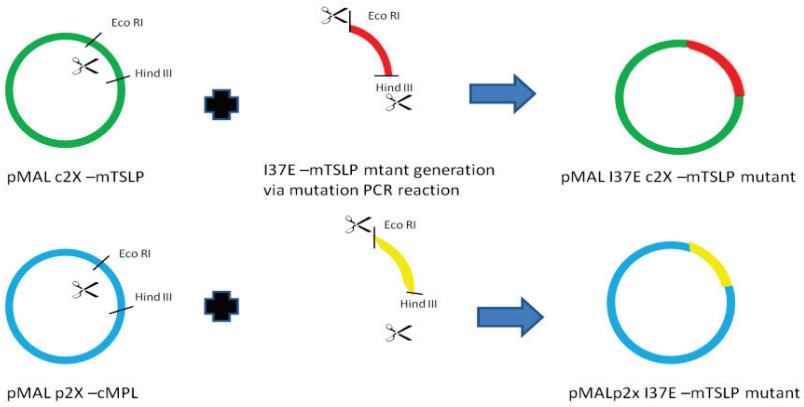

Fig.4.22. Schematic representation of cloning scheme showing the preparation of the pMAL-mTSLP vectors for preparation of mTSLP-MBP fusion protein. The plasmids pMAL-p2X-cMPL and pMAL-c2X-mTSLP were restricted with EcoRI and Hind III enzyme treatments. The mutation I37E coding inserts were generated by causing a mutation in the sequence using mutation PCR. The end results of the cloning were final vectors pMAL-p2X-I37EmTSLP and pMAL-c2X-I37EmTSLP.

The software Ape was used for designing the construct map for pMAL-c2X-I37EmTSLP and pMAL-p2X-I37EmTSLP and the primers I37E mTSLP-MBP For (c2X/p2X), I37E mTSLP-MBP Rev (c2X), I37E mTSLP-MBP Rev (p2X). These primers were then used to amplify the I37E mTSLP mutant gene from pASKIEP-mTSLP construct as a template. These primers were used to initiate a Phusion polymerase medicated mutation PCR reaction using the program as listed in materials and method section 3.2.10. The construct pMAL-p2X-cMPL was modified by excising the cMPL ectodomain using restriction enzymes (see fig 4.22) Eco RI and Hind III and inserting the I37E mTSLP protein expressing gene. The ligated plasmid thus obtained was transformed into *E. coli* Top 10 cells and the cloning effectiveness was verified by a colony PCR. The positive clones were selected and then their plasmids isolated by mini prep. The plasmid DNA was sent for sequencing to verify the sequence. The malE primer which initiates sequence near the 3′ end of malE, 78-81 bases upstream of the primary site in the polylinker, was used for sequencing the plasmid DNA. After making sure that the sequencing yielded no error, the plasmid DNA was used for protein production by transformation into BL-21 DE3 strain (see materials and methods for details).

4.3.6. Expression and purification of I37E mTSLP-MBP fusion protein

The two constructs as above: pMALp2X-I37EmTSLP and pMAL-c2X-I37EmTSLP, were transformed into BL-21 DE 3 (Novagen) competent bacterial cells and the protein production was carried out in a similar way as described above for mTSLP-MBP fusion protein.The molecular weight of the MBP is 42.5 kDa and that of I37E mTSLP is 15 kDa so together, the molecular weight of the fusion protein shall be 57.5 kDa and we must expect a band in the Coomassie blot at this level for the mTSLP-MBP fusion protein.

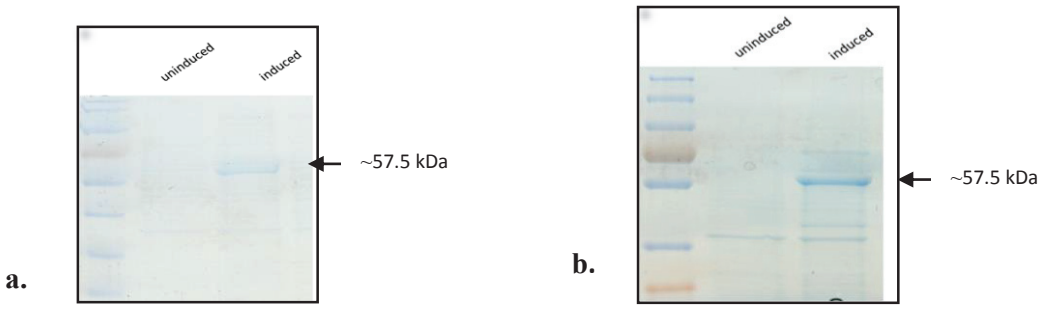

Fig.4.23. Coomassie blot analysis of IPTG induction of BL-21 DE3 cells carrying pMAL-2 series constructs with I37E mTSLP insert. 1 litre of bacterial culture was inoculated with 50 ml of the respective overnight bacterial culture and induced with 1M IPTG at OD 0.5 and shaken for 6 h after induction. a. Comparison of pMAL-p2X-I37EmTSLP-BL21 DE3 bacteria samples (uninduced and induced) in different lanes b. Comparison of pMAL-c2X-I37EmTSLP-BL21 DE3 bacteria samples (uninduced and induced) in different lanes. 20 µl of the bacterial culture was mixed in 50 µl of sample buffer and 20 µl of this mixture is loaded on the gel (Fig. from Karstern Letsch, unpublished results).

pMAL-p2X-I37EmTSLP-BL21 DE3 and pMAL-c2X-I37EmTSLP-BL21 DE3 both show induction as evident by the dark band on the Commassie gels at approximately 57.5 kDa.

Purification by affinity chromatography from the periplasmic/cytoplasmic extracts:

The protein production was carried out in a similar way as that for the mTSLP production. The protein samples could be dialysed in Dialysis buffer (10 mM Tris-HCl; 50 mM NaCl; pH 8.0) depending upon the usage. The proteins samples were run over a 12.5% SDS gel and a Commassie staining was performed (see Fig. 4.24). The concentration of the protein was determined by measuring the concentration on the Nanodrop spectrophotometer or a Bradford assay. Prot Param tool was used to get the actual concentration by dividing it with the extinction coefficient. The value of extinction coefficient is 1.4 for I37E mTSLP-MBP protein.For the periplasmic expressed protein samples shown in figure, the concentration of protein was 3 mg/ml. Therefore, the yield from 1 litre of bacterial culture was approximately 3.1 x10= 31 mg. The coomassie gel showed additional bands and this perhaps point out that the protein undergoes degradation or half transcribed protein fractions are produced. For the cytoplasmic expressed protein samples shown in figure, the concentration of protein was 8.1 mg/ml. Therefore, the yield from 1 litre of bacterial culture was approximately 8.1x10= 81 mg. The coomassie gel showed a distinct band at 57.5 kDa which is the desired protein size. Therefore the cytoplasmic expression of protein yields almost 3 times more protein.

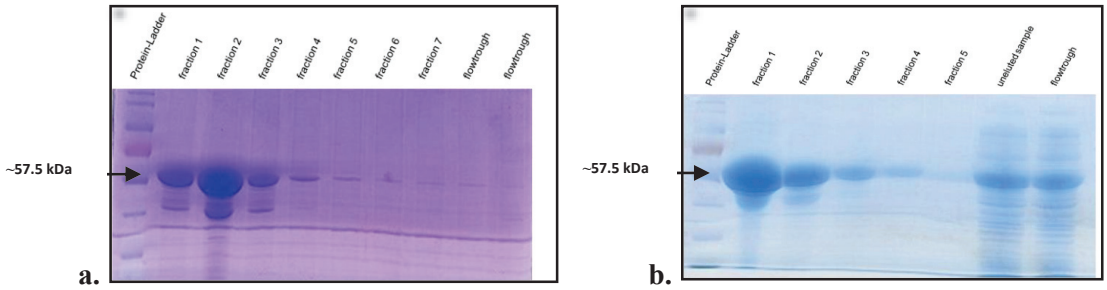

Fig.4.24. Coomassie blot analysis of purified elutes obtained from pMAL-2 series constructs with I37E mTSLP insert. 1 litre of culture was inoculated with 50 ml of the respective overnight bacterial culture and induced with 1M IPTG at OD 0.5 and shaken for 6 h after induction. The cells lysates/periplasmic preparations were passed over amylose column and washed with lysis buffer. After this the protein I37E mTSLP-MBP was eluted by elution buffer. a. pMAL-p2X-I37EmTSLP-BL21 DE3 bacteria produced ImTSLP-MBP from the periplasmic extract which was eluted in fractions of 500 µl each. b. pMAL-c2X-I37EmTSLP-BL21 DE3 cell lysate extract also shows protein production in elutes of fractions of 500 µl. 10 µl of each sample is loaded on the gel.

4.3.7. Characterization of binding activity of I37E mTSLP protein

The fusion protein thus produced above was tested for its binding activity. This was done by an ELISA in which the plate was coated with a fixed amount (500ng/well) of I37E mTSLP-MBP. The various dosages of mTSLPR were then added in increasing dosages. The mTSLPR which binds to the I37E mTSLP-MBP can be detected by antibodies against His tag on mTSLPR and secondary Ab Goat Anti mouse IgG-HRP conjugated. The results obtained are shown in Fig. 4.25.

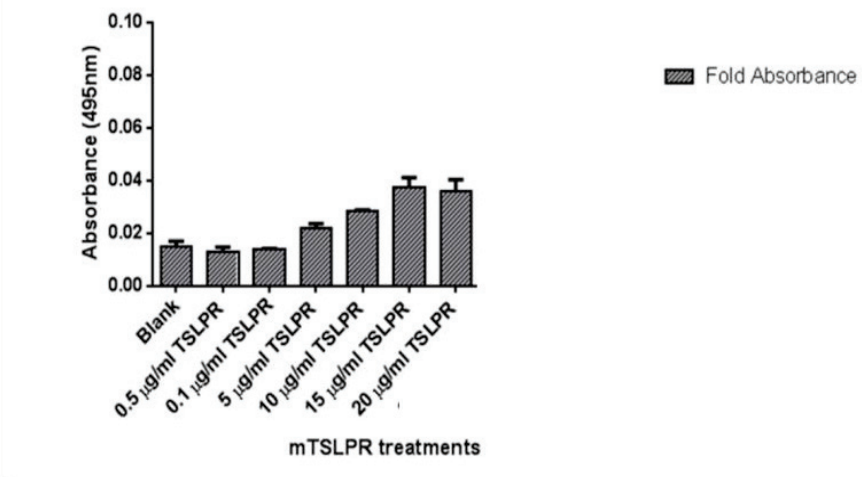

Fig.4.25. ELISA based analysis to detect the binding activity of exo-mTSLPR to ligand I37E mTSLP-MBP. The plate is coated with mTSLP-MBP (50ng/well) in PBS. The mTSLPR was added in different dosages as shown in the graph. The mutant I37E mTSLP which binds to the receptor is detected via primary anti His tag antibody and secondary anti HRP conjugated antibody. The MBP amount is 50ng/well.

It was observed that I37E mTSLP-MBP protein binds to the mTSLPR in a dose dependent manner.

4.3.8. Activity assay on Ba/F3 cellular test system

As seen above, it is confirmed that the I37E mTSLP-MBP protein binds to mTSLPR in an ELISA, the bioactivity was determined by using a Luciferase gene based assay. Approximately 1 million cells starved Ba/F3 cells were transfected with plasmids expressing plasmids expressing hybrid chains exo-mTSLPR-intra-hTSLPR hybrid/exo-mIL-7Rα-intra-hIL-7Rα hybrid and IRF-Luc reporter gene. They were treated with similar dosages of mTSLP and I37E mTSLP-MBP in various dosages as a gradient. The cells were grown for 12-16 h, lysed and reporter gene activity determined on a luminometer. The results obtained are shown in Fig 4.26 on the next page.

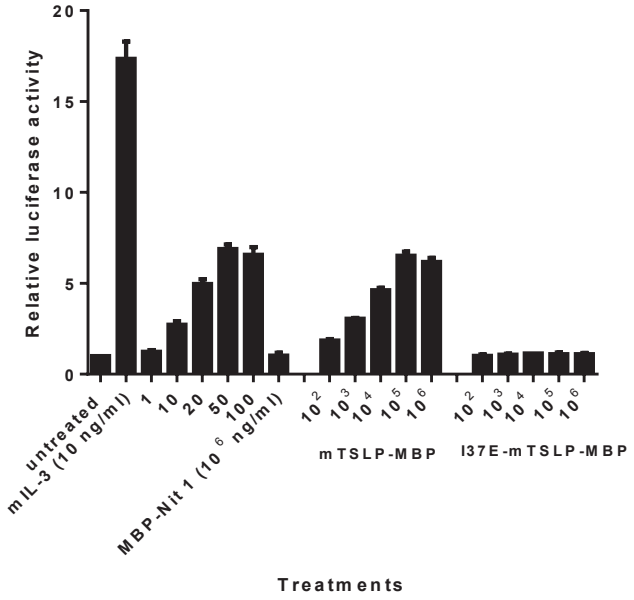

Fig.4.26 Analysis of Ba/F3 luciferase gene based readout to determine the relative bioactivity of I37E mTSLP-MBP fusion protein. The plasmids expressing hybrid chains exo-mTSLPR-intra-hTSLPR hybrid/exo-mIL-7Rα-intra-hIL-7Rα hybrid and IRF-Luc reporter gene were transfected in the Ba/F3 cells using T-16 Amaxa program. The cells were given various treatments with cytokine mTSLP-MBP and I37E mTSLP-MBP in ng/ml. The cells were grown for 16 h, lysed and luciferase activity determined on Luminometer. mIL-3 (20 ng/ml) and mTSLP (various dosages) serves as a positive control for the reporter gene. SD is derived from duplicate samples and shown as error bars. Shown are repesentative data from three independent experiments.

It was observed that the mutant shows no activation of the reporter gene in the Ba/F3 cells as compared to the wild type. The above results show that the mutant binds to the receptor but does not initiates a signal inside the cell.

4.3.9. Functional characterization of the competitive ability of the mutant on Ba/F3 cells

The competitive ability of the mutant was confirmed by using a Luciferase gene based assay. Approximately 1 million cells starved Ba/F3 cells were transfected with plasmids expressing plasmids expressing hybrid chains exo-mTSLPR-intra-hTSLPR hybrid/exo-mIL-7Rα-intra-hIL-7Rα hybrid and IRF-Luc reporter gene. In combination of the activity assay as shown in 4.26 above, the transfected cells were treated with two similar dosages of mTSLP (10^4 and 10^5) ng/ml and an increasing gradient of I37E mTSLP-MBP (10^2-10^6) in various dosage combinations. The cells were grown for 12-16 h, lysed and reporter gene activity determined on a luminometer. The results obtained are shown in Fig 4.27.

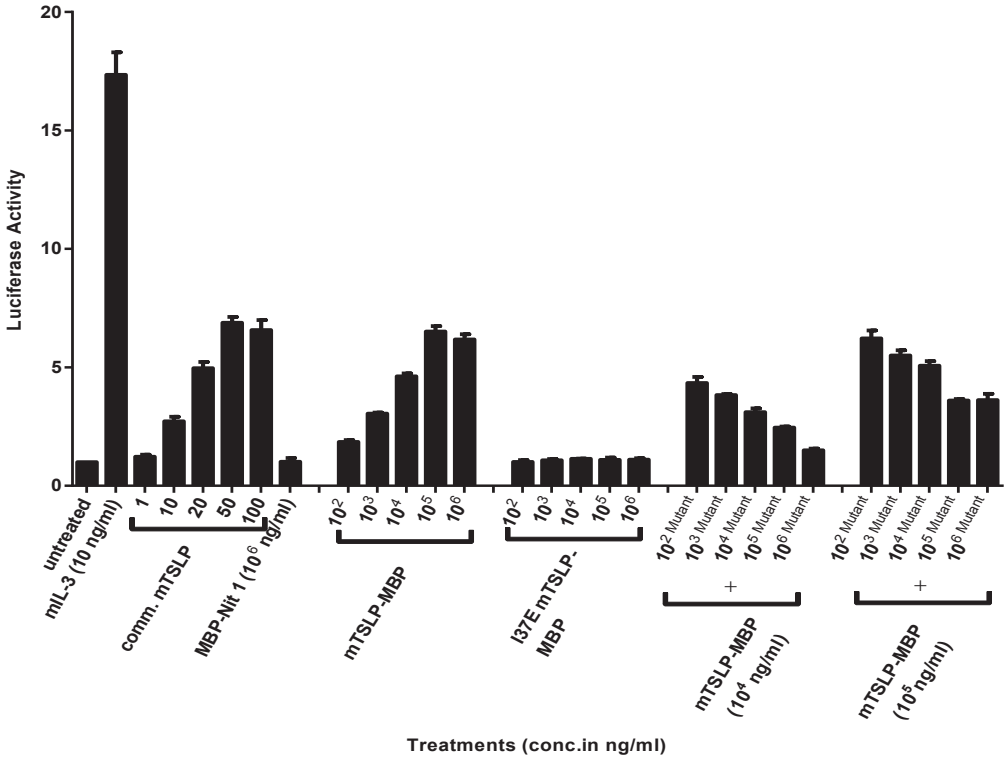

Fig.4.27. Analysis of a Ba/F3 luciferase gene based competition assay between I37E mTSLP-MBP and mTSLP-MBP readout for functional characterization of the bioactivity of the mutant I37E mTSLP-MBP. The plasmids expressing hybrid chains exo-mTSLPR-intra-hTSLPR hybrid/exo-mIL-7Rα-intra-hIL-7Rα hybrid and IRF-Luc reporter gene were transfected in the Ba/F3 cells using T-16 Amaxa program. The cells were given various treatments with cytokine mTSLP-MBP and I37E mTSLP-MBP in ng/ml. The cells were grown for 16 h, lysed and luciferase activity determined on Luminometer.mIL-3 (20 ng/ml) serves as a positive control for the reporter gene. SD is derived from duplicate samples and shown as error bars. Shown is a representative data from three independent experiments.

It was observed that the mutant shows no activation of the reporter gene in the Ba/F3 cells as compared to the wild type. The above results show that the mutant binds to the receptor but does not initiates a signal inside the cell. The mutant I37E mTSLP-MBP actively competes with the mTSLP-MBP thereby decreasing the luciferase signal activity of Ba/F3 cells and thus showing that the mutant is functionally active.

4.4. Studying and characterizing the biological effect of TSLP/I37E antagonist on TSLP responsive dendritic cells.

The Ba/F3 cellular readout system as discussed in section 4.1 was designed to obtain the relative quantification of mTSLP signaling. It does not give a hint about the biological changes it may bring about in the morphology and physiological activity of the target cells. Therefore a need for such a cellular system existed, which could allow us to treat it with mTSLP and then quickly study the changes in the cell via some readout in the form of a dynamic activity of the surface markers. A sensitive system shall be one which could have allowed detection of these changes upon treatment with a sensitive readout such as by flow cytometry.

Dendritic cells obtained from the BMDCs (bone marrow derived cells) of mouse femur bone provide a model for studying the effect of mTSLP. These cells have been observed to exhibit dynamic changes in the expression of surface markers such as OX40L, CD80 and CD86, (Segawa et al., 2014). It has also been observed that TSLP influences the migration (Soumelis et al., 2011) of these cells by influencing the production of some chemokines. Therefore, these cells were chosen for studying migration effects by mTSLP as well as the biological changes on the cell surface markers which occur upon treating them with the antagonistic mutant.

4.4.1. Preparation of the dendritic cells

Dendritic cells were obtained by allowing the BMDCs from the femur of the C57BL/6 black mice under aseptic conditions (Madaan et al., 2014) These cells (1×10^6 cell/ml) were allowed to stick to plastic surface of the petri dishes and mature under the influence of 20 ng/ml of GMCSF (Granular macrophage colony stimulating factor) in RPMI-1640 medium containing 10% heat-inactivated fetal bovine serum, penicillin G/streptomycin (50 µg/ml) in a humidified atmosphere of 5% CO_2/95% air at 37°C for 6 days. The cells were ready on day 7 and this is confirmed by the increase in signals of surface marker $CD11c^+$ which was detected on the flow cytometer. The yield of BMDCs on day 0 was $10x10^6$ cells per femur. The yield of dendritic cells obtained on 6^{th} day was $2x10^6$ cells/per petri dish i.e. 6 million cells in total (see section 3.3.1 of material and methods for the entire procedure of isolation, maturation and purification of dendritic cells).

4.4.2. Characterization of the murine dendritic cells

The dendritic cells are formed by maturation of the cells over a period of 7 days. During this period the cell undergo several morphological and physiological changes under the influence of the cytokine 20 ng/ml GM-CSF in RPMI-1640 media. The cells which mature into the dendritic cell shall start to

float in the medium, where as cells which form the macrophages, usually stick to the base of the petri dish. This unique characteristic can be used to concentrate the dendritic cells and eliminate other cells. A richer concentration could be achieved by magnetic beads but here they were not used.

In order to characterize the cells as obtained from the method as described above, the cells were regularly observed under a microscope and pictures were obtained on various days (day0 - day7) as seen in pictures in Figure. 4.28. The pictures show a visible change in the morphology of the cells. The cells change their shape from round to irregular shaped cells with dendritic processes. The cells appear rolling over the plate.

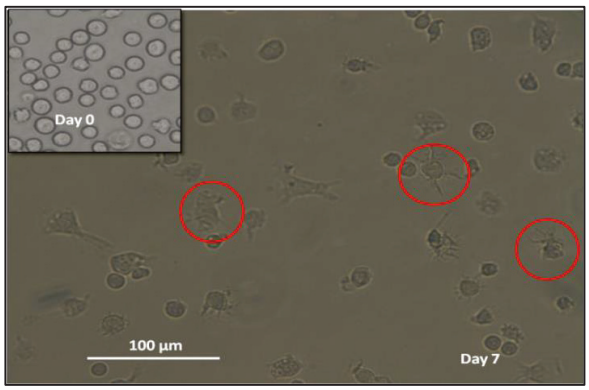

Fig.4.28. Visual characterization of the dendritic cells on a microscope. A snapshot of the microscope (1000x) showing the change in the morphology of the BMDCs to dendritic cells on day 0 (inset image top left corner) and day 7. The red circle highlights the dendritic cells with visible dendrite processes.

The cells were then further analysed using flow cytometry. The cells were stained as per the protocols (see materials and methods section 3.3.10). Three cell samples from day 0 and day 7 were then compared for expression of $CD11c^+$ marker which is a characteristic of the dendritic cells (see Fig. 4.29). Anti mouse $CD11c^+$ marker coupled to PE flurophore was used for this purpose (see materials section 3.3.10).

The gating strategy involved a comparison of the histograms of non stained samples with that of the stained samples. A range gate PE-A+ was applied on the histograms to demarcate the cells producing the signals. These cells which gave signals were traced back on the dot plot and allowed us to know where our population of interest laid. The cells that produced positive stained signals were then gated and this is the gate that has been used for the samples represented below in a square dot plot with FITC and PE filters on X and Y axis. A quadrant Q4 was then defined to enclose the untreated cells inside the quadrant. These are the negatively stained cells. A stained cell shall create a signal which can be detected by a migrated shift into quadrants Q3 and Q2. The comparative shift along with the

statistical count was then observed as a measure of the staining of the 11c^{+}-PE-A+ stained positive cells. Similar gating strategy was applied in all the experiments described ahead.

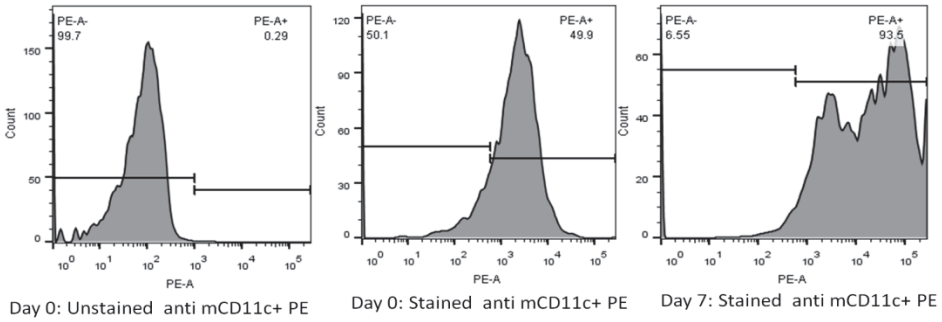

a.

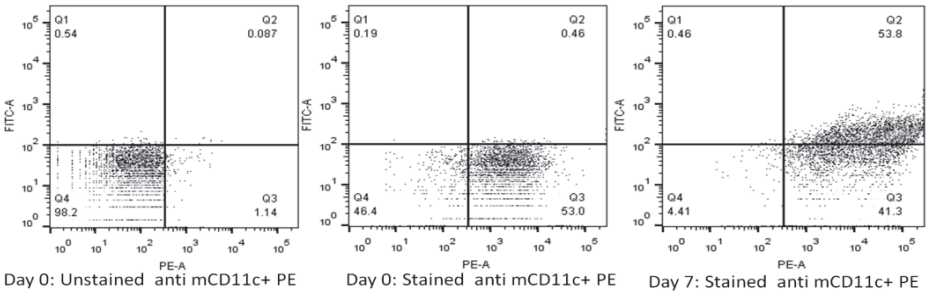

b.

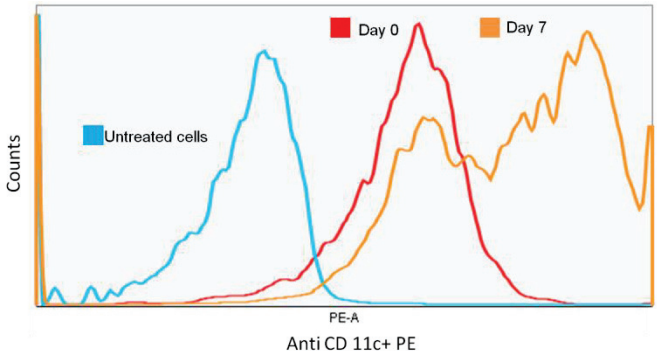

c.

Fig.4.29. Flow cytometry based analysis based characterization of enriched murine dendritic cells. 0.1 million cells/ sample were treated with 1µg of rat anti mouse CD11c+ antibody and were measured on flow cytometer as compared to the unstained sample.

a. Gating strategy: The range gates PE-A- and PE-A+ were applied to the histograms of the unstained and stained cells (10000 count each sample) to locate the positive stained population on the dot plot. The PE-A+ population gate represents the positively stained cells. **b. Dots plot analysis:** Dots plots showing the BMDCs transforming into dendritic cells as compared between unstained and stained samples on day 0 and day 7. The X and the Y axis have filters for PE and FITC signals respectively.**c. Overlay histogram:** An overlay histogram of the PE-A+ signal from dendritic cells obtained on day 0 and day 7 in FL-2 PE channel. The blue curve represents the unstained cells and the red represents the 11c+ positive cells on day 0 while the orange curve represents the 11c^{+} positive cells on day 7.

It was observed that the positive stained cells are located in quadrant Q3 and in time span of 7 days all of them shift towards quadrant Q3 and Q2. An increase in the number of CD11c^{+} cells shows that

the BMDCs have matured into dendritic cells as already visible in the microscopic observations above and the FACS results support the observation made in Fig 4.28. The A shift towards the right was observed on day 7 (shown in orange) as compared to day 0 (shown in red) (see Fig. 4.29 c). The orange curve has 2 peaks, one that of $11c^{+}$cells and other that of $11c^{+}$ negative cells The cells thus obtained and characterized were then ready for further use as a testing system for biological activity of mTSLP.

4.4.3. Evaluation of the biological activity of mTSLP in the supernatant of the keratinocyte derived squamous cell carcinoma cell (KCMH-1)

KCMH-1 is skin keratinocyte derived squamous cell carcinoma cell line obtained from CBA/j mouse (Nakamura et al., 1994), (see materials and methods). This cell line was obtained from our colleague Dr. Hirasawa from Tohoku University, Sendai, Miyagi, Japan. This cell line is known to produce 3 ng/ml of natural murine TSLP on stimulation with 30nM of TPA as established by an ELISA (Segawa et al.2014).

KCMH-1 cells (1×10^5 cell/ml) were grown in α-MEM medium containing 10% heat-inactivated fetal bovine serum, penicillin G/streptomycin (50 μg/ml) in a humidified atmosphere of 5% CO_2/95% air at 37°C for 4 days till they attained confluence. The cells were then stimulated with 30nM of TPA added along with fresh media. The supernatant was collected in 24 h.

A Ba/F3 cell assay was performed to check if the supernatant thus obtained can cause stimulation of the luciferase based STAT-1 reporter gene in the cells. Since the supernatant was in volumes greater than that which can be held in 6 well plate, 25 sq. m flask for suspension cells were used. The plasmids for expressing the hybrid chains and IRF-luc reporter gene were transfected in $1x10^6$ cells Ba/F3 cells (T-16 Amaxa program). The transfected cells were resuspended in residual volume of 2 ml of RPMI-1640 and then were given treatments with various volumes (2, 5, 7 ml) of the mTSLP containing supernatant from KCMH-1 cells. The cells were lysed after 16 h and luciferase gene activity evaluated on a luminometer.

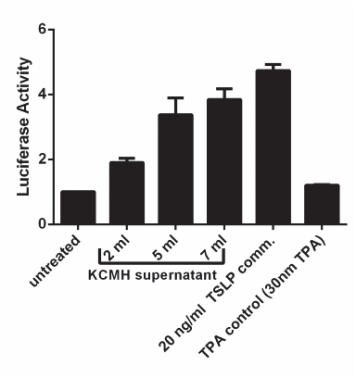

Fig.4.30. Luminometric analysis of the KCMH-1 supernatant response exhibited by the mTSLPR expressing Ba/F3 based IRF-luciferase gene readout system. The plasmids for expressing the hybrid mTSLPR/IL-7 α chains and IRF-luc reporter gene were transfected in the Ba/F3 cells (T-16 Amaxa program). $1x10^6$ cells were given treatments with various volumes of supernatant from KCMH-1 cell (1 ml has approx. 3 ng of mTSLP) as shown in 25 sq. m flasks with residual 2 ml of RPMI-1640 medium. The cells were lysed after 16 h and the relative luciferase gene activity was evaluated on a luminometer.mIL-3 (20 ng/ml) serves as a positive control for the reporter gene (data not shown). SD is derived from duplicate samples and shown as error bars. Shown are representative data from three independent experiments.

The luciferase assay shows an increase in the relative luciferase activity as compared to the untreated cells with increasing volumes of the supernatant from TPA activated KCMH-1 cells. The assay shows that the biological mTSLP present in the KCMH-1 cell supernatant can activate the Ba/F3 Luciferase activity thus proving that the KCMH-1 cells could be stimulated to produce active biological mTSLP containing supernatant.

4.4.4. Studying the effects of mTSLP-MBP and antagonistic I37E mTSLP-MBP mutant on dendritic cell migration

Maria-Isabel Fernanadez (Fernandez et al., 2011) reported that the dendritic cells show migratory behavior across the Boyden chamber when treated with mTSLP. In this experiment (see Fig 4.31 a.) the mature dendritic cells ($1x10^6$) treated with GM-CSF were grown in Boyden migration chamber in the upper well in 500 µl volume and in the lower well various treatments (see Fig, 4.31 b.) of mTSLP-MBP, I37E mTSLP-MBP, their combinations and MBP as control were given in different wells each containing a volume of 1 ml of the RPMI-1640. Cells were grown in RPMI-1640 medium containing 10% heat-inactivated fetal bovine serum, penicillin G/streptomycin (50 µg/ml) in a humidified atmosphere of 5% CO_2/95% air at 37°C for 12 h after treatment. The cells were then fixed, mounted on a slide and seen under a microscope (see materials and methods 3.3.11). The pictures were taken and can be seen in Fig. 4.31 b. The cells were counted by dividing the observed slide area into 3 different parts (see Fig. 4.31 a). The overview of the slide has been shown in Fig.

4.31 b. After counting the cells an approximate quantification analysis was made by plotting the values in Excel (Graph Pad Prism software) and obtaining a X-Y bar diagram (see Fig 4.31. c).

a.

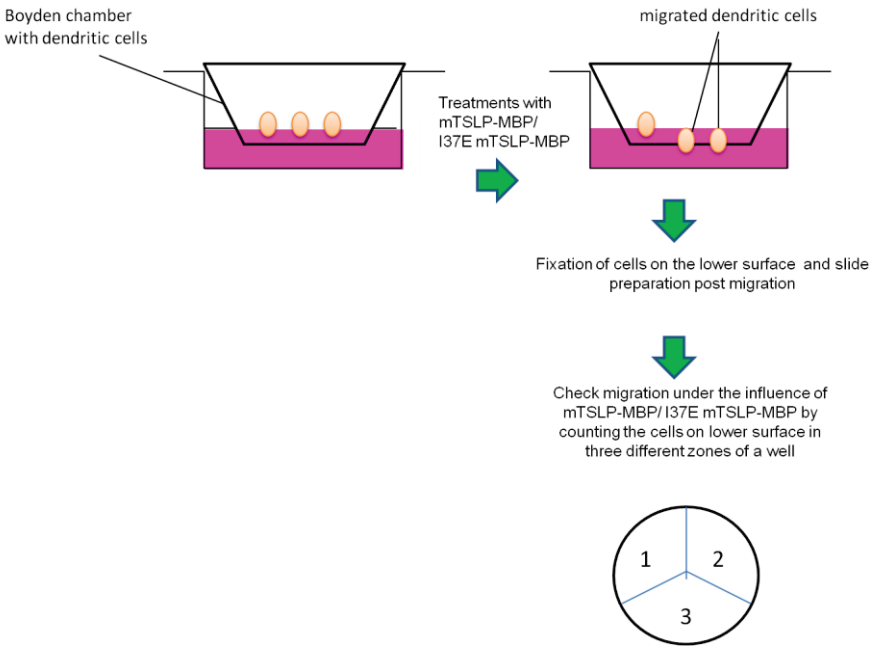

b .

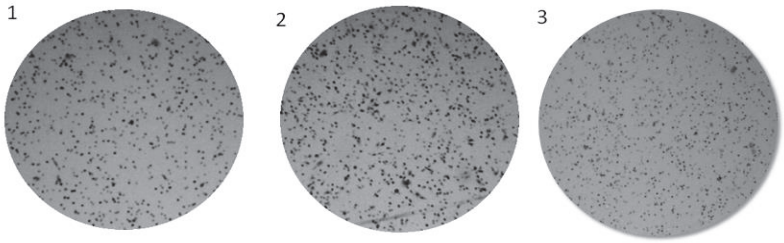

MBP	-	-	-
mTSLP-MBP	-	1000 ng/ml	-
I37E mTSLP-MBP	-	-	1000 ng/ml
Number of cells	**111**	**325**	**130**

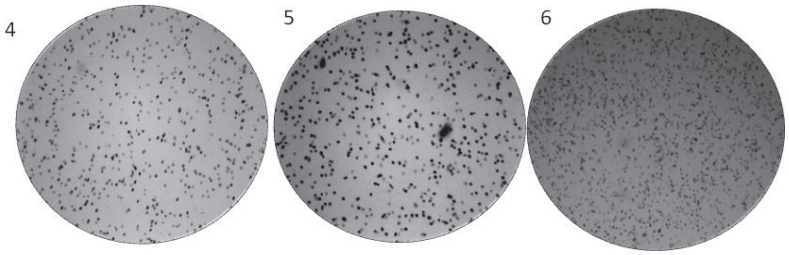

MBP	10 micrograms	-	-
mTSLP-MBP	-	1000 ng/ml	1000 ng/ml
I37E mTSLP-MBP	-	1000 ng/ml	100000 ng/ml
Number of cells	**120**	**299**	**202**

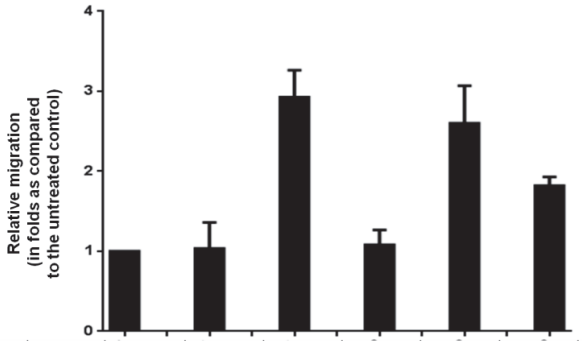

MBP-mTSLP	0	0	1000	0	1000	1000
MBP-I37E-mTSLP	0	0	0	1000	1000	1000000
MBP	0	1000000	0	0	0	0

c.

Treatments (in ng/ml)

Fig.4.31. a. Schematic representation of an experiment to study the relative dendritic cell migration across a membrane in a Boyden chamber under the influence of mTSLP-MBP and I37E mTSLP-MBP. $1x10^6$ GM-CSF treated matured dendritic cells are grown in Boyden migration chamber in the upper well and in the lower well various treatments of mTSLP-MBP, I37E mTSLP-MBP, their combinations and MBP control are given. The cells were grown for 12 h after treatment. The cells are then fixed and seen under a microscope.

b. Analysis of pictures of slides. $1x10^6$ GM-CSF treated matured dendritic cells were grown in Boyden migration chamber as shown in 4.27.a and various treatments of mTSLP-MBP, I37E mTSLP-MBP, their combinations and MBP control are given as shown in the table in this figure. The cells were then fixed and seen under a microscope. The number of cells was counted from three snapshots taken at 1000x magnification (picture data not shown). The counted cells are listed in the table.

c. Statistical analysis of relative dendritic cell migration. $1x10^6$ cells were allowed to migrate under the influence of mTSLP- MBP/I37E mTSLP- MBP treatments made. The mean value of three counts from the fixed cells on the slides obtained above in 4.27 b. were statistically analysed to obtain a bar diagram. The Y axis represents the relative migration (in folds) obtained by mean value analysis as compared to the untreated control. The X axis represents the treatments in ng/ml. The error bars represent the difference in counting cells in the three different regions of the slide area. This is a representative data from 2 sets of independent experiments.

It was observed that the dendritic cells migrated under the influence of mTSLP-MBP and this is reduced when an increased dosage of mutant I37E mTSLP-MBP is added. This shows that the mutant has an inhibitory activity on the migration of the dendritic cells.

4.4.5. Studying the effects of mTSLP containing supernatants obtained from activated KCMH-1 cells on dendritic cells

The initial approach to produce such a system which mimics epithelial secretion of mTSLP in asthmatic condition was taken by Segawa et al., 2014 They used a murine epidermal keratinocyte cell line (KCMH-1) for the production of natural TSLP upon stimulation with different stimulants

and then read the effect of the supernatant as obtained on the OX40L, CD80 and CD86 ligand expression on the surface of the dendritic cells. This system was adopted and applied to study the effects on OX40L expression (see Fig. 4.32) and inhibitory effect of the antagonistic mutant I37E on expressions of OX40L (see Fig. 4.32) and CD80 and CD86 (see Fig. 4.33, 4.34).

KCMH-1 cells (1×10^5 cell/ml) were grown in α-MEM medium containing 10% heat-inactivated fetal bovine serum, penicillin G/streptomycin (50 µg/ml) in a humidified atmosphere of 5% CO_2/95% air at 37°C for 4 days till they attained confluence. The cells were then stimulated with 30nM of TPA added along with fresh media. The supernatant was collected in 24 h.

The dendritic cells (1×10^5 cell/ml) were grown in RPMI-1640 containing 10% heat-inactivated fetal bovine serum, penicillin G/streptomycin (50 µg/ml) in a humidified atmosphere of 5% CO_2/95% air at 37°C. The conditioned media produced by the KCMH-1 cells as described above, in a 1:1 ratio was used to stimulate the dendritic cells (see Fig 4.32 for the experimental scheme). The cells were stained as per the protocol (see materials and methods 3.3.10) and analysed by flow cytometry after 24 h. The quantification of the stimulation is done in terms of the expression of OX40 ligand.

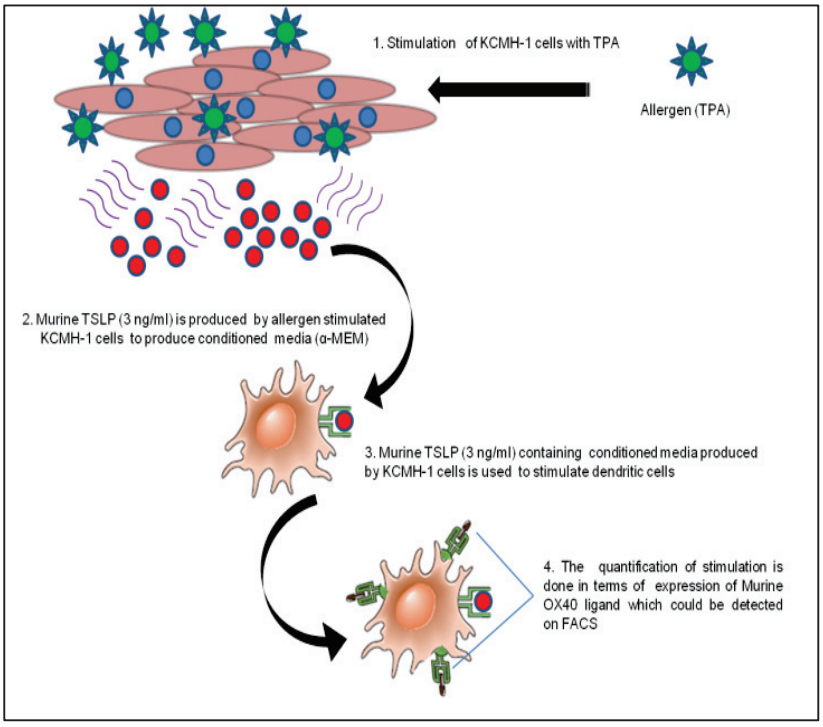

Fig. 4.32. a. The KCMH- Dendritic cell based model: Schematic representation of the production and stimulation of cells. The diagram shows the stimulation of the KCMH-1 (1×10^5 cell/ml) cells by TPA (30nM) and then later stimulation of the 1×10^5 dendritic cells by the KCMH-1 supernatant to produce OX-40 L on its surface.

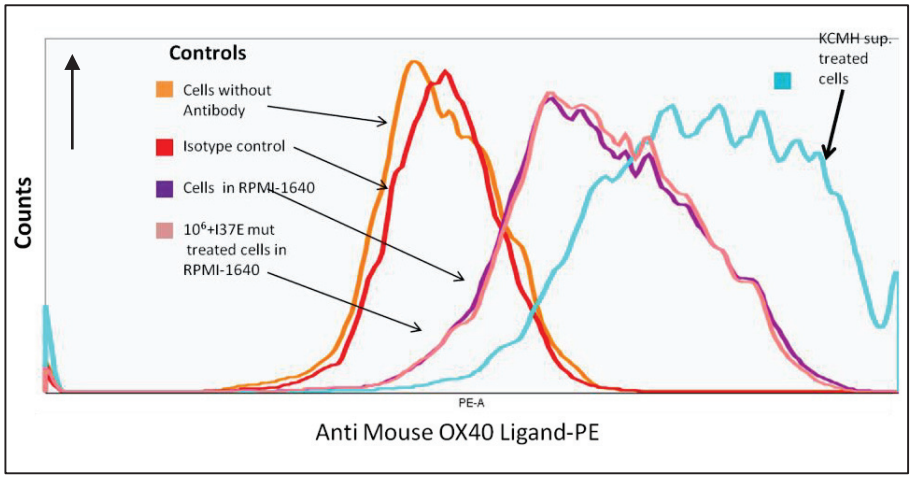

Fig.4.32 b. Flow cytometric analysis of dendritic cells stimulated by KCMH-1 cell supernatant. The $1x10^5$ dendritic cells were stimulated by KCMH-1 cells supernatant for 24 h and were stained by anti mouse 1 µg of anti-OX-40-PE ligand antibody. The signal was analysed using flow cytometry.

It was observed that OX-40 ligand expression on the surface of the dendritic cells in KCMH supernatant treated cells is upregulated on addition of KCMH-1 cell supernatant as indicated by a positive shift in signal towards the right (as indicated by the light blue curve) as compared to the basal expression of OX40 ligands on the dendritic cell surface (violet curve). The isotype control and the use of the Fc blockers ensure that there is no unspecific binding with the Fc receptors. The pink curve represents the curve for cells treated with mutant I37E mTSLP-MBP as a negative control.

4.4.6. Studying the antagonistic effects of I37E mTSLP-MBP mutant on KCMH supernatant induced relative OX-40 ligand expression on the dendritic cellular surface

The supernatant of KCMH cells (1:1 ratio) was used to stimulate the dendritic cells as already described above in 4.4.5. The relative expression of OX40L was studied after adding I37E m-TSLP-MBP in 10^4 and 10^6 ng/ml dosages. The results are shown in Fig. 4.33 b.

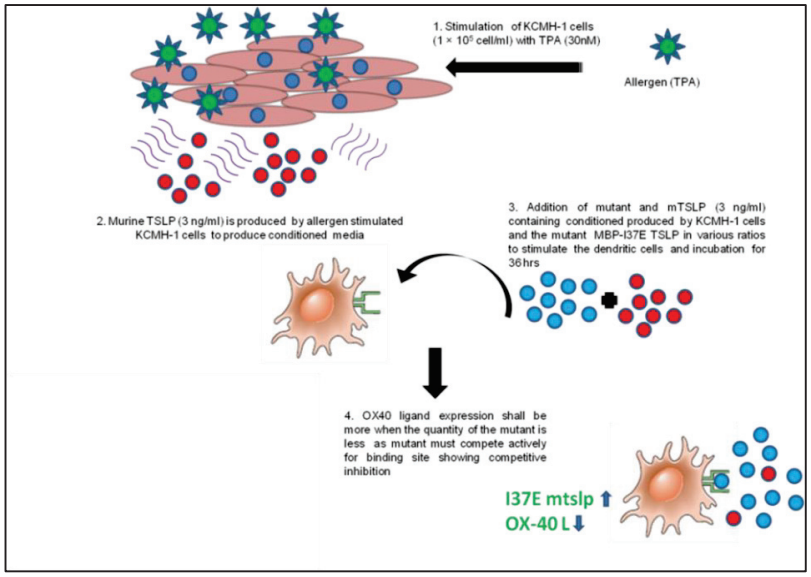

a.

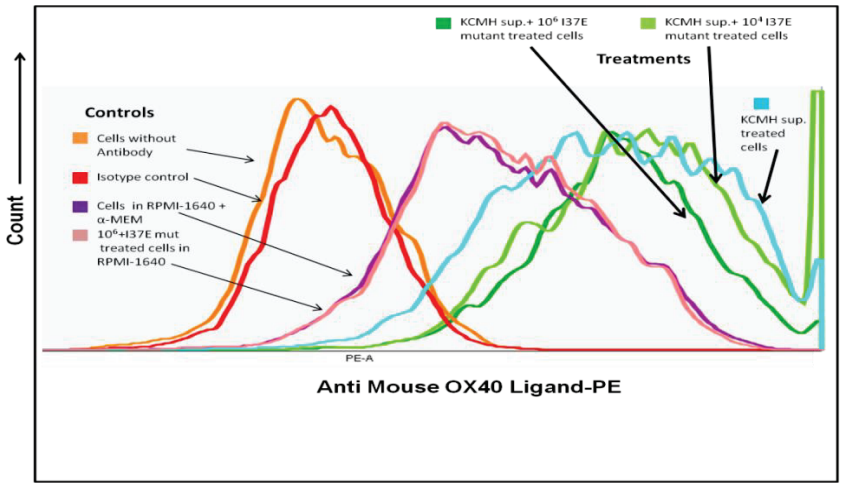

b.

Fig.4.33. KCMH- Dendritic cell based model used for the analysis of inhibitory activity of mutant I37E mTSLP-MBP. a. Schematic representation of the competition assay with dendritic cells. A schematic representation showing the stimulation of the the $1x10^5$ dendritic cells by the mTSLP containing KCMH-1 supernatant (obtained by treating $1x10^5$ KCMH-1 cells by 30nM TPA) to produce OX-40 L on its surface and addition of various dosage of mutant I37E mTSLP-MBP to reduce it. **b. Flow-cytometric analysis of the relative OX40L expression on addition of the mutant dosages.** This relative expression of OX40L was studied after adding I37E mTSLP-MBP in 10^4 (shown by light green curve) and 10^6 (shown by dark green curve) ng/ml dosages. An isotype control (red curve) by IgG1–PE antibody was also performed. Cells without antibody treatment are represented by the orange curve. The cells with only medium (RPMI-1640 + α-MEM) is represented by a violet curve and cells with only mutant is represented as a pink curve.

It was observed that there is a gradual reduction in the relative OX40 L expression with increasing dosage concentrations of the mutant. This indicates that the I37E mTSLP-MBP mutant competes with the wild type TSLP. An isotype control ensures that there is no unspecific binding with the Fc receptors.

4.4.7. Studying the antagonistic effects of I37E mTSLP-MBP mutant on KCMH supernatant induced relative expression of allergic surface markers (CD80 and CD86)

The supernatant of KCMH cells (1:1 ratio) was used to stimulate the dendritic cells as already described above in 4.4.5. I37E mTSLP-MBP treatments were given in 10^4 and 10^6 ng/ml dosages to two different samples. A control with only maximum quantity of mutant was also treated. The treated dendritic cells were (1×10^5 cell/sample) were grown in an incubator with 5% CO_2/95% air at 37°C for 24 h. The relative expression of CD80 and 86 were studied after staining the cells with relevant protocol (see materials and methods). The results are shown in Fig. 4.34 and 4.35.

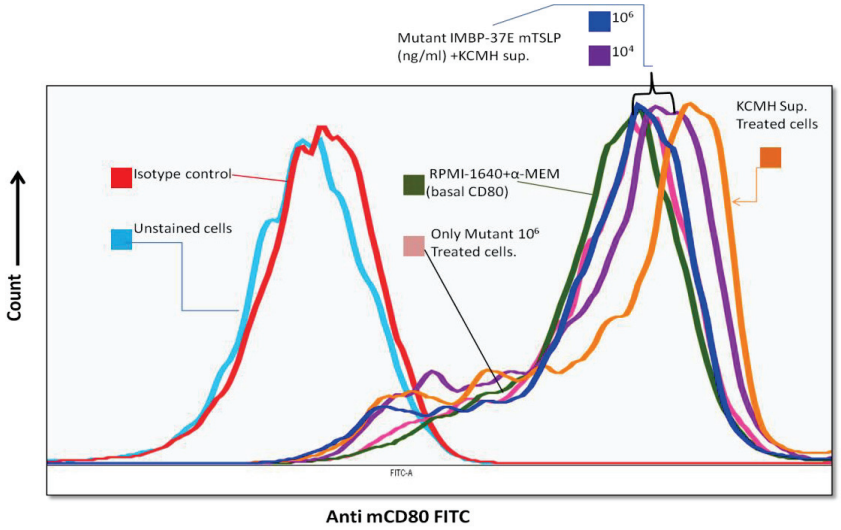

Fig.4.34. Flow-cytometric analysis of the relative change in the CD80 expression on the surface of dendritic cells stimulated by KCMH-1 cell supernatant, on addition of various mutant dosages. 1×10^5 cell dendritic cells were stimulated by KCMH-1 cells supernatant for 24 h and were stained by anti mouse CD80 FITC ligand antibody. The signals were analysed using flow cytometry. The basal CD80 expression is indicated by green curve. The maximum CD 80 expression is indicated by the orange curve. The violet and the blue curve represent the CD80 expression on treatment with two different dosage of the mutant I37E mTSLP-MBP (10^4 and 10^6 ng/ml respectively).The pink curve is the control with only maximum dosage of mutant (10^6 ng/ml). An isotype control (red curve) by IgG1–FITC antibody was also performed (red curve) to show specificity of the antibody. The sky blue curve represents the unstained cells.

It was observed that the KCMH-1 supernatant increased the expression of CD80 ligand on the surface of the mouse dendritic cells (as indicated by the shift between green and orange curves).

The CD80 expression can be brought down significantly brought down by using 10^6 ng/ml of I37E mTSLP-MBP (blue curve).10^4ng/ml I37E mTSLP-MBP also decreases the CD80 expression and thus a dosage dependent decrease of CD80 relative to the increasing concentrations of I37E mTSLP-MBP is seen. The isotype IgG1–FITC controls assure that blocking of Fc recpetors by the blockers is fine and no unspecific bindings take place.

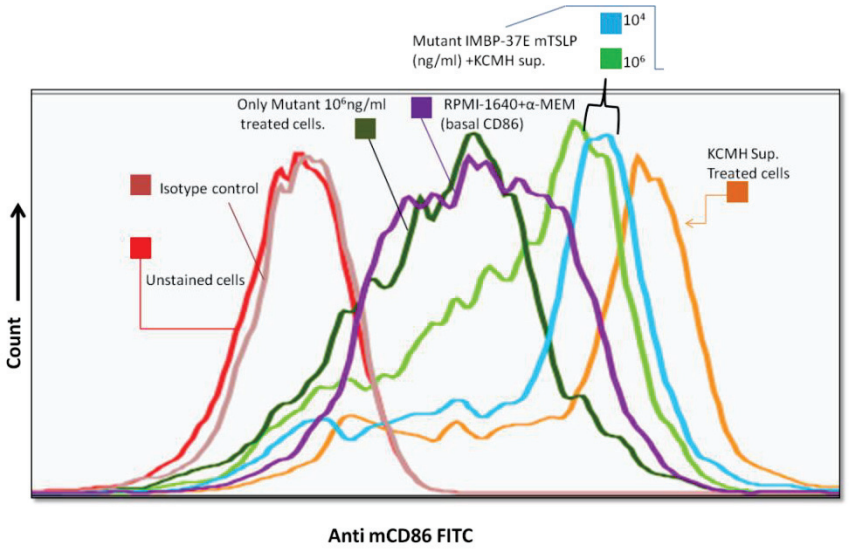

Fig.4.35.Flow-cytometric analysis of the relative change in the CD86 expression on the surface of dendritic cells stimulated by KCMH-1 cell supernatant, on addition of various mutant dosages. 1 × 10^5 cell dendritic cells were stimulated by KCMH-1 cells supernatant for 24 h and were stained by anti mouse CD86 FITC ligand antibody. The signals were analysed using flow cytometry. The basal CD80 expression is indicated by violet curve. The maximum CD86 expression is indicated by the orange curve. The sky blue and light green curves represent the CD86 expression on treatment with two different dosage of the mutant I37E mTSLP-MBP (10^4 and 10^6 ng/ml respectively).The green curve is the control with only maximum dosage of mutant (10^6 ng/ml). An isotype control (light brown) by IgG1–FITC antibody was also performed to show specificity of the antibody. The red curve represents the unstained cells.

In case of CD86 also it was observed that the KCMH-1 supernatant increased the expression of CD86 on the surface of the mouse dendritic cells (as indicated by the shift between orange and violet curves). The CD86 expression could be brought down significantly brought down by using 10^6 ng/ml of I37E mTSLP-MBP mutant (light green curve). The isotype IgG1–FITC controls assure that blocking of the Fc recpetors by the blockers is fine and no unspecific bindings take place.These results indicate that I37E mTSLP- MBP can lower the allergic markers significantly.

5. Discussion

To understand the interaction of a cytokine with its receptor in physiological context, it is necessary to have a cellular readout model. Factor-dependent cell lines have been successfully used in the past as models to study and characterize the functional expression of various growth factor receptors. They have been instrumental in developing bioassays for several cytokines. The reliability of a cell line is vital to the development of successful bioassays. The sensitivity of cell lines during an assay may vary when maintained in continuous cell culture. The process of transfecting a cell line leading to the expression of a cytokine receptor on the surface can be used effectively to create new factor-dependent cell lines. The Ba/F3 cell system provided a quick responding and convenient model to probe the mTSLP signaling pathway and allowed studies related to the effects of the cytokine inhibitors on STAT based reporter gene signaling which served as readout. Ba/F3 is an immortalized murine bone marrow-derived pro-B-cell line which depends on murine IL-3 as a growth and proliferation factor. In the presence of IL-3, Ba/F3 cells show a great resistance towards X-irradiation and the cytotoxic drugs etoposide and cisplatin (Collins, 1992). Ba/F3 cells go through apoptotic cell death through the caspase independent pathway on withdrawing the growth factor (Wirawan et al., 2010). The factor dependence can be switched from mIL-3 to another factor by removal of mIL-3 and transfection of the cells with chains that express relevant cytokine receptors which would be the new dependence factor (Daley et al., 1988). This has been observed in various models for studying the functional reconstitution of growth factor receptors e.g.: IL-3, IL-5 (Bosward et al., 1999) , GM-CSF, Macrophage colony stimulating factor (M-CSF) (Metcalf, et al.,1994, Kitamura et al., 1991, Lutz et al., 2000) and the Ba/F3 cell line dependent on Epo as a growth factor (Sakamaki et al., 1992).

Following the above discussed strategies, initially the cDNA sequences encoding native TSLP receptor chains were cloned into pcDNA3.1 and transfected into the Ba/F3 cells. The reporter gene expression signals were not optimal for the studies. This technical defect was removed by the transfection of the Ba/F3 cells with exo-mTSLPR-intra-hTSLPR/exo-mIL-7Rα-intra-hIL-Rα hybrid receptors along with a STAT1 responsive-IRF reporter gene. This yielded stronger signals when treated with mTSLP. The maximum signal is approximately 6 folds at saturating concentration of mTSLP. Since the internal part of the chains is human, it could associate well with the reporter gene used in the cell. This is the closest artificial model which could be produced in the mouse cells expressing mTSLPR. Further optimization is possible by the rotation of the intercellular domains by introduction of additional amino acids (see results chapter 4.1) based on data from Andreas Wohlmann (Wohlmann, 2014).

This leads to combinations producing better signals than the original, though the structure and orientation of the chains is compromised as compared to the native state. So this may be a shortcoming to not be able to show real state receptor orientation but on the other hands this produces signal approximately 5 fold stronger. The problem still existing is that the cell line is transiently viable for the assays and it is cumbersome to perform assays like proliferation assays as done by Borowski with IL-4 receptor expressing Ba/F3 cells. Such assays when tried with a transient cell line do not work. It must be also noted that the reporter gene assay works only on using the precise amount of DNA for fixed amount of cells for transfections. Therefore, the plan to make mTSLP dependent stable cell line would be instrumental in performing assays like proliferation assays and reporter gene assay with convenience. The possible introduction of expression vectors that could lead to the cytokine production on which the mTSLP-dependent cell line thrives can create an autocrine loop and lead to factor independence. This variant can be used to screen hybridomas for the production of monoclonal antibodies that inhibit mTSLP-dependent proliferation as one possible application. Efforts to make a stable cell line have been tried in past by removing mIL-3 and applying mTSLP selection pressure but have failed. The cells showed growth initially but then died. The limitations could be overcome by a 2 step selection procedure. The first selection could be based on the application of a zeocin antibiotic to obtain cells with domain rotated receptor. Initially the cells shall be given mIL-3. After confirming the presence of domain rotated receptors on the cellular surface by flow cytometry, the cells shall be put to mTSLP selection to remove the dependence on mTSLP. This process is expected to produce a stable cell line which stably expresses domain rotated mTSLPR and is mTSLP dependent.

Soluble receptors can be used as inhibitory tools to disrupt cytokine signaling by competing with the cytokine for binding on to cellular receptors e.g. TNF-α (Seckinger et al., 1990). The mTSLPR soluble exodomain effectively competed with mTSLP for the binding on the receptors expressed on the cells. Therefore it served as a competitive antagonist to interfere with intracellular STAT based luciferase reporter gene activation signals. This is evident by the decreasing signals with the increase of the receptor exo-domain concentrations.

mTSLPR production was optimal for use as a competitor but needs to be further purified by gel filtration to ensure a better starting material for the production of antibody. As the structure of the mTSLPR is known now, the use of critical antigenic epitopes for targeted antibody production is also a possible approach.The mTSLPR antibody produced was non inhibitory (data not shown) though it showed that it could bind to TSLPR expressed on Ba/F3 cells. In a similar approach, Borowski et al. could yield inhibitory antibody producing clones against human TSLPR. The probability to find an antibody using such an approach in single attempt is low. Other hosts (hamster/mouse) for producing such an antibody could be tried. Another approach to produce antibody using autoimmunity against OVA-amine complexes was tried but could yield fewer clones

that survived for some days before dying (data not shown). Such approach could also be re-tried with modifications. The technique of anti-cytokine auto-vaccination is a powerful tool but has remained rather obscure due to various technical problems. A two-step procedure could be used as described by Uyttenhove et al., 2011, which is based on use of purified OVA multimers by size exclusion chromatography after incubation with glutaraldehyde at pH 6. This is followed by incubation of these polymers with the target protein at pH 8.5, this leads to the de-protonation of the reactive amines, resulting in complexes that confer immunogenicity to self-antigens. Uyttenhove et al., 2011 discussed the chemokine granulocyte chemotactic protein-2 (GCP-2)/CXCL6, cytokines GM-CSF, IL-17F, IL-17E/IL-25, IL-27, and TGF-β1, and the MMP-9/gelatinase B as examples. Pre-activated OVA multimers reactive with amine residues can thus provide an efficient carrier for auto-vaccination against 9–90 kDa autologous proteins. This can improve the possible yield of antibody producing hybridoma clones. In addition to the production of mouse mAb against mouse factors, *in vivo*, auto-vaccination offers an alternative to gene inactivation in studies of *in vivo* cytokine function (Zagury et al., 2003). This approach in principle could allow for concomitant inhibition of several cytokines in the same animal, a need for treating the elevated cytokine milieu in Asthma. Another approach as described by Kinoshita (Kinoshita et al., 2005) to prepare 4 monoclonal antibodies against an antigen, prostate-specific membrane antigen (PSMA), for immunotherapy to prevent the *in vivo* growth of lymph node carcinoma of the prostate (LNCaP) tumor could also yield a method. Using computer-aided analysis, they selected the B cell epitopes of PSMA by using various correlates of protein antigenicity and secondary structural predictions according to the algorithm procedure described by Kaumaya et al., 1994. Those peptides which had the transferrin receptor-like domain of PSMA were subjected to analyses. This yielded 4 oligopeptides corresponding to the amino-acid residues of PSMA were selected and listed. A BLAST search at NBCI website (http://ncbi.nlm.nih.gov/BLAST/Blast.cgi) found 3 out of these peptides unique for human PSMA. These peptides were linked to the C-terminal end of the 'promiscuous' measles virus fusion protein (MVF) by a LSPG linker to obtain a T-cell epitope and B-cell epitope chimera. Solid phase synthesis was used to synthesize these oligopeptides followed by purification by HPLC. The molecular weight was checked using Mass spectroscopic analysis. These oligopeptides were used to immunize the mice and develop hybridomas yielding mAbs against the oligonuleotides. These mAbs were specifically targeted to act against the PSMA epitopes. A similar approach could yield oligopeptides which could yield antibodies that bind to the mTSLPR or mTSLP at specific hot spots to impede its activity. Another approach that can be undertaken is single domain antibody generation (van der Linden et al., 1999, Dumoulin et al., 2002). A single-domain antibody comprises of a peptide chain approximately 110 amino acids long with one variable domain (V_H) of a heavy-chain antibody, or of a common IgG. These peptides are heat resistant and have binding affinity towards antigens similar to the whole antibodies. They can be derived from camel and sharks. The complementarity determining region 3 (CDR3), makes then more soluble in water and provides them an ability to bind

epitopes which a normal antibody cannot bind, however a lack of Fc region leads to complement system related cytotoxicity (Dolk et al., 2005, Stanfield et al., 2004). A gene library with several million clones can be produced by reverse transcription and polymerase chain reaction. A single-domain gene library from shark could be screened for antibodies which can bind to the mTSLPR (Gibbs, 2005). Panning and screening techniques like yeast display, phage display or ribosome display could be used to identify the antigen binding clones.

The mTSLP production as a fusion protein was done as there was problem while producing it in bacteria. Similar approaches have been successful for human TSLP but have failed in production of murine TSLP, perhaps due to low homology of mTSLP. Using bacterial production in past, the protein could be secreted into inclusion bodies in bacteria but it showed no activity when purified on a Ni-sepharose column. Similar problems were experienced with IL-4 and refolding buffers and altered conditions had to be used (Andreas Borowski, personal communication). The mTSLP production as a MBP fusion protein yielded considerable amounts of protein in a small amount of time. mTSLP-MBP was bioactive and showed binding to the mTSLPR. The activity of the MBP-fusion proteins is quite low when compared to the commercial mTSLP (see secteeion 4.3). This could be due to the reason that not hundred percent of the total quantity of protein is folded properly. This was not a drawback while studying relative effects in luciferase gene assays but may lead to issues during the animal studies. Too much volume of proteins cannot be administered to the animal. The protein may also be pyrogenic in mice as it may have contamination with bacterial polysaccharides. The cleavage of the protein leads to contamination with factor X and needs another tedious step for purification. These reasons should serve as a motivation to produce proteins in another possible ways like cloning mTSLP in pHL-expression vector and producing it in eukaryotic cell lines like HEK293S MGAT1$^{-/-}$ in (Verstraete et al., 2014) or NS0 cell line from murine myeloma (R&D mTSLP product data sheet). Other plasmids which have been used to produce IL-2 family cytokines could also be tried.

To further elucidate the role of TSLP signaling in diseased condition, the effects of TSLPR blocking via mutant I37E was evaluated. It was observed that I37E binds to the receptors without activity but shows partial competitive effect (see section 4.3). Thus, it is a partial antagonist that competes with the wild type mTSLP in cells activated within a certain concentration range. Efforts need to be made to characterize some effective mutants that are better than this mutant. The initially used bacterial display strategy can be used to characterize some more mutants by random mutations on the hotspot sites where the receptor is binding to the cytokine. This could yield double mutants which may bind or not bind to the TSLPR chain and need Ba/F3 based screening to identify the perfect candidates. *In silico* approaches could be adopted and use of software (Scrödinger) based characterization of mutants based on stimulated molecular docking. One can also think of altering the interface of IL-7

and stabilizing ion pair and counter charges. This approach could lead to the production of superantagonists which may show better affinity to TSLP receptor and thus act as competitors.

No natural human cellular model is available for testing TSLP based inhibitory molecules as there are no TSLPR present on peripheral dendritic cells generated by monocytes (Würtzen et al., 2011, Andreas Wohlmann, personal communication). KCMH-1-Dendritic cell based cellular model was generated to serves as a model for screening of potential allergenicity caused by various allergens/chemicals. This could also serve as model to test inhibitory tools against mTSLP as shown in results section 4.4. This model addresses mTSLP cellular communication network and offers a simple approach and mimics the conditions as present in the allergic animal. Further improvement in this model could be made by using it in an airway liquid based interface. This shall allow it to mimic the cells of the lung. A co-culture with cells is also possible with other population of the blood peripheral blood mononuclear cells (PBMCs) and can yield studies based on CD surface marker dynamics on these cells under inflammatory condition. This model can envisage an outlook of activities in the human system.

For further investigation of the various inhibitory/interfering molecules in mTSLP based signaling in non-transgenic allergic disease models, three types of models could be used: (1) antigen-driven models using ovalbumin (OVA), (2) a protease model and (3) a model of Th2-type contact hypersensitivity. Enhanced levels of mTSLP have been observed in the OVA-induced airway inflammation model, while reduced airway inflammation and goblet cell hyperplasia were observed in TSLPR deficient mice (Shami 2005 et al., Zhou et al., 2005) Epicutaneous immunization of mice with OVA lead to allergic inflammation in the skin, enhanced infiltration of eosinophils, high Th2 cytokine levels and OVA-specific serum IgE, all of them are significantly reduced in TSLPR-deficient mice (R. He et al., 2008). TSLPR deficiency in mice models lead to the attenuation of atherosclerotic lesion development by inhibition of Th17 cells and the promotion of regulatory T cells (C. Wu et al., 2014). TSLP-TSLPR signal-dependent allergic diarrhea with Th2 cytokine production in gastrointestinal tract could also be induced by OVA (Blázquez et al., 2010). In OVA-induced allergic rhinitis, anti-TSLP antibody treatment neutralized the effects of TSLP and reduced its symptoms. Temporary TSLP expression was found to have been induced by mechanical injury in the skin (Oyoshi et al., 2010). In the presence of OVA antigen, DCs isolated from the skin of wild-type mice after mechanical injury elicited increase in IL-4 and IL-13 productions in $CD4^+$ T cells with OVA-specific T cell receptor, whereas DCs from the injured skin of TSLPR-deficient mice or from the skin of un-injured mice induced the production of both the cytokines at a relatively smaller amount (Oyoshi et al., 2010). This study indicates that OVA raised TSLP expression and an increased level of TSLP even temporarily in the skin by mechanical injury, induced antigen-derived Th2 responses by skin DCs.

Proteases also act as allergens. For example, papain, a cysteine protease induced TSLP expression at the injected site of the skin in wild-type mice. Here, TSLP expression was dependent on reactive oxygen species (ROS), toll-like receptor (TLR) 4 and the adaptor protein Toll/Interleukin -1 homology (TIR)-domain-containing adaptor-inducing interferon-β (TRIF) (Tang et al., 2010).

In an experimental model of Th2-type contact hypersensitivity, TSLP was induced using Fluorescein isothiocyanate (FITC) as an allergen (a model for human Th2-type contact hypersensitivity). Dibutyl phthalate, a solvent component used in this model, induced TSLP expression (Larson et al., 2010, Boehme et al., 2008, Shigeno et al.,2009). There was a profound decrease in type-2 immune responses in the skin and in antigen-bearing DCs in the draining lymph node following FITC treatment in the absence of TSLP responses. The DCs migrated but displayed a decreased capacity for promoting $CD4^+$ T cell proliferation (Larson et al., 2010) These studies indicate that the factors OVA, proteases and dibutylphthalate act as inducers of TSLP and this leads to allergic inflammation in mice. So the above discussed mice models can be used for studying the inhibitors depending on the use and various allergic parameters could be evaluated giving us hints about its activity to reduce inflammation in mice. Similar models can be trusted as they have been tried before in case of screening mutants for IL-4 and IL-13.

The latest therapies that are available or being studied to treat asthma have been extensively reviewed by Cezmi A Akdis (Akdis, 2012) and these involve the following:

Corticosteroids as inhalers containing corticosteroids and short and long-acting β2-adrenoceptor agonists (SABAs and LABAs) are the most prevalent advocated asthma treatments for managing Asthma. α-adrenoceptor agonists are used in rhinitis instead to relieve nasal congestion, and non-sedating H1-antihistamines and topical corticosteroids are well-established control therapies. A combination of symptom-relieving and control therapies are used for effective management of most allergies. The corticosteroids suppress the Th2-cell-mediated inflammation by transrepression of inflammatory cytokines and transexpression of the anti inflammatory cytokines, chemokines and adhesion molecules. In smokers and virus-induced exacerbations, the inhaled corticosteroids are rendered ineffective.

β- adrenoreceptor agonists such as Salbutamol and Turbutaline are the most reliable, effective and rapid relieving bronchodilators available at present.They act by binding to the β2-adrenoceptor and stimulating the adenylate cyclase leading to the production of cyclic adenosine 3′5′-monophosphate (cAMP) and activation of protein kinase A. This leads to smooth-muscle relaxation by the phosphorylation of myosin light-chain kinase and by opening of Ca^{2+}-dependent K^+ (K-Ca) channels, thus relieving bronchoconstriction in asthma.

Targeting IgE has been shown in several clinical studies that humanized mAbs bind to the Fc portion of the IgE molecule. Omalizumab is one such antibody that binds to the similar sites that IgE molecules use to attach to FcεRI and proved to be an effective treatment in patients with poorly controlled, moderate to severe allergic asthma or allergic rhinitis. It does not cross-link cell-surface expressed IgE. Omalizumab decreases serum concentration of free IgE (unbound) and the expression of the high-affinity IgE receptor FcεRI on various immune cells. The reticuloendothelial system clears the immune-complexes of IgE and mAb to IgE.

Mast cells inhibition in the airways and conjunctiva, Sodium cromoglicate (SCG) and Nedocromil sodium hinder the allergen-induced early and late-phase responses involving mucosal mast cells induced allergic reponses. These drugs inhibit the flux of chloride ions in mast cells, epithelial cells and neurons thus increasing their activation threshold. Another attractive target is CD63 suface marker on mast cells. These drugs interfere with integrin signalling, localization or trafficking and interacts integrins to modify adhesion to fibronectin and vitronectin. A monoclonal antibody blocking CD63 inhibits FcεRI-mediated activation of mast cells that are adherent to extracellular matrix proteins but not to nonadherent cells.

Cytokine inhibition inside a network that is responsible for the inflammatory processes that lead to asthma and allergy. Immunomodulation of this network through novel biological molecules can produce several therapeutic possibilities to suppress the inflammatory activities. mAbs against several cytokines have been developed and tried in clinical studies. IL-2Rα (CD25) blocking mAb (Daclizumab) is in phase 2 clinical trials and shows efficacy in asthma treatments .It blocks the IL-2Rα on T cells and inhibits the proinflammatory cytokine generation. It showed no negative effects on Treg cell generation *in vivo*. IL-4 Humanized mAb (Pascolizumab) blocks IL-4 signaling. Phase 2 studies have been completed but since the only IL-4 targeting approach was found to be non effective, and developments were ended. Mutated IL-4 (Pitrakinra) blocks IL-4Rα, common to the IL-4 and IL-13 receptors. It showed a reduced allergen response in asthma in the phase 2 clinical trials. Targeting of IL-4 and IL-13 simultaneously by AMG-317 showed some efficacy Blocking mAb to IL-4Rα, also blocks IL-13 in the clinical phase 2 has been completed and showed efficacy. Inhaled oligonucleotide AIR-645 against IL-4Rα, also blocked IL-13 and inhibited effects by allergen challenge. This molecule is in clinical development with phase 2 completed Soluble recombinant human IL-4 receptor (Altrakincept) during phase 1 and 2 clinical trials showed efficacy to control moderate asthma but this was not confirmed during phase 3 trials. Targeting TNF-α is important for treatment of non-controlled asthma. TNF-α Infliximab, chimeric mAb has been already tested in phase 2 for asthma. TNF-α targeting studies have been stopped due to severe side effects, some showed promise while other studies showed no efficacy. The unfavorable risk-benefit ratio is unfavourable for this cytokine target and therefore the target may be dropped. OX-40 ligand blocking mAb to OX40L is in preclinical development in mice. It inhibits the Th2-type immune responses

induced by TSLP but failed to inhibit allergen-induced bronchoconstriction and airway hyperresponsiveness (AHR) in subjects with mild allergic asthma. Several such antibodies have been developed for IL-17, 25 33 and chemokines and are all in clinical phases in mice.

The current therapeutic strategies for mitigation of asthma symptoms are affected by the complexity of the whole disease spectrum and molecular mechanisms. The biomarkers for subgrouping and endotyping are a limitation. Limited information for improvising the existing therapies (for example, currently used inhaled steroid and β-adrenergic agonist combination therapy is effective and relatively inexpensive) and low patient adherence is another issue. The animal studies in small animal models are disappointingly predictive. Most drugs effective in mouse models failed in human clinical trials. The impossibility to study two novel biologicals as a combination where one of them may potentiate the other, until one of them is approved serves as a limiting factor. In this case one of the biologicals may be unlikely to be effective when used alone e.g. cytokine targeting IL-4 etc. In this light, new upstream therapeutic like targets like TSLP which are over expressed and affect a lot of immune cells during inflammation, need to be focused upon.

The present study yielded results that shall be contributing to the studies aimed at targeting the mTSLP/mTSLPR system. Several therapeutic approaches targeting TSLP are in the process of clinical trials. These studies add to further information on the possibilities of using well characterized cellular model systems for studying mTSLP targeting molecules during *in vitro* studies. The studies yield a low cost and efficient way to produce and test bioactivity of mTSLP and efficacy of its mutants *in vitro*. The findings suggest that the I37E mutant characterized in this study could be further improvised with the help of bioinformatics tools to obtain double mutants. The receptor interface structural details offer a chance to enable computational molecular docking and production of several other mutants. Efforts could also be made to obtain super agonists which bind strongly to the TSLPR, even better than mTSLP could and thus can compete with. In addition to the mutant, the receptor protein exo domain produced and characterized in these studies gives hope that their local administration may inhibit Th2-mediated cardinal features of asthma by altering the function of lung DCs. The anti mTSLPR antibody,though non-inhibitory in nature, has been found to bind its target and could be used in enhancing knowledge of the key targets TSLP acts in different stages of allergic diseases which may be further important in enhancing our comprehension of the TSLPR dynamics on the cellular surfaces of various immune cells. TSLP has been shown to activate many other immune and structural cells and therefore such data shall help to understand TSLP related signaling in response to other cytokine. These studies extend our understanding of biological function of TSLP/TSLPR and established the importance of TSLP receptors in atopic diseases.

Since most prevalent atopic asthma is initiated by inhaled allergen exposure, an OVA/HDM induced asthma mouse model system shall provide us further information about the activity of these

inhibitory tools in allergen-specific immune responses during pathogenic asthmatic conditions and therefore such studies shall be performed in near future. However, since mouse models cannot be considered to mimic the full range of clinical manifestations of asthma in humans, humans clinical studies will be required before TSLP can be beyond doubt regarded as a central regulator of allergic asthma. The identification and comprehension of various allergic inflammatory pathways affected by TSLP is therefore a relevant and open dynamic area of active study.

In conclusion, the findings in this thesis provide an insightful understanding about mTSLP based signaling responses during the inflammatory process. The goals of this study to generate mTSLP responsive cell based models which provide quantifiable data and to generate tools to impede mTSLP mediated signaling by antagonists has been met successfully. It can be envisaged that employing these cellular models and tools generated in this study, further investigations could be carried on to study the mTSLP action on various immune cells at molecular level. Since mTSLP influences the immune cell homeostasis at the body's barrier surfaces in association with various chemokines, it engages various immune cells to initiate the inflammatory process during asthma. In this regard, these cellular models could be utilized to investigate the role of various allergens and toxic chemicals in the inflammatory processes. These studies could also provide a foresight into further development of natural human cell based models to study hTSLP activity.

In order to understand and utilize the knowledge about biological intercellular signaling by TSLP, specific information about the promotion and control of TSLPR expression dynamics on various cells must be delineated. In this light it's also important to decrypt whether TSLP evokes similar signaling pathways within different cells. The antibody generated in this study could bind successfully to the surface expressed TSLPR on various immune cells and thus it could be used for probing the dynamics of mTSLPR expression towards cytokine treatments.

The administration of the mutant *in vitro* resulted in down regulation of inflammation markers such as OX40, CD80 and CD86 ligands on the surface of DCs as well as reduction of STAT1 promoted signaling in TSLP responsive Ba/F3 cellular model. These results increase our understanding of the biological function of TSLP/TSLPR signaling and highlight the importance of TSLP in initiation and activation of Th2 skewed responses in atopic diseases. As an improvised study, the natural model could be used to study the effects of TSLP inhibition using the antagonists on various other signaling pathways.

The heterogeneity of various genetic and environmental factors responsible for phenotypic expression in Asthma complicates the desire to design a uniform effective therapy for all the patients. Therefore it becomes essential to find and target upstream molecules involved in cellular immune as a central axis, which makes therapeutic targeting of TSLP desirable. It will be interesting to determine whether the administration of soluble exo-mTSLPR domain and the mutant I37E mTSLP

at the allergen-challenge phase has similar therapeutic effects in OVA/HDM mouse models of Asthma. This study, therefore leaves us open for further interrogation of targeted antagonistic inhibition of mTSLP signaling in animal models in pursuit of a TSLP-orientated therapy.

References

Agrawal, R., Wright, P. W., & Woodfolk, J. (2012). Allergen Induces Dual Upregulation of TSLP Receptor on Circulating Basophils and Dendritic Cells in Atopic Dermatitis. *Journal of Allergy and Clinical Immunology*, *129*(2), AB69.

Akamatsu, T., Watanabe, N., Kido, M., Saga, K., Tanaka, J., Kuzushima, K., Chiba, T. (2008). Human TSLP directly enhances expansion of $CD8^+$ T cells. *Clinical and Experimental Immunology*, *154*(1), 98–106.

Akdis, C. (2012). Therapies for allergic inflammation: refining strategies to induce tolerance. *Nature Medicine*, *18*(5), 736–49.

Allakhverdi, Z., Comeau, M. R., Jessup, H. K., Yoon, B. P., Brewer, A., Chartier, S., Delespesse, G. (2007). Thymic stromal lymphopoietin is released by human epithelial cells in response to microbes , trauma , or inflammation and potently activates mast cells, *204*(2), 253–258.

Allakhverdi, Z., Comeau, M. R., Jessup, H. K., Yoon, B.-R. P., Brewer, A., Chartier, S.,Delespesse, G. (2007). Thymic stromal lymphopoietin is released by human epithelial cells in response to microbes, trauma, or inflammation and potently activates mast cells. *The Journal of Experimental Medicine*, *204*(2), 253–8.

Allakhverdi, Z., Comeau, M. R., Smith, D. E., Toy, D., Endam, L. M., Desrosiers, M., Delespesse, G. (2009). $CD34^+$ hemopoietic progenitor cells are potent effectors of allergic inflammation. *The Journal of Allergy and Clinical Immunology*, *123*(2), 472–8.

Al-Shami, A., Spolski, R., Kelly, J., Fry, T., Schwartzberg, P. L., Pandey, A., Leonard, W. J. (2004). A role for thymic stromal lymphopoietin in CD4(+) T cell development. *The Journal of Experimental Medicine*, *200*(2), 159–68.

Al-Shami, A., Spolski, R., Kelly, J., Keane-Myers, A., & Leonard, W. J. (2005). A role for TSLP in the development of inflammation in an asthma model. *The Journal of Experimental Medicine*, *202*(6), 829–39.

Aspord, C., Pedroza-Gonzalez, A., Gallegos, M., Tindle, S., Burton, E. C., Su, D., Palucka, A. K. (2007). Breast cancer instructs dendritic cells to prime interleukin 13-secreting $CD4^+$ T cells that facilitate tumor development. *The Journal of Experimental Medicine*, *204*(5), 1037–47.

Astrakhan, A., Omori, M., Nguyen, T., Becker-Herman, S., Iseki, M., Aye, T., Rawlings, D. J. (2007). Local increase in thymic stromal lymphopoietin induces systemic alterations in B cell development. *Nature Immunology*, *8*(5), 522–31.

Balkwill, F. R., & Mantovani, A. (2012). Cancer-related inflammation: common themes and therapeutic opportunities. *Seminars in Cancer Biology*, *22*(1), 33–40.

Bell, C. A., Tynan, J. A., Hart, K. C., Meyer, A. N., Robertson, S. C., & Donoghue, D. J. (2000). Rotational coupling of the transmembrane and kinase domains of the Neu receptor tyrosine kinase. *Molecular Biology of the Cell*, *11*(10), 3589–99.

Besin, G., Gaudreau, S., Ménard, M., Guindi, C., Dupuis, G., & Amrani, A. (2008). Thymic stromal lymphopoietin and thymic stromal lymphopoietin-conditioned dendritic cells induce

regulatory T-cell differentiation and protection of NOD mice against diabetes. *Diabetes*, *57*(8), 2107–17.

Biagini Myers, J. M., Martin, L. J., Kovacic, M. B., Mersha, T. B., He, H., Pilipenko, V., Khurana Hershey, G. K. (2014). Epistasis between serine protease inhibitor Kazal-type 5 (SPINK5) and thymic stromal lymphopoietin (TSLP) genes contributes to childhood asthma. *Journal of Allergy and Clinical Immunology*, *134*(4), 891–899.

Bieber, T. (2010). Atopic dermatitis. *Annals of Dermatology*, *22*(2), 125–37.

Biton, M., Levin, A., Slyper, M., Alkalay, I., Horwitz, E., Mor, H., Ben-Neriah, Y. (2011). Epithelial microRNAs regulate gut mucosal immunity via epithelium-T cell crosstalk. *Nature Immunology*, *12*(3), 239–46.

Blázquez, A. B., Mayer, L., & Berin, M. C. (2010). Thymic stromal lymphopoietin is required for gastrointestinal allergy but not oral tolerance. *Gastroenterology*, *139*(4), 1301–9.

Bleck, B., Kazeros, A., Bakal, K., Garcia-Medina, L., Adams, A., Liu, M., Reibman, J. (2015). Coexpression of type 2 immune targets in sputum-derived epithelial and dendritic cells from asthmatic patients. *Journal of Allergy and Clinical Immunology*.

Boehme, S. A., Franz-Bacon, K., Chen, E. P., Sasik, R., Sprague, L. J., Ly, T. W., Bacon, K. B. (2008). A small molecule CRTH2 antagonist inhibits FITC-induced allergic cutaneous inflammation. *International Immunology*, *21*(1), 81–93.

Boguniewicz, M., & Leung, D. Y. M. (2011). Atopic dermatitis: a disease of altered skin barrier and immune dysregulation. *Immunological Reviews*, *242*(1), 233–46.

Bunyavanich S, Schadt EE. Systems Biology of Asthma and Allergic Disease (2015). A Multiscale Approach. *Journal of Allergy and Clinical Immunology,* 135(1): 31-42.

Borowski, A., Vetter, T., Kuepper, M., Wohlmann, A., Krause, S., Lorenzen, T., Friedrich, K. (2013). Expression analysis and specific blockade of the receptor for human thymic stromal lymphopoietin (TSLP) by novel antibodies to the human TSLPRα receptor chain. *Cytokine*, *61*(2), 546–555.

Bosward, K., Emery, D. L., McWaters, P. W., Husband, A. J., & Bendixsen, T. (1999). Characterization of a bioassay for detection of recombinant and native ovine interleukin-5. *Immunology and Cell Biology*, *77*(4), 331–6.

Briot, A., Deraison, C., Lacroix, M., Bonnart, C., Robin, A., Besson, C., Hovnanian, A. (2009). Kallikrein 5 induces atopic dermatitis-like lesions through PAR2-mediated thymic stromal lymphopoietin expression in Netherton syndrome. *The Journal of Experimental Medicine*, *206*(5), 1135–47.

Briot, A., Lacroix, M., Robin, A., Steinhoff, M., Deraison, C., & Hovnanian, A. (2010). Par2 inactivation inhibits early production of TSLP, but not cutaneous inflammation, in Netherton syndrome adult mouse model. *The Journal of Investigative Dermatology*, *130*(12), 2736–42.

Bunyavanich, S., & Schadt, E. E. (2015). Systems biology of asthma and allergic diseases: A multiscale approach. *Journal of Allergy and Clinical Immunology*, *135*(1), 31–42.

Chapiro, E., Russell, L., Lainey, E., Kaltenbach, S., Ragu, C., Della-Valle, V., Bernard, O. A. (2010). Activating mutation in the TSLPR gene in B-cell precursor lymphoblastic leukemia. *Leukemia*,*24*(3),642–5.

Chen, A. I., Mcadam, A. J., Buhlmann, J. E., Scott, S., Lupher, M. L., Greenfield, E. A., Sharpe, A. H. (1999). Ox40-Ligand Has a Critical Costimulatory Role in Dendritic Cell : T Cell Interactions, *11*, 689–698.

Chen, Z.-G., Zhang, T.-T., Li, H.-T., Chen, F.-H., Zou, X.-L., Ji, J.-Z., & Chen, H. (2013). Neutralization of TSLP inhibits airway remodeling in a murine model of allergic asthma induced by chronic exposure to house dust mite. *PloS One*, *8*(1), e51268.

Collins, M. K. (1992). Interleukin 3 protects murine bone marrow cells from apoptosis induced by DNA damaging agents. *Journal of Experimental Medicine*, *176*(4), 1043–1051.

Concepts, C. (2006). The Asthma Epidemic, 2226–2235.

Cookson, W. O. C. (2000). Genetics of asthma and allergic disease. *Human Molecular Genetics*, *9*(16), 2359–2364.

Daley, G. Q., & Baltimore, D. (1988). Transformation of an interleukin 3-dependent hematopoietic cell line by the chronic myelogenous leukemia-specific P210bcr/abl protein. *Proceedings of the National Academy of Sciences of the United States of America*, *85*(23), 9312–6.

De Monte, L., Reni, M., Tassi, E., Clavenna, D., Papa, I., Recalde, H., Protti, M. P. (2011). Intratumor T helper type 2 cell infiltrate correlates with cancer-associated fibroblast thymic stromal lymphopoietin production and reduced survival in pancreatic cancer. *The Journal of Experimental Medicine*, *208*(3), 469–78.

Demehri, S., Morimoto, M., Holtzman, M. J., & Kopan, R. (2009). Skin-derived TSLP triggers progression from epidermal-barrier defects to asthma. *PLoS Biology*, *7*(5).

Dolgachev, V., Petersen, B. C., Budelsky, A. L., Berlin, A. A., & Lukacs, N. W. (2009). Pulmonary IL-17E (IL-25) Production and IL-17RB+ Myeloid Cell-Derived Th2 Cytokine Production Are Dependent upon Stem Cell Factor-Induced Responses during Chronic Allergic Pulmonary Disease. *The Journal of Immunology*, *183*(9), 5705–5715.

Dolk, E., van Vliet, C., Perez, J. M. J., Vriend, G., Darbon, H., Ferrat, G., Verrips, T. (2005). Induced refolding of a temperature denatured llama heavy-chain antibody fragment by its antigen. *Proteins*, *59*(3), 555–64.

Duan, W., Mehta, A. K., Magalhaes, J. G., Ziegler, S. F., Dong, C., Philpott, D. J., & Croft, M. (2010). Innate signals from Nod2 block respiratory tolerance and program T(H)2-driven allergic inflammation. *The Journal of Allergy and Clinical Immunology*, *126*(6), 1284–93.

Dumoulin, M., Conrath, K., Van Meirhaeghe, A., Meersman, F., Heremans, K., Frenken, L. G. J., Matagne, A. (2002). Single-domain antibody fragments with high conformational stability. *Protein Science : A Publication of the Protein Society*, *11*(3), 500–15.

Ebner, S., Nguyen, V. A., Forstner, M., Wang, Y.-H., Wolfram, D., Liu, Y.-J., & Romani, N. (2007). Thymic stromal lymphopoietin converts human epidermal Langerhans cells into antigen-presenting cells that induce proallergic T cells. *The Journal of Allergy and Clinical Immunology*, *119*(4), 982–90.

Ensor, H. M., Schwab, C., Russell, L. J., Richards, S. M., Morrison, H., Masic, D., Moorman, A. V. (2011). Demographic, clinical, and outcome features of children with acute lymphoblastic leukemia and CRLF2 deregulation: results from the MRC ALL97 clinical trial. *Blood*, *117*(7), 2129–36.

Eri, R. D., Adams, R. J., Tran, T. V, Tong, H., Das, I., Roche, D. K.,McGuckin,M. A. (2011). An intestinal epithelial defect conferring ER stress results in inflammation involving both innate and adaptive immunity. *Mucosal Immunology*, *4*(3), 354–64.

Fernandez, M.-I., Heuzé, M. L., Martinez-Cingolani, C., Volpe, E., Donnadieu, M.-H., Piel, M. Soumelis, V. (2011). The human cytokine TSLP triggers a cell-autonomous dendritic cell migration in confined environments. *Blood*, *118*(14), 3862–9.

Fontenot, D., He, H., Hanabuchi, S., Nehete, P. N., Zhang, M., Chang, M., Sastry, K. J. (2009). TSLP production by epithelial cells exposed to immunodeficiency virus triggers DC-mediated mucosal infection of CD4+ T cells. *Proceedings of the National Academy of Sciences of the United States of America*, *106*(39), 16776–81.

Friend, S. L., Hosier, S., Nelson, A., Foxworthe, D., Williams, D. E., & Farr, A. (1994). A thymic stromal cell line supports in vitro development of surface IgM^+ B cells and produces a novel growth factor affecting B and T lineage cells. *Experimental Hematology*, *22*(3), 321–8.

Gao, P.-S., Rafaels, N. M., Mu, D., Hand, T., Murray, T., Boguniewicz, M., Barnes, K. C. (2010). Genetic variants in thymic stromal lymphopoietin are associated with atopic dermatitis and eczema herpeticum. *The Journal of Allergy and Clinical Immunology*, *125*(6), 1403–1407.

Gibbs, W. W. (2005). Nanobodies. *Scientific American*, *293*(2), 78–83.

Gilfillan, A. M., & Tkaczyk, C. (2006). Integrated signalling pathways for mast-cell activation. *Nature Reviews. Immunology*, *6*(3), 218–30.

Gilliet, M., Soumelis, V., Watanabe, N., Hanabuchi, S., Antonenko, S., de Waal-Malefyt, R., & Liu, Y.-J. (2003). Human dendritic cells activated by TSLP and CD40L induce proallergic cytotoxic T cells. *The Journal of Experimental Medicine*, *197*(8), 1059–63.

Gobert, M., Treilleux, I., Bendriss-Vermare, N., Bachelot, T., Goddard-Leon, S., Arfi, V., Ménétrier-Caux, C. (2009). Regulatory T cells recruited through CCL22/CCR4 are selectively activated in lymphoid infiltrates surrounding primary breast tumors and lead to an adverse clinical outcome. *Cancer Research*, *69*(5), 2000–9.

Guan, C., Li, P., Riggs, P.D. and Inouye, H. (1987). (1987). Gene. 67, *Gene*, 21–30.

Guo, P.-F., Du, M.-R., Wu, H.-X., Lin, Y., Jin, L.-P., & Li, D.-J. (2010). Thymic stromal lymphopoietin from trophoblasts induces dendritic cell-mediated regulatory TH2 bias in the decidua during early gestation in humans. *Blood*, *116*(12), 2061–9.

Han, H., Xu, W., Headley, M. B., Jessup, H. K., Lee, K. S., Omori, M., Ziegler, S. F. (2012). Thymic stromal lymphopoietin (TSLP)-mediated dermal inflammation aggravates experimental asthma. *Mucosal Immunology*, *5*(3), 342–51.

Hanabuchi, S., Ito, T., Park, W., Shaw, J. L., Roman, E., Wang, Y., Cao, W. (2012). Thymic Stromal Lymphopoietin-Activated Plasmacytoid Dendritic Cells Induce the Generation of FOXP3$^+$ Regulatory T Cells in Human Thymus. *Journal of Immunology (Baltimore, Md. : 1950)*, *184*(6), 2999–3007.

Harada, M., Hirota, T., Jodo, A. I., Doi, S., Kameda, M., Fujita, K., Tamari, M. (2009). Functional analysis of the thymic stromal lymphopoietin variants in human bronchial epithelial cells. *American Journal of Respiratory Cell and Molecular Biology*, *40*(3), 368–74.

Harada, M., Hirota, T., Jodo, A. I., Hitomi, Y., Sakashita, M., Tsunoda, T.,Tamari, M. (2011). Thymic stromal lymphopoietin gene promoter polymorphisms are associated with susceptibility to bronchial asthma. *American Journal of Respiratory Cell and Molecular Biology*, *44*(6), 787–93.

Hartgring, S. a Y., Willis, C. R., Dean, C. E., Broere, F., van Eden, W., Bijlsma, J. W. J., van Roon, J. a G. (2011). Critical proinflammatory role of thymic stromal lymphopoietin and its receptor in experimental autoimmune arthritis. *Arthritis and Rheumatism*, *63*(7), 1878–87.

He, B., Xu, W., Santini, P. A., Polydorides, A. D., Chiu, A., Estrella, J., Cerutti, A. (2007). Intestinal bacteria trigger T cell-independent immunoglobulin A(2) class switching by inducing epithelial-cell secretion of the cytokine APRIL. *Immunity*, *26*(6), 812–26.

He, R., Oyoshi, M. K., Garibyan, L., Kumar, L., Ziegler, S. F., & Geha, R. S. (2008). TSLP acts on infiltrating effector T cells to drive allergic skin inflammation. *Proceedings of the National Academy of Sciences of the United States of America*, *105*(33), 11875–80.

Headley, M. B., Zhou, B., Shih, W. X., Aye, T., Comeau, M. R., & Ziegler, S. F. (2009). TSLP conditions the lung immune environment for the generation of pathogenic innate and antigen-specific adaptive immune responses. *Journal of Immunology (Baltimore, Md. : 1950)*, *182*(3), 1641–7.

Hirano, R., Hasegawa, S., Hashimoto, K., Haneda, Y., Ohsaki, A., & Ichiyama, T. (2011). Human thymic stromal lymphopoietin enhances expression of CD80 in human CD14$^+$ monocytes/macrophages. *Inflammation Research : Official Journal of the European Histamine Research Society*, *60*(6), 605–10.

Hui, C. C., Asher, I., Heroux, D., Allakhverdi, Z., Delespesse, G., & Denburg, J. A. (2011). Effects of thymic stromal lymphopoietin on cord blood progenitor cell differentiation and hemopoietic cytokine receptors expression. *Allergy, Asthma & Clinical Immunology*, *7*.

Hui, C. C. K., Rusta-Sallehy, S., Asher, I., Heroux, D., & Denburg, J. A. (2014). The effects of thymic stromal lymphopoietin and IL-3 on human eosinophil-basophil lineage commitment: Relevance to atopic sensitization. *Immunity, Inflammation and Disease*, *2*(1), 44–55.

Humbert, M., Menz, G., Ying, S., Corrigan, C. J., Robinson, D. S., Durham, S. R., & Kay, a. B. (1999). The immunopathology of extrinsic (atopic) and intrinsic (non-atopic) asthma: More similarities than differences. *Immunology Today*, *20*(11), 528–533.

Humphreys, N. E., Xu, D., Hepworth, M. R., Liew, F. Y., & Grencis, R. K. (2008). IL-33, a potent inducer of adaptive immunity to intestinal nematodes. *Journal of Immunology (Baltimore, Md. : 1950)*, *180*(4), 2443–9.

Hunninghake, G. M., Soto-Quirós, M. E., Avila, L., Kim, H. P., Lasky-Su, J., Rafaels, N.,Celedón, J. C. (2010). TSLP polymorphisms are associated with asthma in a sex-specific fashion. *Allergy*,*65*(12),1566–75.

Iliev, I. D., Mileti, E., Matteoli, G., Chieppa, M., & Rescigno, M. (2009). Intestinal epithelial cells promote colitis-protective regulatory T-cell differentiation through dendritic cell conditioning. *Mucosal Immunology*, *2*(4), 340–350.

Isaksen, D. E., Baumann, H., Zhou, B., Nivollet, S., Farr, A. G., Levin, S. D., & Ziegler, S. F. (2002). Uncoupling of proliferation and Stat5 activation in thymic stromal lymphopoietin-mediated signal transduction. *Journal of Immunology (Baltimore, Md. : 1950)*, *168*(7), 3288–94.

Iseki, M., Omori-Miyake, M., Xu, W., Sun, X., Takaki, S., Rawlings, D. J., & Ziegler, S. F. (2012). Thymic stromal lymphopoietin (TSLP)-induced polyclonal B-cell activation and autoimmunity are mediated by $CD4^+$ T cells and IL-4. *International Immunology*, *24*(3), 183–95.

Ito, T., Liu, Y., & Arima, K. (2012). Cellular and Molecular Mechanisms of TSLP Function in Human Allergic Disorders - TSLP Programs the " Th2 code " in Dendritic Cells, (September 2011), 35–43.

Ito, T., Wang, Y.-H., Duramad, O., Hori, T., Delespesse, G. J., Watanabe, N., Liu, Y.-J. (2005). TSLP-activated dendritic cells induce an inflammatory T helper type 2 cell response through OX40 ligand. *The Journal of Experimental Medicine*, *202*(9), 1213–23.

Jiang, H., Hener, P., Li, J., & Li, M. (2012). Skin thymic stromal lymphopoietin promotes airway sensitization to inhalant house dust mites leading to allergic asthma in mice. *Allergy*, *67*(8), 1078–82.

Joyce, J. a, & Pollard, J. W. (2009). Microenvironmental regulation of metastasis. *Nature Reviews. Cancer*, *9*(4), 239–52.

Kamekura, R., Kojima, T., Koizumi, J., Ogasawara, N., Kurose, M., Go, M., Sawada, N. (2009). Thymic stromal lymphopoietin enhances tight-junction barrier function of human nasal epithelial cells. *Cell and Tissue Research*, *338*(2), 283–293.

Kashyap, M., Rochman, Y., Spolski, R., Samsel, L., & Leonard, W. J. (2011). Thymic stromal lymphopoietin is produced by dendritic cells. *Journal of Immunology (Baltimore, Md. : 1950)*, *187*(3), 1207–11.

Kato, A., & Schleimer, R. P. (2007). Beyond inflammation: airway epithelial cells are at the interface of innate and adaptive immunity. *Current Opinion in Immunology*, *19*(6), 711–720.

Kaumaya PTP. (1994). '*De novo*' engineering of peptide immunogenic and antigenic determinants as potential vaccines. in: Basava C, Anantharamaiah GM (eds). Peptides: Design, Synthesis and Biological Activity. *Birkhauser: Boston*, 133–164.

Kaur, D., & Brightling, C. (2012). OX40/OX40 ligand interactions in T-cell regulation and asthma. *Chest*, *141*(2), 494–9.

Kim, H. Y., Dekruyff, R. H., & Umetsu, D. T. (2010). review The many paths to asthma : phenotype shaped by innate and adaptive immunity. *Nature Publishing Group*, *11*(7), 577–584. Kim, Y.-M., Kim, Y.-S., Jeon, S. G., & Kim, Y.-K. (2013). Immunopathogenesis of allergic asthma: more than the th2 hypothesis. *Allergy, Asthma & Immunology Research*, *5*(4),189–96.

Kimura, S., Pawankar, R., Mori, S., Nonaka, M., Masuno, S., Yagi, T., & Okubo, K. (2011). Increased expression and role of thymic stromal lymphopoietin in nasal polyposis. *Allergy, Asthma & Immunology Research*, *3*(3), 186–93.

Kinoshita, Y., Kuratsukuri, K., Newman, N., Rovito, P. M., Kaumaya, P. T. P., Wang, C. Y., & Haas, G. P. (2005). Targeting epitopes in prostate-specific membrane antigen for antibody therapy of prostate cancer. *Prostate Cancer and Prostatic Diseases*, *8*(4), 359–63.

Kitajima, M., Lee, H., Nakayama, T., & Ziegler, S. F. (2011). TSLP enhances the function of helper type 2 cells, 1862–1871.

Kitamura, T., Hayashida, K., Sakamaki, K., Yokota, T., Arai, K., & Miyajima, A. (1991). Reconstitution of functional receptors for human granulocyte/macrophage colony-stimulating factor (GM-CSF): evidence that the protein encoded by the AIC2B cDNA is a subunit of the murine GM-CSF receptor. *Proceedings of the National Academy of Sciences of the United States of America*, *88*(12), 5082–6.

Kouzaki, H., O'Grady, S. M., Lawrence, C. B., & Kita, H. (2009). Proteases induce production of thymic stromal lymphopoietin by airway epithelial cells through protease-activated receptor-2. *Journal of Immunology (Baltimore, Md. : 1950)*, *183*(2), 1427–34.

Kuethe, J. W., Prakash, P. S., Midura, E. F., Johnson, B. L., Kasten, K. R., & Caldwell, C. C. (2014). Thymic stromal lymphopoietin mediates the host response and increases mortality during sepsis. *Journal of Surgical Research*, *191*(1), 19–24.

Lambrecht, B. N., & Hammad, H. (2012). The airway epithelium in asthma. *Nature Medicine*, *18*(5), 684–92.

Larson, R. P., Zimmerli, S. C., Comeau, M. R., Itano, A., Omori, M., Iseki, M., Ziegler, S. F. (2010). Dibutyl phthalate-induced thymic stromal lymphopoietin is required for Th2 contact hypersensitivity responses. *Journal of Immunology (Baltimore, Md. : 1950)*, *184*(6), 2974–84.

Lee, H., Headley, M. B., Iseki, M., & Ziegler, S. F. (2012). Cutting Edge: Inhibition of NF- κ B-Mediated TSLP Expression by Retinoid X Receptor.

Lee, H.-C., Headley, M. B., Iseki, M., Ikuta, K., & Ziegler, S. F. (2008). Cutting edge: Inhibition of NF-kappaB-mediated TSLP expression by retinoid X receptor. *Journal of Immunology (Baltimore, Md. : 1950)*, *181*(8), 5189–93.

Lee, H.-C., & Ziegler, S. F. (2007). Inducible expression of the proallergic cytokine thymic stromal lymphopoietin in airway epithelial cells is controlled by NFkappaB. *Proceedings of the National Academy of Sciences of the United States of America*, *104*(3), 914–9.

Lei, L., Zhang, Y., Yao, W., Kaplan, M. H., & Zhou, B. (2011). Thymic stromal lymphopoietin interferes with airway tolerance by suppressing the generation of antigen-specific regulatory T cells. *Journal of Immunology (Baltimore, Md. : 1950)*, *186*(4), 2254–61.

Levin, S. D., Koelling, R. M., Friend, S. L., Isaksen, D. E., Ziegler, S. F., Perlmutter, R. M., & Farr, A. G. (1999). Thymic Stromal Lymphopoietin: A Cytokine That Promotes the Development of IgM B Cells In Vitro and Signals Via a Novel Mechanism 1.

Leyva-Castillo, J. M., Hener, P., Jiang, H., & Li, M. (2013). TSLP produced by keratinocytes promotes allergen sensitization through skin and thereby triggers atopic march in mice. *The Journal of Investigative Dermatology*, *133*(1), 154–63.

Li, D.-J., & Guo, P.-F. (2009). The regulatory role of thymic stromal lymphopoietin (TSLP) in maternal-fetal immune tolerance during early human pregnancy. *Journal of Reproductive Immunology*, *83*(1-2), 106–8.

Li, M., Hener, P., Zhang, Z., Ganti, K. P., Metzger, D., & Chambon, P. (2009). Induction of thymic stromal lymphopoietin expression in keratinocytes is necessary for generating an atopic dermatitis upon application of the active vitamin D3 analogue MC903 on mouse skin. *The Journal of Investigative Dermatology*, *129*(2), 498–502.

Li, M., Hener, P., Zhang, Z., Kato, S., Metzger, D., & Chambon, P. (2006). Topical vitamin D3 and low-calcemic analogs induce thymic stromal lymphopoietin in mouse keratinocytes and trigger an atopic dermatitis. *Proceedings of the National Academy of Sciences*, *103*(31), 11736–11741.

Li, Y.-L., Li, H.-J., Ji, F., Zhang, X., Wang, R., Hao, J.-Q., Dong, L. (2010). Thymic stromal lymphopoietin promotes lung inflammation through activation of dendritic cells. *The Journal of Asthma : Official Journal of the Association for the Care of Asthma*, *47*(2), 117–23.

Lin, Y., Zhong, Y., Shen, W., Chen, Y., Shi, J., Di, J., Saito, S. (2008). TSLP-induced placental DC activation and IL-10 + NK cell expansion : Comparative study based on BALB / c × C57BL / 6 and NOD / SCID × C57BL / 6 pregnant models, 104–117.

Liu, Y.-J. (2007). Thymic stromal lymphopoietin and OX40 ligand pathway in the initiation of dendritic cell-mediated allergic inflammation. *The Journal of Allergy and Clinical Immunology*, *120*(2), 238–44; quiz 245–6.

Loots, G. G., Locksley, R. M., Blankespoor, C. M., Wang, Z. E., Miller, W., Rubin, E. M., & Frazer, K. A. (2000). Identification of a coordinate regulator of interleukins 4, 13, and 5 by cross-species sequence comparisons. *Science (New York, N.Y.)*, *288*(5463), 136–40.

Lu, N., Wang, Y.-H., Wang, Y.-H., Arima, K., Hanabuchi, S., & Liu, Y.-J. (2009). TSLP and IL-7 use two different mechanisms to regulate human CD4+ T cell homeostasis. *The Journal of Experimental Medicine*, *206*(10), 2111–9.

Lutz, P. G., Moog-Lutz, C., Coumau-Gatbois, E., Kobari, L., Di Gioia, Y., & Cayre, Y. E. (2000). Myeloblastin is a granulocyte colony-stimulating factor-responsive gene conferring factor-independent growth to hematopoietic cells. *Proceedings of the National Academy of Sciences of the United States of America*, *97*(4), 1601–6.

Maasho, K., Marusina, A., Reynolds, N. M., Coligan, J. E., & Borrego, F. (2004). Efficient gene transfer into the human natural killer cell line, NKL, using the Amaxa nucleofection system. *Journal of Immunological Methods*, *284*(1-2), 133–40.

Madaan, A., Verma, R., Singh, A. T., Jain, S. K., & Jaggi, M. (2014, February 7). A stepwise procedure for isolation of murine bone marrow and generation of dendritic cells. *Journal of Biological Methods*.

Mantovani, A., Romero, P., Palucka, A. K., & Marincola, F. M. (2008). Tumour immunity: effector response to tumour and role of the microenvironment. *Lancet (London, England)*, *371*(9614), 771–83.

Mazzucchelli, R., Hixon, J. A., Spolski, R., Chen, X., Li, W. Q., Hall, V. L., Durum, S. K. (2008). Development of regulatory T cells requires IL-7Rα stimulation by IL-7 or TSLP. *Blood*, *112*(8), 3283–92.

Mazzucchelli, R. I., Riva, A., & Durum, S. K. (2012). The human IL-7 receptor gene: deletions, polymorphisms and mutations. *Seminars in Immunology*, *24*(3), 225–30.

Menetrier-Caux, C., Gobert, M., & Caux, C. (2009). Differences in Tumor Regulatory T-Cell Localization and Activation Status Impact Patient Outcome. *Cancer Research*, *69*(20), 7895–7898.

Metcalf, D., Willson, T., Rossner, M., & Lock, P. (1994). Receptor insertion into factor-dependent murine cell lines to develop specific bioassays for murine G-CSF and M-CSF and human GM-CSF. *Growth Factors (Chur, Switzerland)*, *11*(2), 145–52.

Miura, Y., Thoburn, C. J., Bright, E. C., Arai, S., & Hess, a D. (2005). Regulation of OX40 gene expression in graft-versus-host disease. *Transplantation Proceedings*, *37*(1), 57–61.

Miyata, M., Hatsushika, K., Ando, T., Shimokawa, N., Ohnuma, Y., Katoh, R., Nakao, A. (2008). Mast cell regulation of epithelial TSLP expression plays an important role in the development of allergic rhinitis. *European Journal of Immunology*, *38*(6), 1487–92.

Morshed, M., Yousefi, S., Stöckle, C., Simon, H.-U., & Simon, D. (2012). Thymic stromal lymphopoietin stimulates the formation of eosinophil extracellular traps. *Allergy*, *67*(9), 1127–37.

Mou, Z., Xia, J., Tan, Y., Wang, X., Zhang, Y., Zhou, B., Han, D. (2009). Overexpression of thymic stromal lymphopoietin in allergic rhinitis. *Acta Oto-Laryngologica*, *129*(3), 297–301.

Mullighan, C. G., Collins-Underwood, J. R., Phillips, L. A. A., Loudin, M. G., Liu, W., Zhang, J., Rabin, K. R. (2009). Rearrangement of CRLF2 in B-progenitor- and Down syndrome-associated acute lymphoblastic leukemia. *Nature Genetics*, *41*(11), 1243–6.

Nagarkar, D. R., Poposki, J. a., Schleimer, R. P., & Kato, a. (2011). Airway Epithelial Cells Directly Promote Th2 Cytokine Production in Mast Cells via Production of IL-1α and TSLP. *Journal of Allergy and Clinical Immunology*, *127*(2), AB165–AB165.

Nguyen, K. D., Vanichsarn, C., & Nadeau, K. C. (2010). TSLP directly impairs pulmonary Treg function: association with aberrant tolerogenic immunity in asthmatic airway. *Allergy, Asthma, and Clinical Immunology : Official Journal of the Canadian Society of Allergy and Clinical Immunology*, *6*(1), 4.

Nishiura, H., Kido, M., Aoki, N., Iwamoto, S., Maruoka, R., Ikeda, A., Watanabe, N. (2012). Increased susceptibility to autoimmune gastritis in thymic stromal lymphopoietin receptor-deficient mice. *Journal of Immunology (Baltimore, Md. : 1950)*, *188*(1), 190–7.

Noble, C. L., Abbas, A. R., Cornelius, J., Lees, C. W., Ho, G.-T., Toy, K., Diehl, L. (2008). Regional variation in gene expression in the healthy colon is dysregulated in ulcerative colitis. *Gut*, *57*(10), 1398–1405.

Noble, C. L., Abbas, A. R., Lees, C. W., Cornelius, J., Toy, K., Modrusan, Z., Diehl, L. (2010). Characterization of intestinal gene expression profiles in Crohn's disease by genome-wide microarray analysis. *Inflammatory Bowel Diseases*, *16*(10), 1717–28.

Oh, M.-H., Oh, S. Y., Yu, J., Myers, A. C., Leonard, W. J., Liu, Y. J., Zheng, T. (2011). IL-13 induces skin fibrosis in atopic dermatitis by thymic stromal lymphopoietin. *Journal of Immunology (Baltimore, Md. : 1950)*, *186*(12), 7232–42.

Olkhanud, P. B., Rochman, Y., Bodogai, M., Malchinkhuu, E., Wejksza, K., Xu, M., Biragyn, A. (2011). Thymic stromal lymphopoietin is a key mediator of breast cancer progression. *Journal of Immunology (Baltimore, Md. : 1950)*, *186*(10), 5656–62.

Olkhanud, P. B., Rochman, Y., Bodogai, M., Malchinkhuu, E., Wejksza, K., Xu, M., Leonard, W. J. (2012). Thymic Stromal Lymphopoietin Is a Key Mediator of Breast Cancer Progression.

Omori, M., & Ziegler, S. (2007). Induction of IL-4 expression in CD4(+) T cells by thymic stromal lymphopoietin. *Journal of Immunology (Baltimore, Md. : 1950)*, *178*(3), 1396–404.

Oyoshi, M. K., Larson, R. P., Ziegler, S. F., & Geha, R. S. (2010). Mechanical injury polarizes skin dendritic cells to elicit a T(H)2 response by inducing cutaneous thymic stromal lymphopoietin expression. *The Journal of Allergy and Clinical Immunology*, *126*(5), 976–84, 984.e1–5.

Palacios, R., & Steinmetz, M. (1985). Il-3-dependent mouse clones that express B-220 surface antigen, contain Ig genes in germ-line configuration, and generate B lymphocytes in vivo. *Cell*, *41*(3), 727–34.

Pandey, A., Ozaki, K., Baumann, H., Levin, S. D., Puel, A., Farr, A. G., Lodish, H. F. (2000). Cloning of a receptor subunit required for signaling by thymic stromal lymphopoietin, *1*(1), 59–64.

Park, L. S., Martin, U., Garka, K., Gliniak, B., Di Santo, J. P., Muller, W., Sims, J. E. (2000). Cloning of the Murine Thymic Stromal Lymphopoietin (Tslp) Receptor: Formation of a Functional Heteromeric Complex Requires Interleukin 7 Receptor. *Journal of Experimental Medicine*, *192*(5), 659–670.

Pedroza-Gonzalez, A., Xu, K., Wu, T.-C., Aspord, C., Tindle, S., Marches, F., Palucka, a K. (2011). Thymic stromal lymphopoietin fosters human breast tumor growth by promoting type 2 inflammation. *The Journal of Experimental Medicine*, *208*(3), 479–90.

Pu, H. H., Duan, J., Wang, Y., Fan, D. X., Li, D. J., & Jin, L. P. (2012). Thymic stromal lymphopoietin promotes the proliferation of human trophoblasts via phosphorylated STAT3-mediated c-Myc upregulation. *Placenta*, *33*(5), 387–91.

Quentmeier, H., Fleckenstein, D., Zaborski, M., & Armstrong, A. (2001). Biotechnical methods section (bts), (December 2000), 1286–1292.

Reche, P., Soumelis, V., Gorman, D. M., Clifford, T., Liu, M., Travis, M., Bazan, J. F. (2001). Human Thymic Stromal Lymphopoietin Preferentially Stimulates Myeloid Cells. *The Journal of Immunology*, *167*(1), 336–343.

Redhu, N. S., Shan, L., Movassagh, H., & Gounni, A. S. (2013). Thymic stromal lymphopoietin induces migration in human airway smooth muscle cells. *Scientific Reports*, *3*, 2301.

Rimoldi, M., Chieppa, M., Salucci, V., Avogadri, F., Sonzogni, A., Sampietro, G. M., Rescigno, M. (2005). Intestinal immune homeostasis is regulated by the crosstalk between epithelial cells and dendritic cells. *Nature Immunology*, *6*(5), 507–14.

Rochman, I., Watanabe, N., Arima, K., Liu, Y.-J., & Leonard, W. J. (2007). Cutting Edge: Direct Action of Thymic Stromal Lymphopoietin on Activated Human CD4+ T Cells. *The Journal of Immunology*, *178*(11), 6720–6724.

Rochman, Y., Kashyap, M., Robinson, G. W., Sakamoto, K., Gomez-Rodriguez, J., Wagner, K.-U., & Leonard, W. J. (2010). Thymic stromal lymphopoietin-mediated STAT5 phosphorylation via kinases JAK1 and JAK2 reveals a key difference fromIL -7-induced signaling. *Proceedings of the National Academy of Sciences of the United States of America*, *107*(45), 19455–60.

Rochman, Y., Spolski, R., & Leonard, W. J. (2009). New insights into the regulation of T cells by gamma(c) family cytokines. *Nature Reviews. Immunology*, *9*(7), 480–90.

Roll, J. D., & Reuther, G. W. (2010). CRLF2 and JAK2 in B-progenitor acute lymphoblastic leukemia: a novel association in oncogenesis. *Cancer Research*, *70*(19), 7347–52.

Rothenberg, M. E., Spergel, J. M., Sherrill, J. D., Annaiah, K., Martin, L. J., Cianferoni, A., Hakonarson, H. (2010). Common variants at 5q22 associate with pediatric eosinophilic esophagitis. *Nature Genetics*, *42*(4), 289–91.

Russell, L. J., Capasso, M., Vater, I., Akasaka, T., Bernard, O. a, Calasanz, M. J., Harrison, C. J. (2009). Deregulated expression of cytokine receptor gene, CRLF2, is involved in lymphoid transformation in B-cell precursor acute lymphoblastic leukemia. *Blood*, *114*(13), 2688–98.

Sakamaki, K., Miyajima, I., Kitamura, T., & Miyajima, A. (1992). Critical cytoplasmic domains of the common beta subunit of the human GM-CSF, IL-3 and IL-5 receptors for growth signal transduction and tyrosine phosphorylation. *The EMBO Journal*, *11*(10), 3541–9.

Seckinger, P., Vey, E., Turcatti, G., Wingfield, P., & Dayer, J. M. (1990). Tumor necrosis factor inhibitor: purification, NH2-terminal amino acid sequence and evidence for anti-inflammatory and immunomodulatory activities. *European Journal of Immunology*, *20*(5), 1167–74.

Segawa, R., Yamashita, S., Mizuno, N., Shiraki, M., Hatayama, T., Satou, N., Hirasawa, N. (2014). Identification of a cell line producing high levels of TSLP: Advantages for screening of anti-allergic drugs. *Journal of Immunological Methods*, *402*(1-2), 9–14.

Semlali, A., Jacques, E., Koussih, L., Gounni, A. S., & Chakir, J. (2010). Thymic stromal lymphopoietin-induced human asthmatic airway epithelial cell proliferation through an IL-13-dependent pathway. *The Journal of Allergy and Clinical Immunology*, *125*(4), 844–50.

Seshasayee, D., Lee, W. P., Zhou, M., Shu, J., Suto, E., Zhang, J., Martin, F. (2007). In vivo blockade of OX40 ligand inhibits thymic stromal lymphopoietin driven atopic inflammation. *The Journal of Clinical Investigation*, *117*(12), 3868–78.

Shane, H. L., & Klonowski, K. D. (2014). A direct and nonredundant role for thymic stromal lymphopoietin on antiviral CD8 T cell responses in the respiratory mucosa. *Journal of Immunology (Baltimore, Md. : 1950)*, *192*(5), 2261–70.

Sherrill, J. D., Gao, P.-S., Stucke, E. M., Blanchard, C., Collins, M. H., Putnam, P. E., Rothenberg, M. E. (2010). Variants of thymic stromal lymphopoietin and its receptor associate with eosinophilic esophagitis. *The Journal of Allergy and Clinical Immunology*, *126*(1), 160–5.

Shi, L., Leu, S.-W., Xu, F., Zhou, X., Yin, H., Cai, L., & Zhang, L. (2008). Local blockade of TSLP receptor alleviated allergic disease by regulating airway dendritic cells. *Clinical Immunology (Orlando, Fla.)*, *129*(2), 202–10.

Shigeno, T., Katakuse, M., Fujita, T., Mukoyama, Y., & Watanabe, H. (2009). Phthalate ester-induced thymic stromal lymphopoietin mediates allergic dermatitis in mice. *Immunology*, *128*(1 Suppl), 849–57.

Shikotra, A., Choy, D. F., Ohri, C. M., Doran, E., Butler, C., Hargadon, B., Bradding, P. (2011). Increased expression of immunoreactive thymic stromal lymphopoietin in patients with severe asthma. *The Journal of Allergy and Clinical Immunology*, *129*(1), 104–111.

Siddiqui, S., Mistry, V., Doe, C., Stinson, S., Foster, M., & Brightling, C. (2010). Airway wall expression of OX40/OX40L and interleukin-4 in asthma. *Chest*, *137*(4), 797–804.

Sims, J. E., Williams, D. E., Morrissey, P. J., Garka, K., Foxworthe, D., Price, V., Paxton, R. J. (2000). Molecular Cloning and Biological Characterization of a Novel Murine Lymphoid Growth Factor. *Journal of Experimental Medicine*, *192*(5), 671–680.

Siracusa, M. C., Kim, B. S., Spergel, J. M., & Artis, D. (2013). Basophils and allergic inflammation. *The Journal of Allergy and Clinical Immunology*, *132*(4), 789–801.

Siracusa, M. C., Saenz, S. A., Hill, D. A., Kim, B. S., Headley, M. B., Doering, T. A., Artis, D. (2011). TSLP promotes interleukin-3-independent basophil haematopoiesis and type 2 inflammation. *Nature*, *477*(7363), 229–33.

Siracusa, M. C., Saenz, S. a., Tait Wojno, E. D., Kim, B. S., Osborne, L. C., Ziegler, C. G., Artis, D. (2013). Thymic Stromal Lymphopoietin-Mediated Extramedullary Hematopoiesis Promotes Allergic Inflammation. *Immunity*, *39*(6), 1158–1170.

Smelter, D. F., Sathish, V., Thompson, M. a, Pabelick, C. M., Vassallo, R., & Prakash, Y. S. (2010). Thymic stromal lymphopoietin in cigarette smoke-exposed human airway smooth muscle. *Journal of Immunology (Baltimore, Md. : 1950)*, *185*(5), 3035–40.

Sokol, C. L., Chu, N.-Q., Yu, S., Nish, S. a, Laufer, T. M., & Medzhitov, R. (2009). Basophils function as antigen-presenting cells for an allergen-induced T helper type 2 response. *Nature Immunology*, *10*(7), 713–20.

Soumelis, V., Reche, P. a, Kanzler, H., Yuan, W., Edward, G., Homey, B., Liu, Y.-J. (2002). Human epithelial cells trigger dendritic cell mediated allergic inflammation by producing TSLP. *Nature Immunology*, *3*(7), 673–80.

Spadoni, I., Iliev, I. D., Rossi, G., & Rescigno, M. (2012). Dendritic cells produce TSLP that limits the differentiation of Th17 cells , fosters Treg development , and protects against colitis, *5*(2), 184–193.

Stanfield, R. L., Dooley, H., Flajnik, M. F., & Wilson, I. A. (2004). Crystal structure of a shark single-domain antibody V region in complex with lysozyme. *Science (New York, N.Y.)*, *305*(5691), 1770–3.

Takai, T. (2012). TSLP Expression: Cellular Sources, Triggers, and Regulatory Mechanisms. *Allergology International*, *61*(1), 3–17.

Tanaka, J., Saga, K., Kido, M., Nishiura, H., Akamatsu, T., Chiba, T., & Watanabe, N. (2010). Proinflammatory Th2 cytokines induce production of thymic stromal lymphopoietin in human colonic epithelial cells. *Digestive Diseases and Sciences*, *55*(7), 1896–904.

Taneda, S., Segerer, S., Hudkins, K. L., Cui, Y., Wen, M., Segerer, M., Alpers, C. E. (2001). Cryoglobulinemic glomerulonephritis in thymic stromal lymphopoietin transgenic mice. *The American Journal of Pathology*, *159*(6), 2355–69.

Tang, H., Cao, W., Kasturi, S. P., Ravindran, R., Nakaya, H. I., Kundu, K., Pulendran, B. (2010). The T helper type 2 response to cysteine proteases requires dendritic cell–basophil cooperation via ROS-mediated signaling. *Nature Immunology*, *11*(7), 608–617.

Tang, T. S., Bieber, T., & Williams, H. C. (2012). Does "autoreactivity" play a role in atopic dermatitis? *The Journal of Allergy and Clinical Immunology*, *129*(5), 1209–1215.

Tasian, S. K., & Loh, M. L. (2011). Understanding the biology of CRLF2-overexpressing acute lymphoblastic leukemia. *Critical Reviews in Oncogenesis*, *16*(1-2), 13–24.

Taylor, B. C., Zaph, C., Troy, A. E., Du, Y., Guild, K. J., Comeau, M. R., & Artis, D. (2009). TSLP regulates intestinal immunity and inflammation in mouse models of helminth infection and colitis. *The Journal of Experimental Medicine*, *206*(3), 655–67.

Torgerson, D. G., Ampleford, E. J., Chiu, G. Y., Gauderman, W. J., Gignoux, C. R., Graves, P. E., Nicolae, D. L. (2011). Meta-analysis of genome-wide association studies of asthma in ethnically diverse North American populations. *Nature Genetics*, *43*(9), 887–92.

Tsai, K.-H., Tsai, F.-J., Lin, H.-J., Lin, H.-J., Liu, Y.-H., Liao, W.-L., & Wan, L. (2012). Thymic stromal lymphopoietin gene promoter polymorphisms and expression levels in Graves' disease and Graves' ophthalmopathy. *BMC Medical Genetics*, *13*, 116.

Umetsu, D. T., & Dekruyff, R. H. (2006). Immune dysregulation in asthma. *Current Opinion in Immunology*, *18*(6), 727–32.

Uyttenhove, C., Marillier, R. G., Tacchini-Cottier, F., Charmoy, M., Caspi, R. R., Damsker, J. M., Van Snick, J. (2011). Amine-reactive OVA multimers for auto-vaccination against cytokines and other mediators: perspectives illustrated for GCP-2 in L. major infection. *Journal of Leukocyte Biology*, *89*(6), 1001–7.

Van Bodegom, D., Zhong, J., Kopp, N., Dutta, C., Kim, M.-S., Bird, L., Weinstock, D. M. (2012). Differences in signaling through the B-cell leukemia oncoprotein CRLF2 in response to TSLP and through mutant JAK2. *Blood*, *120*(14), 2853–63.

Van der Linden, R. H., Frenken, L. G., de Geus, B., Harmsen, M. M., Ruuls, R. C., Stok, W., Verrips, C. T. (1999). Comparison of physical chemical properties of llama VHH antibody fragments and mouse monoclonal antibodies. *Biochimica et Biophysica Acta*, *1431*(1), 37–46.

Vercelli, D. (2008). Discovering susceptibility genes for asthma and allergy. *Nature Reviews. Immunology*, *8*(3), 169–82.

Verstraete, K., van Schie, L., Vyncke, L., Bloch, Y., Tavernier, J., Pauwels, E., Savvides, S. N. (2014). Structural basis of the proinflammatory signaling complex mediated by TSLP. *Nature Structural & Molecular Biology*, *21*(4), 375–82.

Vosshenrich, C. A. J., Cumano, A., Müller, W., Di Santo, J. P., & Vieira, P. (2003). Thymic stromal-derived lymphopoietin distinguishes fetal from adult B cell development. *Nature Immunology*, *4*(8), 773–9.

Watanabe, N., Hanabuchi, S., Marloie-Provost, M.-A., Antonenko, S., Liu, Y.-J., & Soumelis, V. (2005). Human TSLP promotes CD40 ligand-induced IL-12 production by myeloid dendritic cells but maintains their Th2 priming potential. *Blood*, *105*(12), 4749–51.

Watanabe, N., Hanabuchi, S., Soumelis, V., Yuan, W., Ho, S., de Waal Malefyt, R., & Liu, Y.-J. (2004). Human thymic stromal lymphopoietin promotes dendritic cell-mediated CD4+ T cell homeostatic expansion. *Nature Immunology*, *5*(4), 426–34.

Watanabe, N., Wang, Y.-H., Lee, H. K., Ito, T., Wang, Y.-H., Cao, W., & Liu, Y.-J. (2005). Hassall's corpuscles instruct dendritic cells to induce $CD4^{+}CD25^{+}$ regulatory T cells in human thymus. *Nature*, *436*(7054), 1181–5.

West, E. E., Kashyap, M., & Leonard, W. J. (2012). TSLP: A Key Regulator of Asthma Pathogenesis. *Drug Discovery Today. Disease Mechanisms*, *9*(3-4), 1–6.

Wirawan, E., Vande Walle, L., Kersse, K., Cornelis, S., Claerhout, S., Vanoverberghe, I., Vandenabeele, P. (2010). Caspase-mediated cleavage of Beclin-1 inactivates Beclin-1-induced autophagy and enhances apoptosis by promoting the release of proapoptotic factors from mitochondria. *Cell Death & Disease*, *1*, e18.

Wohlmann, A., Sebastian, K., & Krause, S. (2010). Signal transduction by the atopy-associated human thymic stromal lymphopoietin (TSLP) receptor depends on Janus kinase function, Biol Chem. 2010 Feb-Mar; 391(2-3):181-6.

Wong, C. K., Hu, S., Cheung, P. F. Y., & Lam, C. W. K. (2010). Thymic Stromal Lymphopoietin Induces Chemotactic and Prosurvival Effects in Eosinophils. *American Journal of Respiratory Cell and Molecular Biology*, *43*(3), 305–315.

Wu, C., He, S., Peng, Y., Kushwaha, K. K., Lin, J., Dong, J., Li, D. (2014). TSLPR deficiency attenuates atherosclerotic lesion development associated with the inhibition of TH17 cells and the promotion of regulator T cells in ApoE-deficient mice. *Journal of Molecular and Cellular Cardiology*, *76*, 33–45.

Wu, H.-X., Guo, P.-F., Jin, L.-P., Liang, S.-S., & Li, D.-J. (2010). Functional regulation of thymic stromal lymphopoietin on proliferation and invasion of trophoblasts in human first-trimester pregnancy. *Human Reproduction (Oxford, England)*, *25*(5), 1146–52.

Würtzen, P. a., Koed, G. K., Grauert, G., Papazian, D., Hansen, S., & Lund, K. (2011). Freshly isolated CD11c+ mDC express the TSLPR and responds to TSLP while pDC and *in vitro* cultured MoDC do not. *Journal of Allergy and Clinical Immunology*, *127*(2), AB93–AB93.

Wynn, T. A. (2004). Fibrotic disease and the T(H)1/T(H)2 paradigm. *Nature Reviews. Immunology*, *4*(8), 583–94.

Xu, G., Zhang, L., Wang, D. Y., Xu, R., Liu, Z., Han, D. M., Li, H. B. (2010). Opposing roles of IL-17A and IL-25 in the regulation of TSLP production in human nasal epithelial cells. *Allergy*, *65*(5), 581–9.

Yang, X.-P., Ghoreschi, K., Steward-Tharp, S. M., Rodriguez-Canales, J., Zhu, J., Grainger, J. R., Laurence, A. (2011). Opposing regulation of the locus encoding IL-17 through direct, reciprocal actions of STAT3 and STAT5. *Nature Immunology*, *12*(3), 247–54.

Ying, S., Connor, B. O., Ratoff, J., Meng, Q., Mallett, K., Cousins, D., Zhang, G. (2012). Thymic Stromal Lymphopoietin Expression Is Increased in Asthmatic Airways and Correlates with Expression of Th2-Attracting Chemokines and Disease Severity.

Yoo, J., Omori, M., Gyarmati, D., Zhou, B., Aye, T., Brewer, A., Ziegler, S. F. (2005). Spontaneous atopic dermatitis in mice expressing an inducible thymic stromal lymphopoietin transgene specifically in the skin. *The Journal of Experimental Medicine*, *202*(4), 541–9.

Zagury, D., Le Buanec, H., Bizzini, B., Burny, A., Lewis, G., & Gallo, R. C. (2003). Active versus passive anti-cytokine antibody therapy against cytokine-associated chronic diseases. *Cytokine & Growth Factor Reviews*, *14*(2), 123–37.

Zaph, C., Troy, A. E., Taylor, B. C., Berman-Booty, L. D., Guild, K. J., Du, Y., Artis, D. (2007). Epithelial-cell-intrinsic IKK-beta expression regulates intestinal immune homeostasis. *Nature*, *446*(7135), 552–6.

Zeuthen, L. H., Fink, L. N., & Frokiaer, H. (2008). Epithelial cells prime the immune response to an array of gut-derived commensals towards a tolerogenic phenotype through distinct actions of thymic stromal lymphopoietin and transforming growth factor-beta. *Immunology*, *123*(2), 197–208.

Zhang, Z., Hener, P., Frossard, N., Kato, S., Metzger, D., Li, M., & Chambon, P. (2009). Thymic stromal lymphopoietin overproduced by keratinocytes in mouse skin aggravates experimental asthma. *Proceedings of the National Academy of Sciences of the United States of America*, *106*(5), 1536–41.

Zhou, B., Comeau, M. R., De Smedt, T., Liggitt, H. D., Dahl, M. E., Lewis, D. B., Ziegler, S. F. (2005). Thymic stromal lymphopoietin as a key initiator of allergic airway inflammation in mice. *Nature Immunology*, *6*(10), 1047–53

Zhou, B., Headley, M. B., Aye, T., Tocker, J., Comeau, M. R., & Ziegler, S. F. (2008). Reversal of thymic stromal lymphopoietin-induced airway inflammation through inhibition of Th2 responses. *Journal of Immunology (Baltimore, Md. : 1950)*, *181*(9), 6557–62.

Ziegler, S. F., & Liu, Y. (2006). Thymic stromal lymphopoietin in normal and pathogenic T cell development and function, *7*(7), 709–714.

Appendix I. Plasmid Maps

1. pcDNA3.1 mTSLPR-His 6X

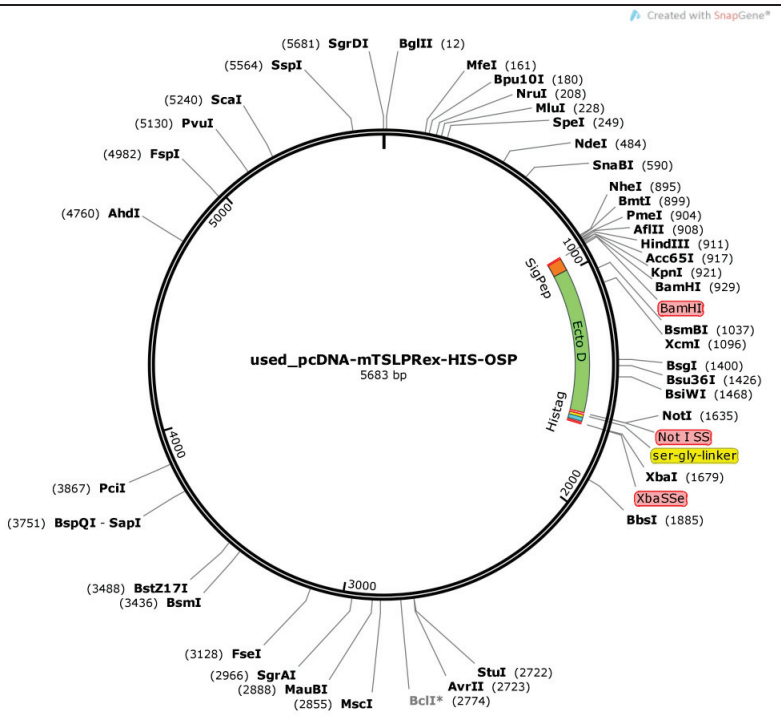

2. pcDNA3.1 mTSLPR-TraN-His8x

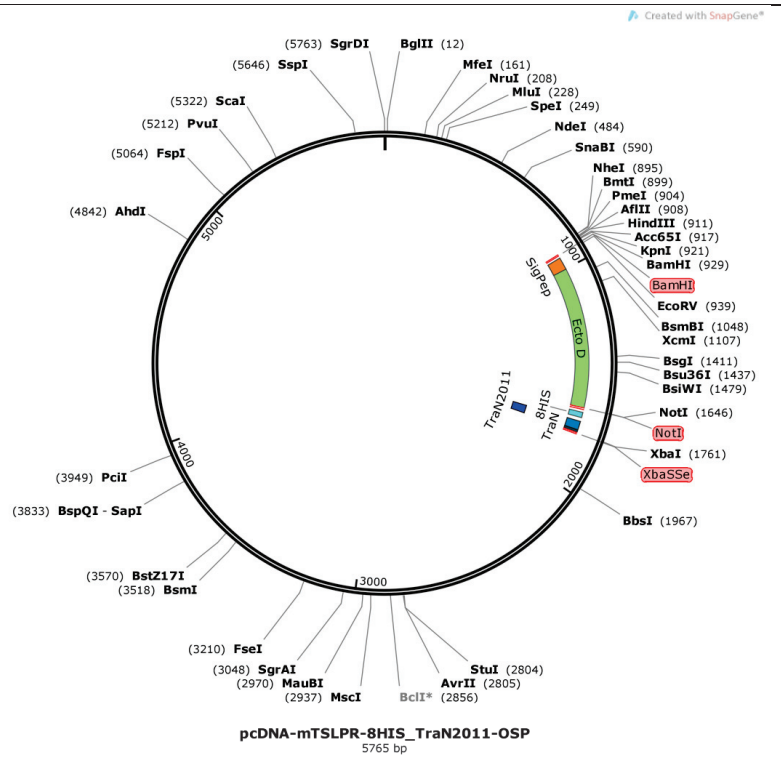

3. pcDNA3.1-mIL7Raex-hIL7Raint-HYB

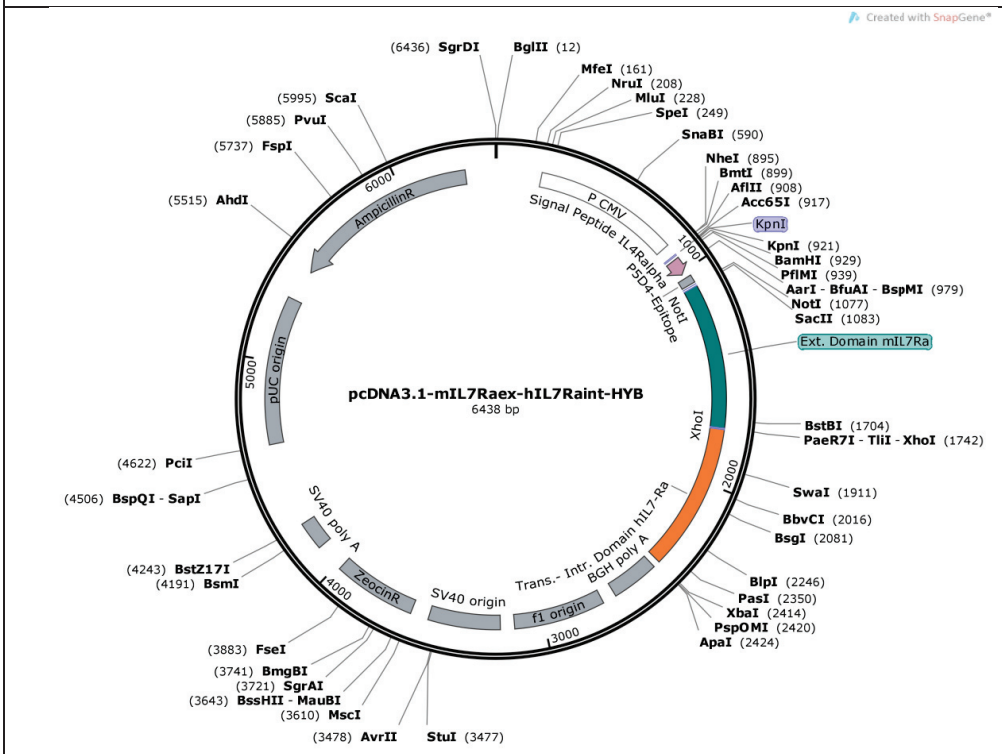

4. pcDNA3.1-mTSLPRex-hTSLPRint-HYB

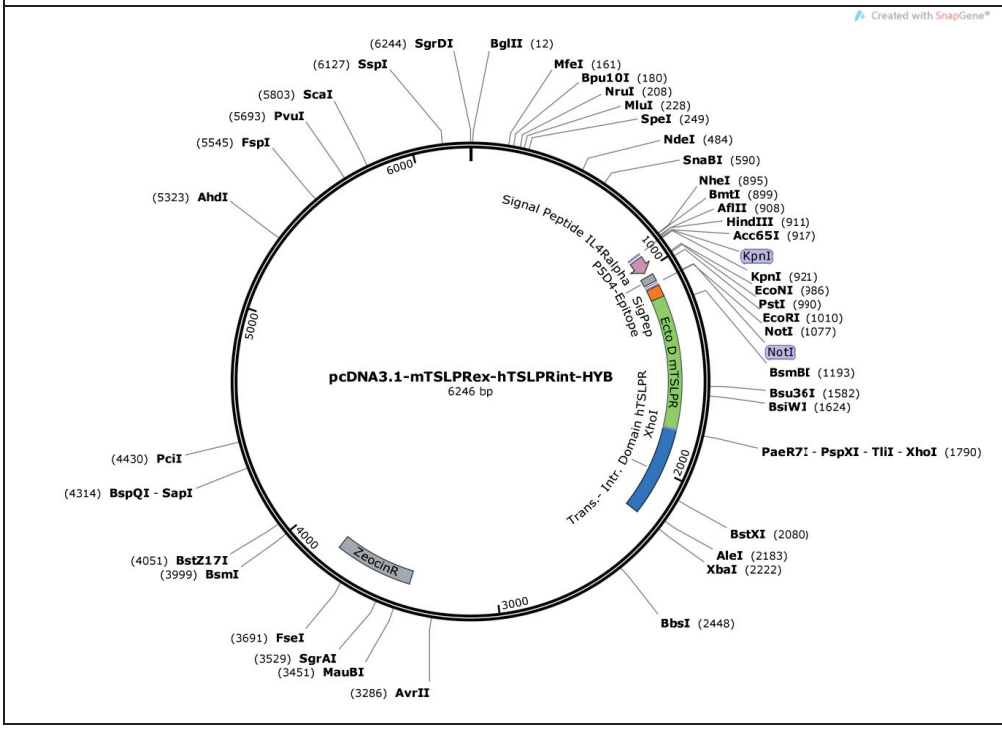

5. pMAL-c2X-mTSLP (In mutant form I37E, Isoleucine replaced by glutamate at position 37 by PCR)

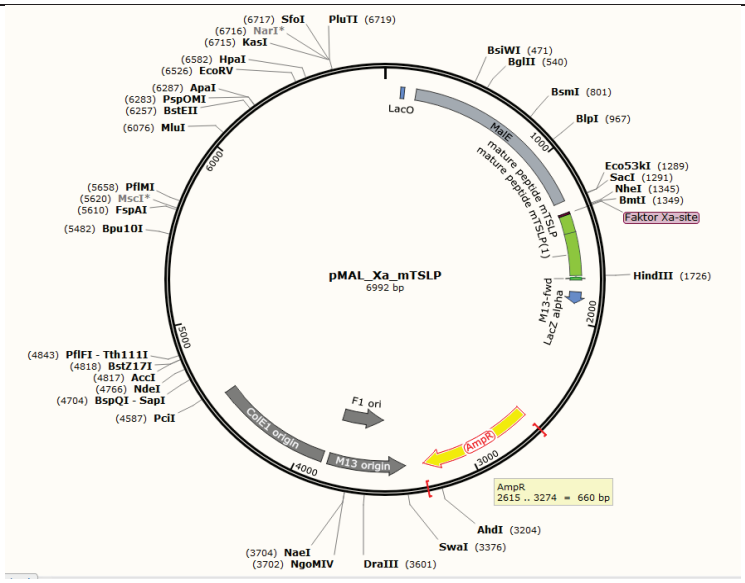

6.pMAL-p2X-mTSLP (In mutant form I37E, Isoleucine replaced by glutamate at position)

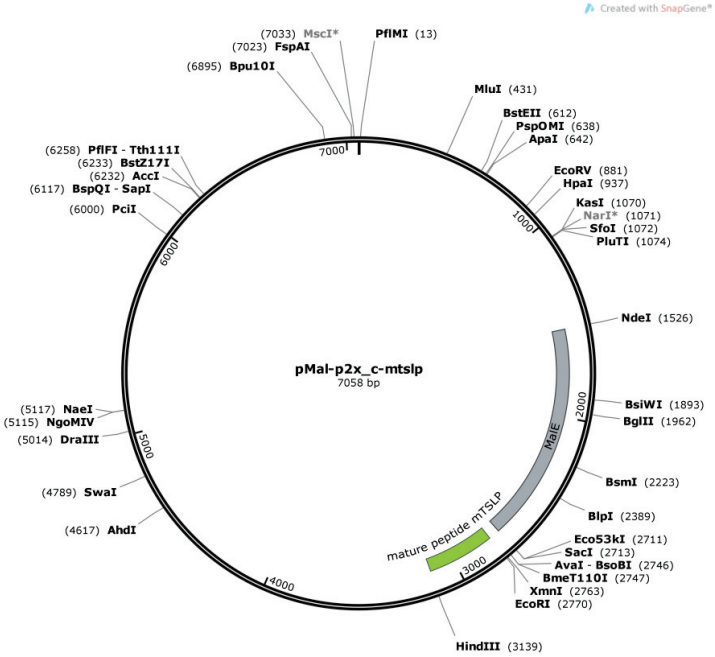

Appendix II. List of Tables and Figures

List of tables

Table II/1. List of figures	
Table No.	**Description**
Table 1.1.	Effect of TSLP on various immune cells.
Table 1.2.	Specific targeting of mTSLP pathway in mice
Table 3.1.	List of used laboratory equipment
Table 3.2.	List of used laboratory consumables
Table 3.3.	List of chemicals and reagents used
Table 3.4.	List of other chemicals and reagents
Table 3.5.	List of commercial buffers
Table 3.6.	List of self-made buffers
Table 3.7.	List of enzymes
Table 3.8.	List of antibiotics
Table 3.9.	List of commercial kits
Table 3.10.	List of antibodies
Table 3.11.	List of primary cells
Table 3.12.	List of eukaryotic cell lines
Table 3.13.	List of bacterial strains
Table 3.14.	pcDNA3.1 + (Neo/Zeo) -derived receptor expression constructs
Table 3.15.	pMAL-c2X derived expression constructs (see Appendix.)
Table 3.16.	pGL3-basic derived expression constructs (see Appendix)
Table 3.17.	Oligonucleotide sequence
Table 3.18.	Cytokines and factors used
Table 3.19.	Software
Table 3.20.	Components of a plasmid digestion reaction
Table 3.21.	Principle of PCR
Table 3.22.	Reaction mixture
Table 3.23.	Composition of 12.5% gels
Table 4.1.	(a)Composition of chains with rotated domains (b) combination of chains
Table II/1	List of tables
Table II/2	List of figures
Table III/1	Accesion numbers

List of figures

Table II/2. List of figures	
Fig No.	**Description**
Fig.1.1.	Receptors for γc family cytokines and TSLP
Fig.1.2.	A cellular scheme showing mechanism of TSLP action.
Fig.1.3.	a. The structure of mTSLP and b. mTSLP-TSLPR interaction.
Fig.1.4.	Diseases in which TSLP has a direct or suspected role.
Fig.3.1.	Plasmid map of the vector pcDNA3.1 (+) Neo. The vector is derived from Invitrogen and is suitable for the expression of recombinant proteins in eukaryotic system (Product Information from Invitrogen).
Fig.3.2	The pMAL-2 vectors expression system for production of mTSLP. pMAL-
Fig.3.3	Plasmid map of the vector pGL3-basic.
Fig.3.4.	Steps involved in the generation of the dendritic cells from the bone marrow cells from C57BL/6J mice
Fig.3.5.	A schematic overview of the chemical reactions underlying the Promega Luciferase® Reporter Assay.
Fig.3.6.	The pMAL-2 vectors expression system for production of mTSLP .
Fig.4.1.	Flow cytometric analysis of mTSLPR receptor expression on the surface of the transfected Ba/F3 cell line:
Fig.4.3.	Generation of the hybrid plasmids.
Fig.4.4.	Flow cytometric analysis of hybrid receptor chain expression on the surface of the transfected Ba/F3 cell line.
Fig 4.5.	Analysis of signalling activity of the murine TSLP hybrid receptor chains with Ba/F3 luciferase gene readout system
Fig.4.6.	Effects of relative domain rotations in the transmembrane region.
Fig.4.7.	Phusion PCR production of insert exo-mTSLPR.
Fig.4.8	a. Schematic linear illustration of mTSLPR His6x plasmid gene sequence including restriction sites.
	b. Schematic illustration of mTSLPR His8x TraN sequence including restriction sites.
Fig.4.9.	Western blot showing comparative expression of mTSLPR in HEK 293T cells transfected with pcDNA3.1 exo-mTSLPR-His 8xTraN by Amaxa and Turbofect.

Fig.4.26.	Analysis of Ba/F3 luciferase gene based readout to determine the relative bioactivity of I37E mTSLP-MBP fusion protein.
Fig.4.27.	Analysis of a Ba/F3 luciferase gene based competition assay between I37E mTSLP-MBP and mTSLP-MBP readout for functional characterization of the bioactivity of the mutant I37E mTSLP-MBP
Fig.4.28.	Visual characterization of the dendritic cells on a microscope.
Fig.4.29.	Flow cytometry based analysis based characterization of enriched murine dendritic cells:
Fig.4.30.	Luminometric analysis of the KCMH-1 supernatant response exhibited by the mTSLPR expressing Ba/F3 based IRF-luciferase gene readout system.
Fig. 4.31.	a. Schematic representation of an experiment to study the relative dendritic cell migration across a membrane in a Boyden chamber under the influence of mTSLP-MBP and I37E mTSLP-MBP. b. Analysis of pictures of slides c. Statistical analysis of relative dendritic cell migration.
Fig. 4.32.	a. The KCMH- Dendritic cell based model: Schematic representation of the production and stimulation of cells. b. Flow cytometric analysis of dendritic cells stimulated by KCMH-1 cell supernatant
Fig.4.33.	The KCMH- Dendritic cell based model used for analysis of inhibitory activity of mutant I37E mTSLP-MBP. a. Schematic representation of the competition assay with dendritic cells. b. Flow-cytometric analysis of the relative OX40L expression on addition of the mutant dosages.
Fig.4.34.	Flow-cytometric analysis of the relative change in the CD80 expression on the surface of dendritic cells stimulated by KCMH-1 cell supernatant, on addition of various mutant dosages.
Fig.4.35.	Flow-cytometric analysis of the relative change in the CD86 expression on the surface of dendritic cells stimulated by KCMH-1 cell supernatant, on addition of various mutant dosages

Appendix III. DNA Sequences

Table III/1. Accession number

DNA	Accession number
hTSLPR	NM_022148.3
mTSLPR	NM_002185.3
mIL-7Rα	NM_008372.4
mTSLPR	NM_016715.4
mTSLP	NM_021367.2

Acknowledgement

I would like to extend my gratitude to the people who generously contributed to the work presented in this thesis.

Special mention goes to my enthusiastic and erudite supervisor, Prof. Dr. Karlheinz Friedrich. My PhD has been an amazing experience and I thank Karlheinz wholeheartedly, not only for his tremendous academic support, but also for giving me so many wonderful opportunities to be creative and independently design sub projects and above all his motivation in times of crisis. His war cry 'Go for it' filled me up with energy and ended all despair of the struggle towards yielding meaningful results.

Similar, profound gratitude goes to Prof. Dr. Baniahmad and Prof. Dr. Alexander Berndt, who have been my critical reviewers and advising members of my thesis committee. The meetings with all the supervisors have been remarkably helpful to control the timelines of delivery and evaluation of the results.

I highly appreciate Andreas Wohlmann, Andreas Borowski, Jens Bratsch, Sebastian Krause, Susanne Jennek, Karsten Letsch and Simone Mueller for sharing their technical expertise and contributing with time, material and completion of various sub-projects.

Special mention goes to Nadine Knutti and Kritan Gautam in enriching me with the philosophy of 'art of happy living' and creating a positive environment around me. Special thanks to AG Mosig and AG Huber allowing me to use their equipments in their labs.

Finally, thanks to Mom and Dad, Anshu, Saurabh, Nisha and niece Saanvi for their everlasting support and encouragement. A special thanks to my wife Shivani for her support and help towards creation of thesis. I shall like to dedicate this thesis to my family and my supervisor Prof. Dr. Friedrich.

Sworn Declaration

I hereby declare that

my doctoral thesis abides by the regulations of the Faculty of Medicine, Friedrich Schiller University.

the content in this thesis has been created by me and all works, personal communication, and sources have been cited appropriately.

the creation of this work has been supervised and supported and assessed by: Prof. Dr. Karlheinz Friedrich and Prof. Dr. A. Baniahmad.

the assistance of a doctoral consultant was not used and that no third parties have received either direct or indirect monetary benefits from me for work associated with the submitted dissertation.

I have not submitted the contents of this dissertation as a subject for a governmental or other scientific examination.

I have not submitted this or an in major parts similar work as a dissertation to any other university.

Jena, 16.12.15

Place, Date

Signature

Curriculum Vitae

Nilabh Ranjan

Teichgraben 3
Jena, Germany-07743
+49 15773384886
ranjan.nilabh@gmail.com

Education

Jan 2012- till date	PhD, IZKF Research Scholar, Friedrich Schiller University, Germany
2004 - 2006	M.Sc., Biotechnology, Chhatrapati Shahu Ji Maharaj University, India
2000 - 2004	Bachelor of Science (B.Sc.), University of Lucknow, India
1999 - 2000	ISC, Biology, City Montessori Degree College, India
1998	ICSE, St. Thomas High School, Lucknow

Honors and Awards

June-August 2015	DAAD short term PhD grant, Graduate academy Jena
May 2013	Immunotools IT Box Award 2013, Immunotools GmbH, Germany
April 2013 - April 2015	DAAD Support Scholarship for International tutors, Graduate Academy Jena
Jan 2012 - Jan2015	IZKF PhD Graduate Scholarship IZKF, Jena, Germany
June 2009 and Dec. 2005	CSIR-UGC Lectureship National Eligibility Test
April 2007 - June 2007	Department of Biotechnology Project Fellowship

Publications

Abstracts

- (Poster) Thymic Stromal Lymphopoietin (TSLP) and its receptor as targets for the development of anti-inflammatory and anti-leukemic inhibitory agents. (FEBS Congress, Berlin, July 2015).
- (Poster) Antagonistic targeting of Thymic Stromal Lymhopoietin (TSLP) signaling in murine cellular models. DZL Breath Summer School, Hannover June, 2015.

- The Thymic Stromal Lymphopoietin (TSLP) receptor in asthma and cancer: Influence on pathogenesis parameters and specific blockade by novel inhibitory antibodies. 16th Joint Meeting Signal Transduction Receptors, Mediators and Genes, Nov 2012.
- (Poster) Studies towards targeting Thymic Stromal Lymhopoietin (TSLP) and STAT (Signal transducers and activators of transcription) pathways for therapeutic amelioration of Asthma bronchiale. In proceedings of UGMLC/DZL-Symposium 2012, Volume: Pneumologie 2012; 66-A220).
- (Talk) Paradigm Shift in Cytotoxicity Tests from in-vivo to *in-vitro* for Antiasthmatic Drug (Published in Abstract Book at NCIHD'06 Kanpur).
- (Poster) Immunobiology of Transplantation and Immuno-suppression. (Published in Abstract Book at NCIHD'2006 Kanpur).
- (Poster) STAT 3 Peptide expressions in the leukocyte population of broncho alveolar lavage fluid (BALF) of asthmatic mice. (Published in Toxicology International Special silver jubilee edition, pp43, Nov'05).

Paper

- Blockade of Thymic Stromal Lymphopoietin (TSLP) receptor inhibits TSLP-driven proliferation and signalling in lymphoma cells from a subset of B-ALL patients.
  Tina Vetter, Andreas Borowski, Andreas Wohlmann, Nilabh Ranjan, Michael Kuepper, Susanne Badura, Oliver G. Ottman, and Karlheinz Friedrich, Journal of Cancer Research and Clinical Oncology (JCRCO), (Submission under progress)

16.12.15, Jena